QC
807.5
.U6
W6
no.291
c.2

NOAA Technical Memorandum ERL ETL-291

WAVE SCATTERING AT LOW GRAZING ANGLES: NEW PERTURBATION THEORY

M.I. Charnotskii

Environmental Technology Laboratory
Boulder, Colorado
August 1998

noaa NATIONAL OCEANIC AND ATMOSPHERIC ADMINISTRATION / Environmental Research Laboratories

NOAA Technical Memorandum ERL ETL-291

WAVE SCATTERING AT LOW GRAZING ANGLES: NEW PERTURBATION THEORY

Mikhail I. Charnotskii
Science and Technology Corporation

QC
807.5
.U6
W6
no. 291

c. 2

LIBRARY

N.O.A.A.
U S Dept. of Commerce

Environmental Technology Laboratory
Boulder, Colorado
August 1998

UNITED STATES DEPARTMENT OF COMMERCE

William M. Daley
Secretary

NATIONAL OCEANIC AND ATMOSPHERIC ADMINISTRATION

D. JAMES BAKER
Under Secretary for Oceans and Atmosphere/Administrator

Environmental Research Laboratories

James L. Rasmussen
Director

NOTICE

Mention of a commercial company or product does not constitute an endorsement by NOAA/ERL. Use for publicity or advertising purposes, of information from this publication or concerning proprietary products or the tests of such products, is not authorized.

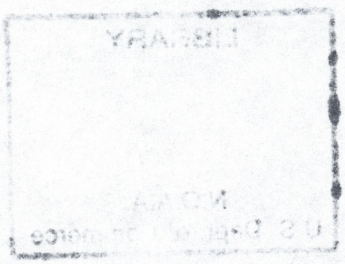

TABLE OF CONTENTS

WAVE SCATTERING AT LOW GRAZING ANGLES: NEW PERTURBATION THEORY

Mikhail I. Charnotskii
Science and Technology Corporation

Abstract

We examine wave scattering by a periodic surface in the presence of low-grazing scattered modes. We find that in the case of the Neuman boundary condition the surface is characterized by effective impedance and corresponding Brewster angle. Conventional perturbation theory appears to be valid only when all scattering grazing angles are larger than the effective Brewster angle. We develop a new perturbation expansion that is valid when one of the scattered modes propagates below the effective Brewster angle. The scattering amplitude is found to be nonlinear in terms Fourier components of the heights. This development resolves the existing contradiction between the low-grazing scattering results by Barrick [1] and Tatarskii/Charnotskii [2, 3] for a periodic surface case. We propose a uniform perturbation approximation which combines the conventional and low-grazing angles perturbation results and incorporates the effective surface impedance. In particular this theory describes the sign change of the reflection coefficient when the incidence angle approaches zero.

Similar results have been obtained for the special case of two grazing modes. The effective surface impedance does not exist in this case, but there is a critical angle separating the validity domains of the conventional and low-grazing angles perturbation theories. We found that the reflection coefficient reduces substantially in the vicinity of the critical angle. At the same time, the backscatter increases significantly.

1. INTRODUCTION

We discuss here the specifics of wave scattering by a plane in an average surface when either one of or both the incidence and/or scattering grazing angles are small. This situation is of a significant practical interest for a ground-based active and passive radar studies of the ocean surface, and for a long-path propagation along the ocean surface.

For the finite impedance surfaces and Dirichlet problem both numerical results of [1] for the periodic surface, and very general analytical results of [2, 3] predict that the continuous scattering amplitude is proportional to the small grazing angle. This result is also supported by the conventional perturbation theory.

However, there is a certain controversial aspect to the Neuman case:

- Numerical results of Barrick [1] show the same type of grazing behavior as for the finite impedance and Dirichlet surfaces. Besides that, Barrick asserts that the reflection coefficient of the slightly rough Neuman surface changes its sign from +1 to -1 when the grazing incidence angle tends to zero. This conclusion is supported by the theoretical results of Bass and Fuks [4] for an average field above a statistically rough surface.
- Analytical results of Tatarskii and Charnotskii [2, 3] predict, however, that for a plane in average, but otherwise arbitrary Neuman rough surface, the continuous scattering amplitude saturates at a finite limit when the grazing angle approaches zero. This conclusion is supported by the conventional perturbation theory. Other supporting evidence comes from

the model problem of scattering by a single bump at the plane, which is presented in Appendix A.

It is reasonable to expect that the problem should be simplified by the fact that there is an additional small parameter besides the small angle. For example, one can expect a quick and easy solution in the case when roughness heights are small. However, when the small incidence/scattering angle is combined with the perturbation theory we face a problem with two small parameters: small scattering or incidence angle $\alpha << 1$, and small roughness height in the wavelength scale, $kh << 1$. If scattering amplitude is an analytical function of these two parameters at zero then there exists a universal limiting behavior of the scattering amplitude when $\alpha \to 0$ and $kh \to 0$. This limit would not depend on the specific way by which the origin at the (α, kh) plane is approached. It would appear that for the Dirichlet and finite impedance problems. this is the case.

When scattering amplitude is not an analytic function of α and kh at zero, it is possible to obtain the different limits when $\alpha \to 0$ and $kh \to 0$, depending on what kind of relation exists between α and kh. We found that this is the case for the Neuman problem. We will show that at least for Neuman scattering with a finite number of propagating diffraction orders this is indeed the case, and for the scattering amplitudes we have:

$$\lim_{\alpha \to 0}\left(\lim_{kh \to 0}\right) \neq \lim_{kh \to 0}\left(\lim_{\alpha \to 0}\right). \tag{1.1}$$

The left-hand part of this formula corresponds to the conventional perturbation theory, where the small-height assumption is made first, and then the small-angle case is analyzed. The major result of the paper is the development of the a new perturbation expansion that corresponds to the right-hand part of (1.1). We call it Grazing Perturbation (GP) expansion for brevity.

In Chapter 2 we introduce the major integral equation for scalar wave scattering by a plane an in average rough surface with an impedance boundary condition. We present the details of the existing discrepancy in the small-grazing angle behavior predictions by Barrick [1] and Tatarskii/Charnotskii [2, 3].

In Chapter 3 we introduce the necessary formalism for the one-dimensional periodic surface scattering, and derive the principal equations of our numerical analysis.

In Chapter 4 we discuss the intrinsic limitations of the Conventional Perturbation (CP) theory in the presence of one or two low-grazing modes. We show that incorporation of the higher-order term extends the validity domain of the CP formulas, and estimate the CP validity domains for one and two low-grazing mode cases.

In Chapter 5 we develop a new, grazing perturbation (GP-I) theory that is valid in the presence of a single grazing mode. We discuss the validity domain of the GP-I formulas, role of the higher-order GP-I terms, and the reciprocity of the GP-I formulas. We introduce the effective surface impedance and Brewster angle and show that CP-I together with GP-I form a complete set of asymptotes with the effective Brewster angle being the border between them.

Chapter 6 mirrors Chapter 5, but discussion is concentrated on the specific case of the two low-grazing scattered orders. We call it the GP-II approximation to distinguish it from the previous case. We show that it is not feasible to introduce the effective impedance in this case, but there exists the critical grazing angle that separates the validity domains of the CP-II and CP-II approximations.

In Chapter 7 we propose two sets of formulas that represent the Uniform Perturbation (UP) approximations that are valid for the small roughness heights but arbitrary values of the scattering angles.

We present the overview of our major results in the Conclusion and discuss the limitations associated with the surface periodicity.

Appendix A presents an important example of the scattering problem, scattering by a plane with a single bump. This example shows that our periodic surface results cannot be extended to the non-periodic, rough surface case in a straightforward manner.

Appendix B contains some details of our numerical technique.

2. INTEGRAL EQUATIONS FOR THE SCATTERING PROBLEM.

2.1 Principal Equations

Consider the 3-D scattering problem for the scattering of a plane wave:

$$E_{IN}(\mathbf{r},z,\mathbf{q}_0)=\exp(i\mathbf{r}\cdot\mathbf{q}_0+\nu_0 z) \tag{2.1}$$

by the rough surface $\Sigma:\{z=\varsigma(\mathbf{r})\}$.

A scattered wave satisfies the homogeneous Helmholtz's equation

$$\left[k^2+\nabla^2\right]E_{SC}(\mathbf{r},z,\mathbf{q}_0)=0 \tag{2.2}$$

in the region $z>\varsigma(\mathbf{r})$, and the impedance boundary condition

$$\frac{\partial E_{TOT}(\mathbf{r},\varsigma(\mathbf{r}),\mathbf{q}_0)}{\partial n(\mathbf{r})}+ikZE_{TOT}(\mathbf{r},z,\mathbf{q}_0)=0 \tag{2.3}$$

at the surface. Here, the total field is:

$$E_{TOT}(\mathbf{r},z,\mathbf{q}_0)\equiv E_{IN}(\mathbf{r},z,\mathbf{q}_0)+E_{SC}(\mathbf{r},z,\mathbf{q}_0).$$

The scattered field above the highest point of the surface has the form:

$$E_{SC}(\mathbf{r},z,\mathbf{q}_0)=\iint\frac{d\mathbf{q}}{k\nu(\mathbf{q})}S(\mathbf{q},\mathbf{q}_0)\exp\left[i\mathbf{q}\cdot\mathbf{r}+i\nu(\mathbf{q})z\right]. \tag{2.4}$$

This definition of the scattering amplitude $S(\mathbf{q},\mathbf{q}_0)$ corresponds to the angular density of the scattered field. A pair of integral equations for the surface fields and scattering amplitude can be derived from Green's formula applied to the region $z^*>z>\varsigma(\mathbf{r})$ and a pair of functions $E_{TOT}(\mathbf{r},z,\mathbf{q}_0)$ and $\exp\left[i\mathbf{q}\cdot\mathbf{r}\pm i\nu(\mathbf{q})z\right]$,and have the following form:

$$\iint d\mathbf{r}E(\mathbf{r},\mathbf{q}_0)\left[\nu(\mathbf{q})+\mathbf{q}\cdot\nabla\varsigma(\mathbf{r})+kZ\sqrt{1+\left|\nabla\varsigma(\mathbf{r})\right|^2}\right]\exp\left[-i\mathbf{q}\cdot\mathbf{r}+i\nu(\mathbf{q})\varsigma(\mathbf{r})\right] \tag{2.5}$$
$$=8\pi^2\nu_0\delta(\mathbf{q}-\mathbf{q}_0),$$

$$\iint d\mathbf{r}E(\mathbf{r},\mathbf{q}_0)\left[\nu(\mathbf{q})-\mathbf{q}\cdot\nabla\varsigma(\mathbf{r})-kZ\sqrt{1+\left|\nabla\varsigma(\mathbf{r})\right|^2}\right]\exp\left[-i\mathbf{q}\cdot\mathbf{r}-i\nu(\mathbf{q})\varsigma(\mathbf{r})\right] \tag{2.6}$$
$$=\frac{8\pi^2}{k}S(\mathbf{q},\mathbf{q}_0).$$

Here we introduced the notation $E(\mathbf{r},\mathbf{q}_0)\equiv E_{TOT}\left(\mathbf{r},\varsigma(\mathbf{r}),\mathbf{q}_0\right)$ for the surface value of the total field.

Integration by part of the terms with $\nabla\varsigma(\mathbf{r})$ in (2.5) and (2.6) allows us to present these equations in the alternative form:

$$\iint d\mathbf{r}E(\mathbf{r},\mathbf{q}_0)\left[\frac{k^2}{\nu(\mathbf{q})}+kZ\sqrt{1+\left|\nabla\varsigma(\mathbf{r})\right|^2}\right]\exp\left[-i\mathbf{q}\cdot\mathbf{r}+i\nu(\mathbf{q})\varsigma(\mathbf{r})\right] \tag{2.7}$$
$$+\frac{i}{\nu(\mathbf{q})}\iint d\mathbf{r}\exp\left[-i\mathbf{q}\cdot\mathbf{r}+i\nu(\mathbf{q})\varsigma(\mathbf{r})\right]\left[\mathbf{q}\cdot\nabla E(\mathbf{r},\mathbf{q}_0)\right]=8\pi^2\nu_0\delta(\mathbf{q}-\mathbf{q}_0),$$

$$\iint d\mathbf{r}E(\mathbf{r},\mathbf{q}_0)\left[\frac{k^2}{\nu(\mathbf{q})}-kZ\sqrt{1+\left|\nabla\varsigma(\mathbf{r})\right|^2}\right]\exp\left[-i\mathbf{q}\cdot\mathbf{r}-i\nu(\mathbf{q})\varsigma(\mathbf{r})\right] \tag{2.8}$$
$$+\frac{i}{\nu(\mathbf{q})}\iint d\mathbf{r}\exp\left[-i\mathbf{q}\cdot\mathbf{r}-i\nu(\mathbf{q})\varsigma(\mathbf{r})\right]\left[\mathbf{q}\cdot\nabla E(\mathbf{r},\mathbf{q}_0)\right]=\frac{8\pi^2}{k}S(\mathbf{q},\mathbf{q}_0).$$

Using the Fourier transform of the surface field :

$$E(\mathbf{r},\mathbf{q}_0)\equiv\iint d\mathbf{p}\hat{E}(\mathbf{p},\mathbf{q}_0)\exp(i\mathbf{p}\cdot\mathbf{r}), \tag{2.9}$$

we present these equations as follows:

$$\iint d\mathbf{r}\iint d\mathbf{p}\hat{E}(\mathbf{p},\mathbf{q}_0)\left[\frac{k^2-\mathbf{p}\cdot\mathbf{q}}{\nu(\mathbf{q})}+kZ\sqrt{1+\left|\nabla\varsigma(\mathbf{r})\right|^2}\right]\exp\left[i(\mathbf{p}-\mathbf{q})\cdot\mathbf{r}+i\nu(\mathbf{q})\varsigma(\mathbf{r})\right] \tag{2.10}$$
$$=8\pi^2\nu_0\delta(\mathbf{q}-\mathbf{q}_0),$$

$$\iint d\mathbf{r}\iint d\mathbf{p}\hat{E}(\mathbf{p},\mathbf{q}_0)\left[\frac{k^2-\mathbf{p}\cdot\mathbf{q}}{v(\mathbf{q})}-ikZ\sqrt{1+\left|\nabla\varsigma(\mathbf{r})\right|^2}\right]\exp\left[i(\mathbf{p}-\mathbf{q})\cdot\mathbf{r}-iv(\mathbf{q})\varsigma(\mathbf{r})\right] \tag{2.11}$$
$$=\frac{8\pi^2}{k}S(\mathbf{q},\mathbf{q}_0).$$

While this last equations look more complicated than the original equations (2.5) and (2.6), it has certain advantages when used for the periodic surface.

2.2 Reciprocity and Energy Conservation

Application of Green's formula to the pair of fields $E_{TOT}(\mathbf{r},z,\mathbf{q}_1)$ and $E_{TOT}(\mathbf{r},z,\mathbf{q}_2)$ over the same domain as in the previous section proves the **reciprocity** of the scattering amplitude:

$$S(\mathbf{q}_1,\mathbf{q}_0)=S(-\mathbf{q}_1,-\mathbf{q}_0). \tag{2.12}$$

Energy conservation follows from application of Green's formula to the pair of fields $E_{TOT}(\mathbf{r},z,\mathbf{q}_1)$ and $E^*{}_{TOT}(\mathbf{r},z,\mathbf{q}_2)$ with $|\mathbf{q}_1|,|\mathbf{q}_2|<k$:

$$\iint\limits_{|\mathbf{q}|<k}\frac{d\mathbf{q}}{kv(\mathbf{q})}S(\mathbf{q},\mathbf{q}_1)S^*(\mathbf{q},\mathbf{q}_2)=kv_1\delta(\mathbf{q}_2-\mathbf{q}_1)-\frac{k^2}{4\pi^2}\mathrm{Re}(Z)\iint d\mathbf{r}E(r,\mathbf{q}_1)E^*(r,\mathbf{q}_0). \tag{2.13}$$

For the Dirichlet and Neuman boundary conditions (2.13) simplifies to

$$\iint\limits_{|\mathbf{q}|<k}\frac{d\mathbf{q}}{kv(\mathbf{q})}S(\mathbf{q},\mathbf{q}_1)S^*(\mathbf{q},\mathbf{q}_2)=kv_1\delta(\mathbf{q}_2-\mathbf{q}_1). \tag{2.14}$$

2.3 Conventional Perturbation Results

Perturbation solution of the scattering problem seeks the surface field and the scattering amplitude in the form of the Taylor functional series in $\varsigma(\mathbf{r})$:

$$\begin{aligned}E(\mathbf{r},\mathbf{q}_0)&=E^{(0)}(\mathbf{r},\mathbf{q}_0)+E^{(1)}(\mathbf{r},\mathbf{q}_0)+E^{(2)}(\mathbf{r},\mathbf{q}_0)+..\\ S(\mathbf{q}_1,\mathbf{q}_0)&=S^{(0)}(\mathbf{q}_1,\mathbf{q}_0)+S^{(1)}(\mathbf{q}_1,\mathbf{q}_0)+S^{(2)}(\mathbf{q}_1,\mathbf{q}_0)+..\end{aligned} \tag{2.15}$$

Substitution of (2.15) into (2.5) and (2.6) and equating of the similar orders in $\varsigma(\mathbf{r})$ provide the following results for up to the second order in $\varsigma(\mathbf{r})$:

$$E(\mathbf{r},\mathbf{q}_0)=2\frac{\nu_0}{\nu_0+kZ}\exp(i\mathbf{r}\cdot\mathbf{q}_0)$$
$$-2i\frac{\nu_0}{\nu_0+kZ}\iint d\mathbf{q}'\hat{\varsigma}(\mathbf{q}'-\mathbf{q}_0)\frac{\left[k^2-\mathbf{q}'\cdot\mathbf{q}_0+kZ\nu(\mathbf{q}')\right]}{\nu(\mathbf{q}')+kZ}\exp(i\mathbf{r}\cdot\mathbf{q}')$$
$$+\frac{\nu_0}{\nu_0+kZ}\iint\frac{d\mathbf{q}'}{\nu(\mathbf{q}')+kZ}\iint d\mathbf{p}\hat{\varsigma}(\mathbf{p}-\mathbf{q}_0)\hat{\varsigma}(\mathbf{q}'-\mathbf{p})\exp(i\mathbf{r}\cdot\mathbf{q}')\Big\{\nu(\mathbf{q}')\left[k^2-\mathbf{q}'\cdot\mathbf{q}_0\right] \tag{2.16}$$
$$+kZ\left[\nu^2(\mathbf{q}')+(\mathbf{p}-\mathbf{q}_0)\cdot(\mathbf{q}'-\mathbf{p})\right]-2\frac{\left[k^2-\mathbf{p}\cdot\mathbf{q}_0+kZ\nu(\mathbf{p})\right]\left[k^2-\mathbf{q}'\cdot\mathbf{p}+kZ\nu(\mathbf{q}')\right]}{\nu(\mathbf{p})+kZ}\Big\},$$

$$S(\mathbf{q}_1,\mathbf{q}_0)=k\nu_0\frac{\nu_0-kZ}{\nu_0+kZ}\delta(\mathbf{q}_1-\mathbf{q}_0)$$
$$-2ik\frac{\nu_0}{\nu_0+kZ}\frac{\nu_1}{\nu_1+kZ}\hat{\varsigma}(\mathbf{q}_1-\mathbf{q}_0)\left(k^2-\mathbf{q}_1\cdot\mathbf{q}_0+kZ\right)$$
$$-k\frac{\nu_0}{\nu_0+kZ}\frac{\nu_1}{\nu_1+kZ}\iint d\mathbf{p}\hat{\varsigma}(\mathbf{p}-\mathbf{q}_0)\hat{\varsigma}(\mathbf{q}_1-\mathbf{p}) \tag{2.17}$$
$$\times\left\{kZ\left[q_1^2-p^2-\mathbf{p}\cdot(\mathbf{q}_0-\mathbf{q}_1)\right]-2\frac{\left[k^2-\mathbf{p}\cdot\mathbf{q}_0+kZ\nu(\mathbf{p})\right]\left[k^2-\mathbf{q}_1\cdot\mathbf{p}+k^2Z^2\right]}{\nu(\mathbf{p})+kZ}\right\}.$$

Here, $\hat{\varsigma}(\mathbf{q})$ is the Fourier transform of roughness heights:

$$\varsigma(\mathbf{r})=\iint d\mathbf{q}\hat{\varsigma}(\mathbf{q})\exp(i\mathbf{q}\cdot\mathbf{r}).$$

For the Dirichlet case, $Z\to\infty$ we have the standard result:

$$S(\mathbf{q}_1,\mathbf{q}_0)=-k\nu_0(\mathbf{q}_1-\mathbf{q}_0)+2ik\nu_0\nu_1\hat{\varsigma}(\mathbf{q}_1-\mathbf{q}_0)$$
$$+2k\nu_0\nu_1\iint d\mathbf{p}\hat{\varsigma}(\mathbf{p}-\mathbf{q}_0)\hat{\varsigma}(\mathbf{q}_1-\mathbf{p})\nu(\mathbf{p}). \tag{2.18}$$

For the Neuman problem, $Z\to 0$, the surface field is:

$$E(\mathbf{r},\mathbf{q}_0)=2\exp(i\mathbf{r}\cdot\mathbf{q}_0)-2i\iint d\mathbf{q}'\hat{\varsigma}(\mathbf{q}'-\mathbf{q}_0)\frac{\left[k^2-\mathbf{q}'\cdot\mathbf{q}_0\right]}{\nu(\mathbf{q}')}\exp(i\mathbf{r}\cdot\mathbf{q}')$$
$$+\iint d\mathbf{q}'\iint d\mathbf{p}\hat{\varsigma}(\mathbf{p}-\mathbf{q}_0)\hat{\varsigma}(\mathbf{q}'-\mathbf{p})\exp(i\mathbf{r}\cdot\mathbf{q}')\left\{\left[k^2-\mathbf{q}'\cdot\mathbf{q}_0\right]-2\frac{\left[k^2-\mathbf{p}\cdot\mathbf{q}_0\right]\left[k^2-\mathbf{q}'\cdot\mathbf{p}\right]}{\nu(\mathbf{q}')}\right\}, \tag{2.19}$$

and the scattering amplitude is

$$S(\mathbf{q}_1,\mathbf{q}_0)=k\nu_0\delta(\mathbf{q}_1-\mathbf{q}_0)-2ik\hat{\varsigma}(\mathbf{q}_1-\mathbf{q}_0)\left[k^2-\mathbf{q}_1\cdot\mathbf{q}_0\right]$$
$$-2k\iint d\mathbf{p}\hat{\varsigma}(\mathbf{p}-\mathbf{q}_0)\hat{\varsigma}(\mathbf{q}_1-\mathbf{p})\frac{\left[k^2-\mathbf{p}\cdot\mathbf{q}_0\right]\left[k^2-\mathbf{q}_1\cdot\mathbf{p}\right]}{\nu(\mathbf{p})}. \tag{2.20}$$

The CP series for the Fourier transform of the surface field can be derived directly from (2.10) or from (2.16). In either case:

$$\hat{E}(\mathbf{q},\mathbf{q}_0)=2\frac{\nu_0}{\nu_0+kZ}\delta(\mathbf{q}-\mathbf{q}_0)$$
$$-2i\frac{\nu_0}{\nu_0+kZ}\hat{\varsigma}(\mathbf{q}-\mathbf{q}_0)\frac{\left[k^2-\mathbf{q}\cdot\mathbf{q}_0+kZ\nu(\mathbf{q})\right]}{\nu(\mathbf{q})+kZ}$$
$$+\frac{\nu_0}{(\nu_0+kZ)(\nu(\mathbf{q})+kZ)}\iint d\mathbf{p}\hat{\varsigma}(\mathbf{p}-\mathbf{q}_0)\hat{\varsigma}(\mathbf{q}-\mathbf{p})\Big\{\nu(\mathbf{q})\left[k^2-\mathbf{q}\cdot\mathbf{q}_0\right] \tag{2.21}$$
$$+kZ\left[\nu^2(\mathbf{q})+(\mathbf{p}-\mathbf{q}_0)\cdot(\mathbf{q}-\mathbf{p})\right]-2\frac{\left[k^2-\mathbf{p}\cdot\mathbf{q}_0+kZ\nu(\mathbf{p})\right]\left[k^2-\mathbf{q}\cdot\mathbf{p}+kZ\nu(\mathbf{q})\right]}{\nu(\mathbf{p})+kZ}\Big\}.$$

For the Neuman case we have:

$$\hat{E}(\mathbf{q},\mathbf{q}_0)=2\delta(\mathbf{q}-\mathbf{q}_0)-2i\hat{\varsigma}(\mathbf{q}-\mathbf{q}_0)\frac{\left[k^2-\mathbf{q}\cdot\mathbf{q}_0\right]}{\nu(\mathbf{q})}$$
$$+\frac{1}{\nu(\mathbf{q})}\iint d\mathbf{p}\hat{\varsigma}(\mathbf{p}-\mathbf{q}_0)\hat{\varsigma}(\mathbf{q}-\mathbf{p})\left\{\nu(\mathbf{q})\left[k^2-\mathbf{q}\cdot\mathbf{q}_0\right]-2\frac{\left[k^2-\mathbf{p}\cdot\mathbf{q}_0\right]\left[k^2-\mathbf{q}\cdot\mathbf{p}\right]}{\nu(\mathbf{p})}\right\}. \tag{2.22}$$

The notable feature of CP formulas for the Neuman problem (2.19), (2.20) and (2.22) is a singularity of at $|\mathbf{q}|=k$. It looks like it will be present in all the higher-order terms of the series as well. However, this is an integrable singularity, and it causes no principal problems.

2.4 Grazing Angle Behavior

2.4.1 Perturbation Results

Consider the low grazing angle behavior of the scattered field for the finite incident angle first. In this case $\nu_1=k\sin\alpha_1<<k$. Perturbation formula (2.17) shows that for the finite impedance and for the Dirichlet case we have: $S(\mathbf{q}_1,\mathbf{q}_0)\propto\alpha_1{}^1$. However, for the Neuman case from (2.20) we have $S(\mathbf{q}_1,\mathbf{q}_0)\propto\alpha_1{}^0$. There is no universal limit of the scattering amplitude when both $Z\to 0$, and $\alpha_1\to 0$ because scattering amplitude is not an analytical function of Z and α_1 at zero. Formally this is quite obvious from (2.17) due to the presence of the $(\nu+kZ)^{-1}$ multipliers.

In order get more insight into the behavior of the scattering amplitude when both $Z \to 0$, and $\alpha_1 \to 0$, we need to specify how this zero is approached. If we assume that the Brewster angle is $\beta \approx |Z|$, then for $\alpha_1 \to 0$, and $\alpha_1 > \beta$, we have $S(\mathbf{q}_1, \mathbf{q}_0) \propto \alpha_1^{\,0}$, Neuman-type behavior. However, when $\alpha_1 \to 0$ but $\alpha_1 < \beta$, we have $S(\mathbf{q}_1, \mathbf{q}_0) \propto \alpha_1$, which is a Dirichlet-type behavior. In principle, when $Z \to 0$, and $\alpha_1 = t\beta$ for certain constant t we are able to obtain everything in between.

When both incident and scattering angles are small, for the finite impedance and Dirichlet case we have $S(\mathbf{q}_1, \mathbf{q}_0) \propto (\alpha_1 \alpha_0)^1$. When $Z \to 0$ first and then $\alpha_{0,1} \to 0$, which corresponds to the Neuman case, we have $S(\mathbf{q}_1, \mathbf{q}_0) \propto (\alpha_1 \alpha_0)^0$. This complies with the reciprocity, as expected. The situation in general is similar to the low-grazing scattering case in a sense that there is no universal behavior when both impedance and incident/scattering angle approach zero.

In formal terms all this discussion corresponds to the left-hand side of (1.1), when we allow $k\eta \to 0$ first and then use the fact that $\alpha_i << 1$. We see that the Dirichlet and Neuman problems exhibit a different behavior in this CP limit. It is also clear that in the CP limit the scattering amplitude is not an analytical function of the surface impedance and scattering angle at zero.

2.4.2 Low-Grazing Scattering Discrepancy

Unfortunately, our analytical capabilities are quite limited for the non-perturbation case due to the lack of an exact solution of the problem. However, we are still able to draw some general conclusions by examining the principal integral equations. If we subtract (2.5) from (2.6) we can present the scattering amplitude in the form:

$$S(\mathbf{q}_1, \mathbf{q}_0) = k\nu_0 \delta(\mathbf{q}_1 - \mathbf{q}_0) - \frac{i\nu_1 k}{4\pi^2} \iint d\mathbf{r} E(\mathbf{r}, \mathbf{q}_0) \exp(-i\mathbf{q}_1 \cdot \mathbf{r}) \sin[\nu_1 \varsigma(\mathbf{r})]$$
$$- \frac{k}{4\pi^2} \iint d\mathbf{r} E(\mathbf{r}, \mathbf{q}_0) \exp(-i\mathbf{q}_1 \cdot \mathbf{r}) \left[\mathbf{q}_1 \cdot \nabla\varsigma(\mathbf{r}) + kZ\sqrt{1 + |\nabla\varsigma(\mathbf{r})|^2} \right] \cos[\nu_1 \varsigma(\mathbf{r})]. \tag{2.23}$$

If we add (2.5) to (2.6) we have:

$$S(\mathbf{q}_1, \mathbf{q}_0) = -k\nu_0 \delta(\mathbf{q}_1 - \mathbf{q}_0) + \frac{\nu_1 k}{4\pi^2} \iint d\mathbf{r} E(\mathbf{r}, \mathbf{q}_0) \exp(-i\mathbf{q}_1 \cdot \mathbf{r}) \cos[\nu_1 \varsigma(\mathbf{r})]$$
$$+ \frac{ik}{4\pi^2} \iint d\mathbf{r} E(\mathbf{r}, \mathbf{q}_0) \exp(-i\mathbf{q}_1 \cdot \mathbf{r}) \left[\mathbf{q}_1 \cdot \nabla\varsigma(\mathbf{r}) + kZ\sqrt{1 + |\nabla\varsigma(\mathbf{r})|^2} \right] \sin[\nu_1 \varsigma(\mathbf{r})]. \tag{2.24}$$

Both equations are exact and give the same values of the scattering amplitude for any conditions. Note also that the δ-type terms are not equal to the correct plane-surface specular component in both cases. The correct term according to (2.17) should read:

$$S^{(0)}(\mathbf{q}_1, \mathbf{q}_0) = k\nu_0 \frac{\nu_0 - kZ}{\nu_0 + kZ} \delta(\mathbf{q}_1 - \mathbf{q}_0). \tag{2.25}$$

We are also able to present equations (2.10), (2.11) in the form:

$$4\pi^2[\nu_1+kZ]\hat{E}(\mathbf{q}_1,\mathbf{q}_0)+kZ\iint d\mathbf{r}\iint d\mathbf{p}\hat{E}(\mathbf{p},\mathbf{q}_0)\left[\sqrt{1+|\nabla\varsigma(\mathbf{r})|^2}-1\right]\exp[i(\mathbf{p}-\mathbf{q}_1)\cdot\mathbf{r}]$$
$$+\iint d\mathbf{r}\iint d\mathbf{p}\hat{E}(\mathbf{p},\mathbf{q}_0)\left[k^2-\mathbf{p}\cdot\mathbf{q}_1+kZ\nu_1\sqrt{1+|\nabla\varsigma(\mathbf{r})|^2}\right] \tag{2.26}$$
$$\times\exp[i(\mathbf{p}-\mathbf{q}_1)\cdot\mathbf{r}]\frac{\exp[+i\nu_1\varsigma(\mathbf{r})]-1}{\nu_1}=8\pi^2\nu_0\delta(\mathbf{q}_1-\mathbf{q}_0),$$

$$4\pi^2[\nu_1-kZ]\hat{E}(\mathbf{q}_1,\mathbf{q}_0)-kZ\iint d\mathbf{r}\iint d\mathbf{p}\hat{E}(\mathbf{p},\mathbf{q}_0)\left[\sqrt{1+|\nabla\varsigma(\mathbf{r})|^2}-1\right]\exp[i(\mathbf{p}-\mathbf{q}_1)\cdot\mathbf{r}]$$
$$+\iint d\mathbf{r}\iint d\mathbf{p}\hat{E}(\mathbf{p},\mathbf{q}_0)\left[k^2-\mathbf{p}\cdot\mathbf{q}_1-kZ\nu(\mathbf{q}_1)\sqrt{1+|\nabla\varsigma(\mathbf{r})|^2}\right] \tag{2.27}$$
$$\times\exp[i(\mathbf{p}-\mathbf{q}_1)\cdot\mathbf{r}]\frac{\exp[-i\nu_1\varsigma(\mathbf{r})]-1}{\nu_1}=\frac{8\pi^2}{k}S(\mathbf{q}_1,\mathbf{q}_0),$$

where all the terms have no singularities at $\nu(\mathbf{q}_1)\to 0$.

For the Neuman case these equations reduce to:

$$8\pi^2\nu_0\delta(\mathbf{q}_1-\mathbf{q}_0)=4\pi^2\nu_1\hat{E}(\mathbf{q}_1,\mathbf{q}_0)$$
$$+\iint d\mathbf{r}\iint d\mathbf{p}\hat{E}(\mathbf{p},\mathbf{q}_0)[k^2-\mathbf{p}\cdot\mathbf{q}_1]\exp[i(\mathbf{p}-\mathbf{q}_1)\cdot\mathbf{r}]\frac{\exp[i\nu_1\varsigma(\mathbf{r})]-1}{\nu_1}, \tag{2.28}$$

$$\frac{8\pi^2}{k}S(\mathbf{q}_1,\mathbf{q}_0)=4\pi^2\nu_1\hat{E}(\mathbf{q}_1,\mathbf{q}_0)$$
$$+\iint d\mathbf{r}\iint d\mathbf{p}\hat{E}(\mathbf{p},\mathbf{q}_0)[k^2-\mathbf{p}\cdot\mathbf{q}_1]\exp[i(\mathbf{p}-\mathbf{q}_1)\cdot\mathbf{r}]\frac{\exp[-i\nu_1\varsigma(\mathbf{r})]-1}{\nu_1}. \tag{2.29}$$

We will use these equations in the next chapters to investigate the specific case of scattering by a periodic surface.

If for the Neuman case we formally let $\mathbf{q}_1\to k\hat{\mathbf{q}}_1$ in (2.23), we have:

$$S(k\hat{\mathbf{q}}_1,\mathbf{q}_0)=k\nu_0\delta(k\hat{\mathbf{q}}_1-\mathbf{q}_0)-\frac{k^2}{4\pi^2}\hat{\mathbf{q}}_1\cdot\iint d\mathbf{r}\nabla\varsigma(\mathbf{r})E(\mathbf{r},\mathbf{q}_0)\exp(-ik\hat{\mathbf{q}}_1\cdot\mathbf{r}). \tag{2.30}$$

Since the first term at the right-hand part of (2.30) represents the reflected field for the plane Neuman surface, the integral at the right-hand part of (2.30) represents the diffusive component of the scattered field. This integral converges at least in the case when the roughness disappears

at large distances, $\nabla\varsigma(\mathbf{r})\to 0$ when $|\mathbf{r}|\to 0$. This means that $S(\mathbf{q}_1,\mathbf{q}_0)\propto\alpha_1^{\,0}$ at small grazing angles. Note also that this result is not limited by the small heights assumption, but is supported by the perturbation theory results discussed earlier in this section. This conclusion was presented by Tatarskii and Charnotskii in [2,3].

Another point of view was presented by Barrick in [1]. Actually his analysis was done for a periodic surface, but we present the general case version here. If we formally let $\nu(\mathbf{q}_1)\to 0$, which means that $\mathbf{q}_1\to k\hat{\mathbf{q}}_1$, in (2.28) and (2.29) then:

$$\begin{aligned}&8\pi^2\nu_0\delta(k\hat{\mathbf{q}}_1-\mathbf{q}_0)=ik\iint d\mathbf{r}\iint d\mathbf{p}\hat{E}(\mathbf{p},\mathbf{q}_0)[k-\mathbf{p}\cdot\hat{\mathbf{q}}_1]\exp[i(\mathbf{p}-k\hat{\mathbf{q}}_1)\cdot\mathbf{r}]\varsigma(\mathbf{r})\\&=4\pi^2 ik\iint d\mathbf{p}\hat{E}(\mathbf{p},\mathbf{q}_0)[k-\mathbf{p}\cdot\hat{\mathbf{q}}_1]\hat{\varsigma}(k\hat{\mathbf{q}}_1-\mathbf{p}),\end{aligned}\tag{2.31}$$

$$\begin{aligned}&\frac{8\pi^2}{k}S(k\hat{\mathbf{q}}_1,\mathbf{q}_0)=-ik\iint d\mathbf{r}\varsigma(\mathbf{r})\iint d\mathbf{p}\hat{E}(\mathbf{p},\mathbf{q}_0)[k-\mathbf{p}\cdot\hat{\mathbf{q}}_1]\exp[i(\mathbf{p}-k\hat{\mathbf{q}}_1)\cdot\mathbf{r}]\\&=-4\pi^2 i\iint d\mathbf{p}\hat{E}(\mathbf{p},\mathbf{q}_0)[k^2-\mathbf{p}\cdot\mathbf{q}_1]\hat{\varsigma}(k\hat{\mathbf{q}}_1-\mathbf{p}).\end{aligned}\tag{2.32}$$

From (2.31) and (2.32) it is obvious that

$$S(k\hat{\mathbf{q}}_1,\mathbf{q}_0)=-k\nu_0\delta(k\hat{\mathbf{q}}_1-\mathbf{q}_0).\tag{2.33}$$

This means that at small observation angles the Neuman rough surface behaves as a plane with the Dirichlet boundary condition. This mimics the result obtained by Barrick in [1] for a periodic surface. This conclusion is also supported by the theoretical results of Bass and Fuks [4] for an average field above a statistically rough surface. We did not even need to solve for $\hat{E}(\mathbf{p},\mathbf{q}_0)$ to come to the conclusion (2.33). However, this solution implies that the integral at the right-hand parts of (2.31) and (2.32) converge, and the surface field satisfies the equation:

$$\iint d\mathbf{p}'\hat{E}(k\hat{\mathbf{q}}-\mathbf{p}',\mathbf{q}_0)(\mathbf{p}'\cdot\hat{\mathbf{q}})\hat{\varsigma}(\mathbf{p}')=-2i\frac{\nu_0}{k}\delta(k\hat{\mathbf{q}}-\mathbf{q}_0).\tag{2.34}$$

It is difficult to make any conclusions regarding the existence of a solution for this equation; however, it is quite obvious that this equation does not have a solution in the conventional perturbation sense (2.15).

From (2.24) it follows that for the Neuman problem and $\mathbf{q}_1\to k\hat{\mathbf{q}}_1$ we formally have:

$$S(k\hat{\mathbf{q}}_1,\mathbf{q}_0)=-k\nu_0\delta(k\hat{\mathbf{q}}_1-\mathbf{q}_0)+\frac{\nu_1 k}{4\pi^2}\iint d\mathbf{r}E(\mathbf{r},\mathbf{q}_0)\exp(-ik\hat{\mathbf{q}}_1\cdot\mathbf{r})\left[1+ik\hat{\mathbf{q}}_1\cdot\nabla\varsigma(\mathbf{r})\varsigma(\mathbf{r})\right].\tag{2.35}$$

Since according to (2.33) the first term at the right-hand part of (2.35) represents the reflected field, the second component is the diffusive scattered field and at small scattering angles we have $S(\mathbf{q}_1,\mathbf{q}_0)\propto\alpha_1^{\,1}$. This conclusion is based on the assumption that the integral at the right-hand part of (2.35) converges. It is not possible to check this assumption for the general case, but

if one uses the CP result (2.19) for the surface field it is easy to find that the integral diverges at least in the term-by-term sense. This is not surprising, of course, since the -1 reflection coefficient and $S(\mathbf{q}_1,\mathbf{q}_0)\propto\alpha_1^{\,1}$ are in clear contradiction to the CP result (2.20).

It is instructive to note that although both derivations start from the exact integral equations (2.5) and (2.6), Tatarskii/Charnotskii's arguments rely to some extent on the CP results, but Barrick's analysis uses equation (2.34), which does not have a CP solution. This gives a hint that the CP solution needs to be examined more accurately for a small grazing angle case. The rest of the paper is devoted to the resolution of this contradiction. We limit our discussion to the case of a one-dimensional periodic surface from this point on, but we will address the possible consequences of this restricted approach at the end of the paper.

The Dirichlet and finite-impedance scattering problems do not carry this type of controversy with them since both Tatarskii/Charnotskii and Barrick analyses result in the same $O\left(\alpha_1^{\,1}\right)$ dependence at the small grazing angles. Therefore, the following discussion is concentrated on the Neuman problem.

3. ONE-DIMENSIONAL PERIODIC SURFACE

In this chapter we introduce the necessary formalism for scattering from a periodic one-dimensional surface.

3.1 One-Dimensional Roughness

Consider a surface with 1-D roughness:

$$\varsigma(\mathbf{r})=\varsigma(x,y)=\eta(x). \tag{3.1}$$

In this case the total surface field has the form: $E(\mathbf{r},\mathbf{q}_0)\equiv E\left(x,y,q_{0_x},q_{0_y}\right)=E\left(x,q_{0_x}\right)\exp\left(iyq_{0_y}\right)$, and from (2.6) it follows that

$$S(\mathbf{q},\mathbf{q}_0)\equiv S\left(q_x,q_y,q_{0_x},q_{0_y}\right)=kT\left(q_x,q_{0_x}\right)\delta\left(q_y-q_{0_y}\right). \tag{3.2}$$

Instead of (2.4) the scattered field is presented as:

$$E_{SC}(\mathbf{r},z,\mathbf{q}_0)=\exp\left(iq_{0_y}y\right)\int\frac{dq_x}{\nu(q_x)}T\left(q_x,q_{0_x}\right)\exp\left[iq_xx+i\nu(q_x)z\right]. \tag{3.3}$$

Our principal equations (2.5) and (2.6) can be simplified to:

$$\int dxE(x,q_0)\left[\nu(q)+q\eta'(x)+kZ\sqrt{1+\left|\eta'(x)\right|^2}\right]\exp\left[-iqx+i\nu(q)\eta(x)\right]=4\pi\nu_0\delta(q-q_0), \tag{3.4}$$

$$\int dxE(x,q_0)\left[\nu(q)-q\eta'(x)-kZ\sqrt{1+\left|\eta'(x)\right|^2}\right]\exp\left[-iqx-i\nu(q)\eta(x)\right]=4\pi T(q,q_0), \tag{3.5}$$

where we dropped subscript $_x$ for brevity.

Integral equations (2.10) and (2.11) can be simplified as follows

$$\int dx \int dp \hat{E}(p,q_0)\left[\frac{k^2 - pq}{\nu(q)} + kZ\sqrt{1+|\eta'(x)|^2}\right]\exp\left[i(p-q)x + i\nu(q)\eta(x)\right] = 4\pi\nu_0\delta(q-q_0), \tag{3.6}$$

$$\int dx \int dp \hat{E}(p,q_0)\left[\frac{k^2 - pq}{\nu(q)} - ikZ\sqrt{1+|\eta'(x)|^2}\right]\exp\left[i(p-q)x - i\nu(q)\eta(x)\right] = 4\pi T(q,q_0). \tag{3.7}$$

3.2 Periodic Surface

Consider now a periodic surface with period L :

$$\eta(x+L) = \eta(x). \tag{3.8}$$

In this case Fourier transform of the height function has the form:

$$\hat{\eta}(p) = \sum_{n=-\infty}^{\infty} \eta_n \delta(p - n\kappa), \tag{3.9}$$

where $\kappa = \frac{2\pi}{L}$.

The surface field is pseudoperiodic, meaning that:

$$\hat{E}(q,q_0) = \sum_{n=-\infty}^{\infty} e_n \delta(q - q_0 - n\kappa). \tag{3.10}$$

The scattering amplitude for the periodic surface has the form:

$$T(q,q_0) = \sum_{m=-\infty}^{\infty} T_m(q_0)\nu_m \delta(q - q_m), \tag{3.11}$$

where $q_m = q_0 + m\kappa$, are the horizontal components of the wave vectors of diffraction orders, and $\nu_m = \nu(q_m)$. This definition of the discrete scattering amplitudes allows us to present the scattered field above the highest point of the surface as a sum of plane waves:

$$E_{sc}(x,z,q_0) = \sum_{m=-\infty}^{\infty} T_m(q_0)\exp(iq_m x + i\nu_m z). \tag{3.12}$$

Integral equations (3.6) and (3.7) can now be transformed to linear algebraic form

$$2\nu_0\delta_{m,0} = e_m(q_0)(\nu_m + kZ)$$
$$+\sum_{n=-\infty}^{\infty} e_n(q_0)\left[i\left(k^2 - q_m q_n + kZ\nu_m\right)p_{m-n}(\nu_m) + kZr_{m-n} + ikZ\nu_m \sum_{l=-\infty}^{\infty} r_l p_{m-n-l}(\nu_m)\right], \tag{3.13}$$

$$2\nu_m T_m(q_0) = e_m(q_0)(\nu_m - kZ)$$
$$+\sum_{n=-\infty}^{\infty} e_n(q_0)\left[-i\left(k^2 + q_m q_n - kZ\nu_m\right)p_{m-n}(-\nu_m) - kZr_{m-n} + ikZ\nu_m \sum_{l=-\infty}^{\infty} r_l p_{m-n-l}(-\nu_m)\right]. \tag{3.14}$$

Equations (3.13) and (3.14) hold for $m = 0,\pm1,\pm2,\ldots$ We use in (3.13) and (3.14) the following Fourier series:

$$\sqrt{1+|\eta'(x)|^2} = 1 + \sum_{l=-\infty}^{\infty} r_l \exp(il\kappa x)\ , \tag{3.15}$$

and

$$\exp\left(\pm i\nu\eta(x)\right) = 1 \pm i\nu \sum_{n=-\infty}^{\infty} p_n(\pm\nu)\exp(in\kappa x)\,. \tag{3.16}$$

Note that when $\nu\eta(x) << 1$, we have

$$p_m(\pm\nu) \approx \eta_m \pm \frac{i\nu}{2}\sum_{p=-\infty}^{\infty}\eta_{m-p}\eta_p\,. \tag{3.17}$$

For the Neuman case, $Z = 0$, equations (3.13) and (3.14) reduce to:

$$2\nu_0\delta_{m,0} = e_m(q_0)\nu_m + i\sum_{n=-\infty}^{\infty} e_n(q_0)\left(k^2 - q_m q_n\right)p_{m-n}(\nu_m), \tag{3.18}$$

$$2\nu_m T_m(q_0) = e_m(q_0)\nu_m - i\sum_{n=-\infty}^{\infty} e_n(q_0)\left(k^2 - q_m q_n\right)p_{m-n}(-\nu_m)\,. \tag{3.19}$$

Similar to the rough surface case equations (2.23) and (2.24), in order to calculate the scattering amplitude when the surface field is known, instead of (3.19) one can use the difference of (3.18) and (3.19):

$$T_m(q_0) = \delta_{m,0} - \frac{i}{2\nu_m}\sum_{n=-\infty}^{\infty} e_n(q_0)\left(k^2 - q_m q_n\right)\left[p_{m-n}(\nu_m) + p_{m-n}(-\nu_m)\right], \tag{3.20}$$

or the sum of (3.18) and (3.19):

$$T_m(q_0) = -\delta_{m,0} + e_m(q_0) + \frac{i}{2\nu_m}\sum_{n=-\infty}^{\infty} e_n(q_0)\left(k^2 - q_m q_n\right)\left[p_{m-n}(\nu_m) - p_{m-n}(-\nu_m)\right]. \tag{3.21}$$

For the further development of perturbation solutions the last formula is more convenient since the sum at the right-hand part contains the terms $\left[p_{m-n}(\nu_m) - p_{m-n}(-\nu_m)\right]$ that are at least of the second order in heights as it follows from (3.17). Therefore, in most cases the first two terms at the right-hand part of (3.21) will be sufficient.

We can obtain a formal series solution for $e_m(q_0)$ by iterating equation (3.18) for the surface field and substituting the series into (3.20). The results are as follows:

$$e_m(q_0) = 2\delta_{m,0} + 2a_{m,0} + 2\sum_{n_1=-\infty}^{\infty} a_{m,n_1} a_{n_1,0} + 2\sum_{n_1,n_2=-\infty}^{\infty} a_{m,n_2} a_{n_2,n_1} a_{n_1,0} + \ldots, \tag{3.22}$$

$$T_m(q_0) = \delta_{m,0} + \left(a_{m,0} + b_{m,0}\right) + \sum_{n_1=-\infty}^{\infty}\left(a_{m,n_1} + b_{m,n_1}\right)a_{n_1,0} + \sum_{n_1,n_2=-\infty}^{\infty}\left(a_{m,n_2} + b_{m,n_2}\right)a_{n_2,n_1} a_{n_1,0} + \ldots. \tag{3.23}$$

Here, we introduced the notations:

$$a_{m,n} = \frac{\left(k^2 - q_m q_n\right)}{\nu_m} p_{m-n}(\nu_m), \quad b_{m,n} = \frac{\left(k^2 - q_m q_n\right)}{\nu_m} p_{m-n}(-\nu_m). \tag{3.24}$$

We will use these series in the next chapter to examine the validity domain of the CP series in the presence of grazing orders.

For the Dirichlet case, $Z \to \infty$, we introduce the surface sources as follows:

$$g_m(q_0) = \frac{kZ}{\nu_m}\left[e_m(q_0) + \sum_{l=-\infty}^{\infty} r_{m-l} e_l(q_0)\right], \quad m = 0, \pm 1, \pm 2, .., \tag{3.25}$$

and equations (3.13) and (3.14) reduce to

$$2\delta_{m,0} = g_m(q_0) + i\sum_{n=-\infty}^{\infty} \nu_n p_{m-n}(\nu_m) g_n(q_0), \tag{3.26}$$

$$2T_m(q_0) = -g_m(q_0) + i\sum_{n=-\infty}^{\infty} \nu_n p_{m-n}(-\nu_m) g_n(q_0). \tag{3.27}$$

Similar to (3.21) it is convenient to replace equation (3.27) by the difference of (3.27) and (3.26):

$$T_m(q_0) = \delta_{m,0} - g_m(q_0) - \frac{i}{2}\sum_{n=-\infty}^{\infty} \nu_n \left[p_{m-n}(\nu_m) - p_{m-n}(-\nu_m) \right] g_n(q_0) \tag{3.28}$$

3.3 Reciprocity and energy conservation

Reciprocity for the one-dimensional periodic surface follows from substitution of (3.11) into (2.12):

$$\frac{T_m(q_0)}{\nu(q_0)} = \left. \frac{T_m(p_0)}{\nu(p_0)} \right|_{p_0 = -q_m} \tag{3.29}$$

It is worth noting that in (3.29) we deal with two different scattering problems: a direct problem with the incidence vector q_0 and scattering vectors $q_m = q_0 + m\kappa$, and a reciprocal problem with the incidence vector $p_0 = -q_m$ and scattering vectors $p_n = p_0 + n\kappa$. These two sets of modes are different in general for the arbitrary q_0.

Energy conservation follows from (2.14) and (3.2), (3.11):

$$\sum_{\text{Prop}} \left| T_m(q_0) \right|^2 \nu_m = \nu_0 . \tag{3.30}$$

Here the sum is over of the propagating modes only. This equation merely means that the power inflow across the plane $z = const$ above the surface from the incident wave is equal to the power outflow through the same plane carried by the scattered waves.

Also from (2.14) and (3.2), (3.11) we have:

$$\sum_{\text{Prop}(n)} T_m(q_0) T^*_{m+n}(q_{-n}) \nu_m = 0. \tag{3.31}$$

Integer parameter n is restricted so that $-n$ is a propagating order. The sum here is over all m such that m and $m+n$ are propagating orders. Equation (3.31) means that in the case when the surface is illuminated from the two directions simultaneously, the interference of the scattered fields causes no changes in the power outflow across the plane $z = const$.

4. CONVENTIONAL PERTURBATION SOLUTION FOR A PERIODIC SURFACE

4.1 General Discussion

We start with the CP series for the surface fields and scattering amplitudes:

$$e_m(q_0)=e_m^{(0)}(q_0)+e_m^{(1)}(q_0)+..,\ T_m(q_0)=T_m^{(0)}(q_0)+T_m^{(1)}(q_0)+.., \tag{4.1}$$

where $^{(n)}$-th term is $O\left(k^n\eta^n\right)$. From (3.13) and (3.14), and using (3.16) and the fact that $r_l=O\left(\kappa^2\eta^2\right)$, in the zero and first-order in $k\eta$ we have:

$$e_m(q_0)=\frac{2\nu_0}{(\nu_0+kZ)}\delta_{m,0}-\frac{2i\nu_0\left(k^2-q_mq_0+kZ\nu_m\right)}{(\nu_0+kZ)(\nu_m+kZ)}\eta_m, \tag{4.2}$$

$$T_m(q_0)=\frac{(\nu_0-kZ)}{(\nu_0+kZ)}\delta_{m,0}-\frac{2i\nu_0\left[k^2-q_mq_0-k^2Z^2\right]}{(\nu_0+kZ)(\nu_m+kZ)}\eta_m. \tag{4.3}$$

After accounting for the difference in definitions of scattering amplitudes, these are exactly the rough surface perturbation results (2.17) and (2.21), when $\hat{\varsigma}(\mathbf{p})$ is replaced by (3.1) and (3.9).

For the Neuman case we have (first three orders):

$$\begin{aligned}e_m(q_0)&=2\delta_{m,0}-2i\frac{\left(k^2-q_mq_0\right)}{\nu_m}\eta_m\\&+\sum_{p=-\infty}^{\infty}\eta_{m-p}\eta_p\left[\left(k^2-q_mq_0\right)-2\frac{\left(k^2-q_mq_p\right)\left(k^2-q_pq_0\right)}{\nu_m\nu_p}\right],\end{aligned} \tag{4.4}$$

$$T_m(q_0)=\delta_{m,0}-2i\frac{\left(k^2-q_mq_0\right)}{\nu_m}\eta_m-2\sum_{p=-\infty}^{\infty}\eta_{m-p}\eta_p\frac{\left(k^2-q_mq_p\right)\left(k^2-q_pq_0\right)}{\nu_p\nu_m}. \tag{4.5}$$

These formulas can be derived directly from the rough surface perturbation result (2.20) and (2.22) when Fourier transform of the heights is given by (3.9). The leading terms of (4.4) can also be obtained from the exact set of equations (3.18) if we assume that $k\eta<<1$, and $|e_0|>>|e_m|$. In this case (3.18) can be simplified to:

$$\begin{cases}e_0(q_0)\nu_0=2\nu_0\\e_m(q_0)\nu_m+ie_0(q_0)\left(k^2-q_mq_0\right)\eta_m=0\end{cases}. \tag{4.6}$$

The solution of (4.6) readily provides the first two terms at the right-hand part of (4.4). The higher-order terms can be obtained under the same assumptions if one keeps higher-order terms when approximating equation (3.18).

It is well known that changes of the d.c. component of the height function η_0 affect the scattering amplitudes in a very simple a priory known way. Namely:

$$T_m(q_0)\big|_{\eta_0} = T_m(q_0)\big|_{\eta_0=0} \exp\left[-i(\nu_m + \nu_0)\right].$$

Unfortunately, the perturbation theory fails to take advantage of this fundamental property of the scattering amplitude, and enters formula (4.5) the same way as all the other components η_m. In particular it creates the linear in heights term for the specular reflection coefficient $T_0(q_0)$. We will overcome this drawback of the perturbation theory in the following discussion by assuming that $\eta_0 = 0$. Of course this can always be accomplished by the proper choice of the coordinate origin.

If we keep the first three terms of (4.5) for $T_0(q_0)$ and the first leading term for the other $T_m(q_0)$, then the energy conservation principle (3.30) is obeyed with accuracy up to the $O(k^2\eta^2)$. The graph of Figure 4.1 presents the comparison of the CP results calculated with this accuracy (dashed curves) to the numerical solution of equations (3.18) and (3.21) (solid curves) for a wide range of incidence angles. The details of the numerical solution are presented in Appendix B.

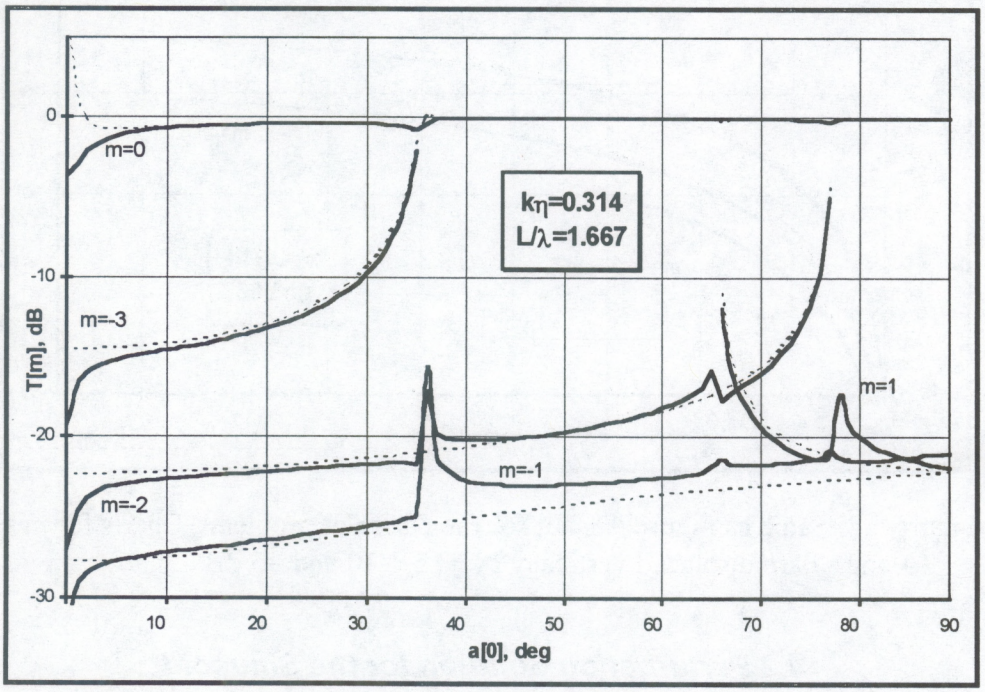

Figure 4.1. Comparison of the numerical and the first-order CP results.

The low-grazing angle modes appear at grazing incidence angles of $\alpha_0 \approx 78.5^0$, $\alpha_0 \approx 66.4^0$ and $\alpha_0 \approx 36.9^0$, when the $m=-2$, $m=1$ and $m=-3$ diffraction orders are at grazing, and at $\alpha_0 = 0^0$ when the incident and specular waves are at grazing. One can see that mode magnitudes increase significantly when a certain mode approaches grazing. In the theory of diffraction gratings this effect is called Rayleigh anomalities [7]. At first glance it appears that the first-order CP provides a good approximation for the grazing order itself; however, the more detailed investigation in the following chapter finds that this is not true for very small grazing angles. It is also evident that when one mode reaches the grazing position it substantially affects the rest of the scattering spectrum. Quite naturally the first-order perturbation theory fails to reflect this coupling. The most distinct feature of the chart, however, is a complete failure of the perturbation theory at the low-grazing incident angles.

Figure 4.2 presents the same data as Figure 4.1 but for the Dirichlet problem. Unlike the Neuman case these curves are almost featureless. The accuracy of the perturbation theory is uniform across the range of the incidence angles. If the vicinities of the low-grazing angle events are excluded, the accuracy of the perturbation theory is about the same for the Neuman and Dirichlet cases.

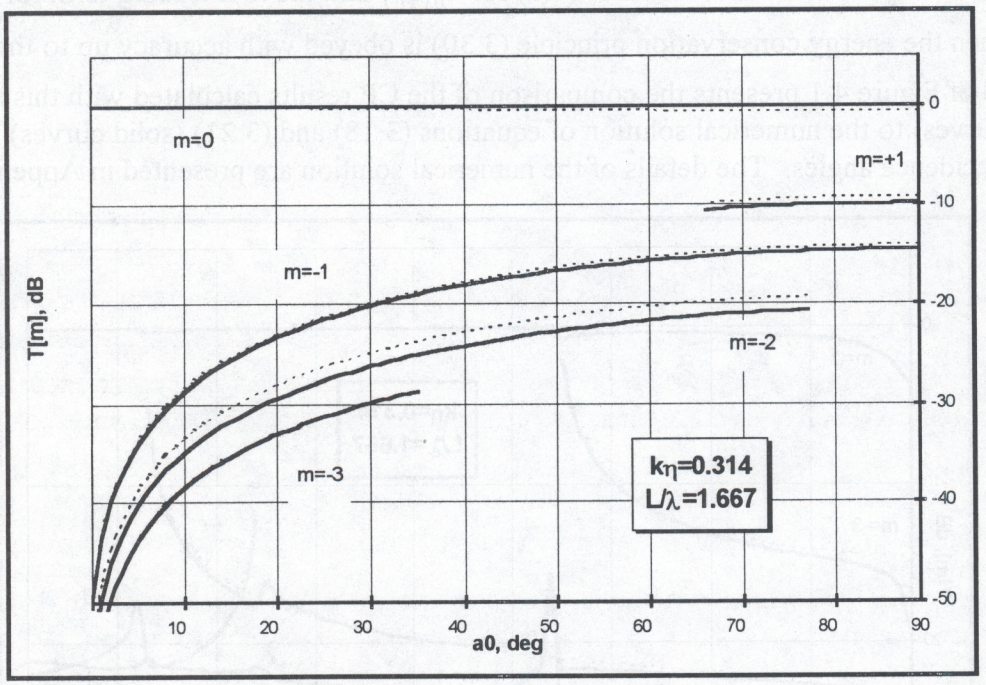

Figure 4.2. Same as Figure 4.1 but for the Dirichlet problem. Charts for m = +1, -1 and -2 are displaced vertically by +15, =10 and =5 dB.

4.2 Perturbation Solution for the Sinusoid

The sinusoidal surface profile $\eta(x) = \eta_0 \cos(\kappa x)$ is rather popular as a model for a numerical check of analytical results. In particular it was used in [1] to study the forward and back scattering at small-grazing angles. However, in our opinion this model has some undesirable features, and we avoid using it in our further discussion.

From (3.9) for the sinusoidal profile we have:

$$\hat{\eta}_m(x) = \frac{\eta_0}{2}\left(\delta_{m,1} + \delta_{m,-1}\right). \tag{4.7}$$

Using this result in (4.5) we obtain the scattering amplitude in the following form:

$$\begin{aligned} T_m(q_0) = {} & \delta_{m,0}\left\{1 - \frac{\eta_0^2}{2}\left[\frac{\left(k^2 - q_0 q_1\right)\left(k^2 - q_1 q_0\right)}{\nu_1 \nu_0} + \frac{\left(k^2 - q_0 q_{-1}\right)\left(k^2 - q_{-1} q_0\right)}{\nu_{-1} \nu_0}\right]\right\} \\ & -i\eta_0 \delta_{m,1} \frac{\left(k^2 - q_1 q_0\right)}{\nu_1} - i\eta_0 \frac{\left(k^2 - q_{-1} q_0\right)}{\nu_{-1}} \delta_{m,-1} \\ & -\frac{\eta_0^2}{2}\delta_{m,-2} \frac{\left(k^2 - q_{-2} q_{-1}\right)\left(k^2 - q_{-1} q_0\right)}{\nu_{-1} \nu_{-2}} - \frac{\eta_0^2}{2}\delta_{m,2} \frac{\left(k^2 - q_2 q_1\right)\left(k^2 - q_1 q_0\right)}{\nu_1 \nu_2} + O\left(k^3 \eta_0^3\right). \end{aligned} \tag{4.8}$$

Obviously, the first-order in η_0 terms produce only a pair of diffraction orders: +1 and -1. The second-order terms produce a triplet of the diffraction orders: +2, 0 and -2, and so on. This is impelled by the sparsity of the surface spectrum. Since we are interested in the periodic surface only as a model of the random rough surface, it is more natural to assume that the surface has the dense spectrum, and even in the first order of perturbation theory all the scattering modes are actually excited according to the formula (4.5). Therefore, we will not use the sinusoidal surface for further numerical calculations but generate surfaces with a dense spectrum.

4.3 Grazing Angle Behavior of the Conventional Perturbation Solution

In this section we examine the validity domain of the CP solution (4.5) of the Neuman problem in the presence of grazing mode(s). The Dirichlet case and the finite impedance case are not of great interest at low-grazing angles since formulas (4.2) and (4.3) are analytical at $\nu_m \to 0$. The situation is dramatically different for the Neuman case, since as it is clear from (4.4) and (4.5) the surface field and scattering amplitudes are singular when $\nu_m \to 0$.

It is clear from (4.5) and the more general series (3.23) that when no grazing modes are allowed the CP solution is valid for $k\eta << 1$. We found, however, that the presence of the additional small parameter, small grazing angle of the diffraction order, affects the validity domain of the CP solution.

Since we are concerned with the case when the number of propagating modes is not large, we typically can have only one grazing propagating mode. This case is discussed in detail in subsection 4.3.1. Under certain conditions on the radiation wavelength, grating period, and incidence angle (Littrow mounting) it is also possible that two grazing modes are present. If so, then one mode necessarily propagates in the positive direction of the x axis and the other in the negative direction. This sounds like an exotic situation, but we need to address it since it includes the important backscatter case. The two grazing modes case is discussed in detail in subsection 4.3.2.

4.3.1 Single Grazing Order

Suppose now that for certain $m = m^*$ the m^*-th diffraction order is close to grazing, i.e. we the have $\nu_{m^*} << k$. The corresponding scattering grazing angle $\alpha_{m^*} = \sin^{-1}\left(\frac{\nu_{m^*}}{k}\right) << 1$.

When the **incident wave is not grazing** it is quite clear that for $m \neq m^*$ the sum in (4.5) contains the term:

$$-2\eta_{m-m^*}\eta_{m^*}\frac{\left(k^2 - q_m q_{m^*}\right)\left(k^2 - q_{m^*}q_0\right)}{\nu_{m^*}\nu_m} = O\left(\frac{k^2\eta^2}{\alpha_{m^*}}\right). \tag{4.9}$$

It is also clear that the multiple sums corresponding to the higher orders in (3.23) contain the terms proportional to $\alpha_{m^*}^{-2}, \alpha_{m^*}^{-3}$ and so on.

For a sufficiently small grazing angle the term presented by the formula (4.9) can become larger than the second term in (4.5) which is of the order of $O(k\eta)$. This essentially ruins the original assumption of the perturbation theory that the higher-order in $k\eta$ terms are smaller than the lower-order ones. Obviously this means that the validity of the CP-I theory is restricted somehow by the presence of the grazing diffraction mode. We now need to estimate the condition under which the CP-I theory is valid. It seems natural to impose the condition that the second term in (4.5) is larger than the one given by (4.9). The results would be the inequality $\alpha_{m^*} > k\eta$. However, if we keep the (4.9) term in our CP formulas we should be concerned about the value of the neglected higher-order terms only. More detailed analysis of the higher terms of the iteration series (3.23) shows that among the terms proportional to the $\alpha_{m^*}^{-2}$ the leading one has the order $O\left(\frac{k^4\eta^4}{\alpha_{m^*}^2}\right)$, and the leading proportional to $\alpha_{m^*}^{-3}$ term is $O\left(\frac{k^6\eta^6}{\alpha_{m^*}^3}\right)$, and so on. This gives the following validity condition for the CP:

$$\alpha_{m^*} > k^2\eta^2, \tag{4.10}$$

which is a less restrictive inequality than $\alpha_{m^*} > k\eta$. Hence, it makes sense to add a simple term in the form of (4.9) to the first-order CP formulas to expand the validity domain of the result. This is illustrated by the chart in Figure 4.3, where calculated results are compared to the first-order CP and the first order CP which is corrected by the term (4.9) for $m^* = -2$, and $m = -1$ and different heights. Obviously the correction improves the accuracy of the approximation, but what is most important is that the domain where the corrected CP is accurate, but the first-order perturbation is invalid is getting wider when $k\eta \to 0$. This indicates that the CP validity domain is extended by the correction term (4.9). It is worth noting that addition of more higher-order terms would not expand the validity domain any further. The sketch of the validity domain of the CP-I approximation at the $(\alpha_{m^*}, k\eta)$ plane is presented in Figure 4.4.

For the grazing order itself, $m = m^*$, the first-order in heights term is $O\left(\frac{k\eta}{\alpha_{m^*}}\right)$. It is easy to show that the sum in (4.5) cannot produce the term proportional to the $\alpha_{m^*}^{-2}$, but the third-

order in heights sum from (3.23) contains the $O\left(\frac{k^3\eta^3}{\alpha_{m^*}^2}\right)$ term. Therefore the CP formula for the grazing order is valid under the same condition (4.10) as was derived for the non-grazing modes.

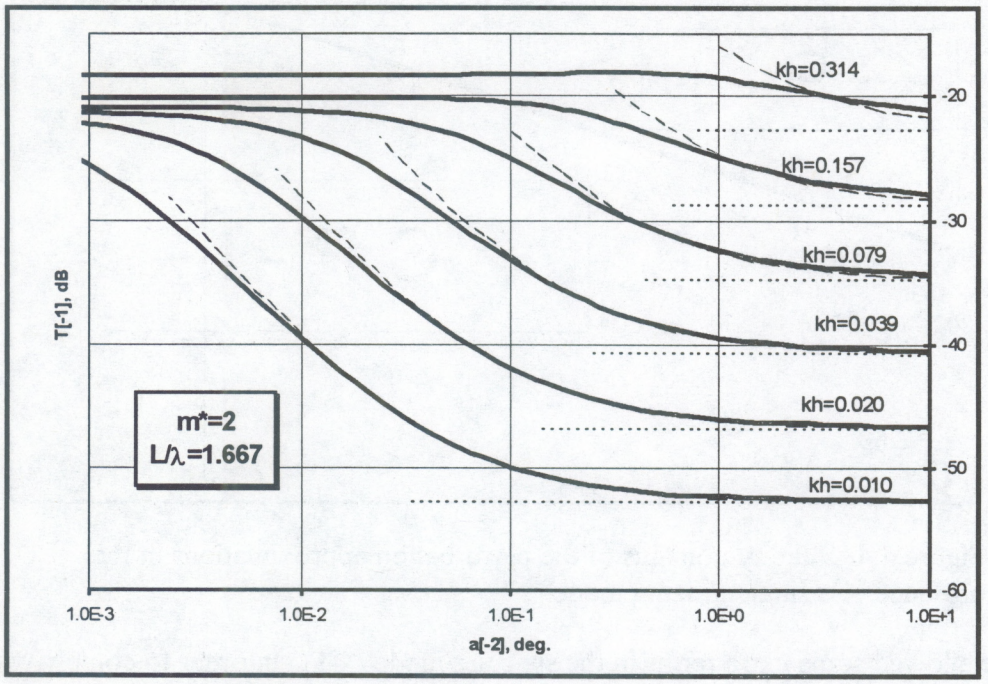

Figure 4.3. Validity domain of the perturbation theory. Heavy solid curves - calculations, dotted lines - first-order perturbation, long-dashed - term (4.9) included.

Finally, scattering amplitudes in the CP approximation can be presented in the following form:

$$T_0(q_0) = 1 - 2\sum_{n\neq 0} \frac{\left(k^2 - q_0 q_n\right)^2}{\nu_0 \nu_n} |\eta_n|^2 + O\left(\frac{k^4\eta^4}{\alpha_{m^*}^2}\right), \tag{4.11}$$

$$T_{m^*}(q_0) = -2i\eta_{m^*} \frac{\left(k^2 - q_{m^*} q_0\right)}{\nu_{m^*}} + O\left(\frac{k^3\eta^3}{\alpha_{m^*}^2}\right), \tag{4.12}$$

$$T_m(q_0) = -2i\eta_m \frac{\left(k^2 - q_m q_0\right)}{\nu_m} - 2\eta_{m-m^*}\eta_{m^*} \frac{\left(k^2 - q_m q_{m^*}\right)\left(k^2 - q_{m^*} q_0\right)}{\nu_{m^*}\nu_m} + O\left(\frac{k^4\eta^4}{\alpha_{m^*}^2}\right), \quad m \neq 0, m^*. \tag{4.13}$$

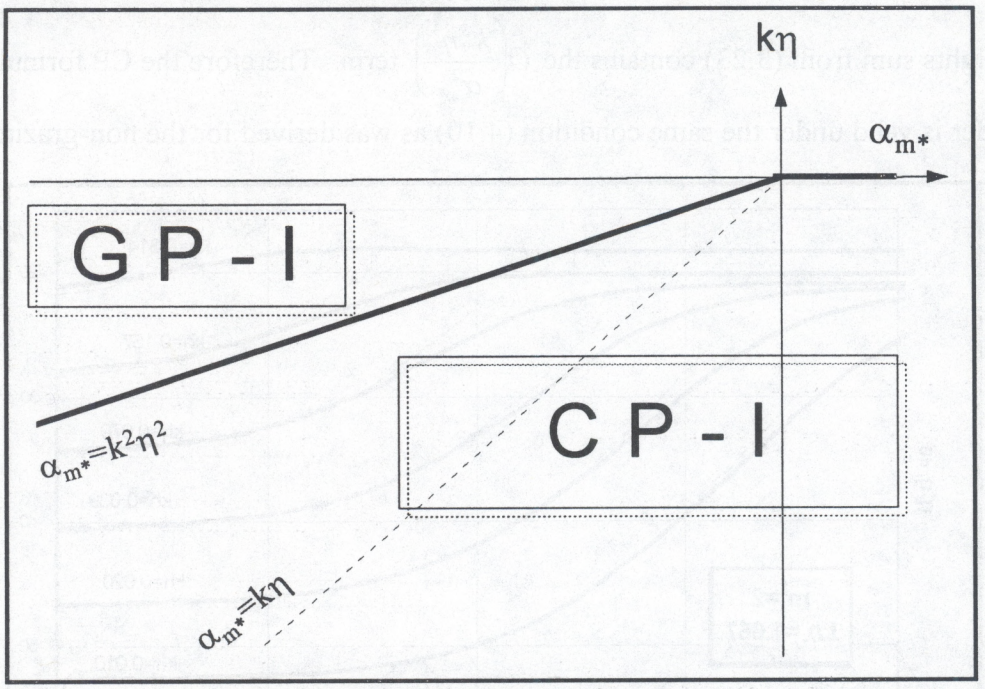

Figure 4.4. Validity domains of the perturbation approximations in the presence of a single grazing mode.

We allowed some extra terms in the specular mode (4.11) in order to comply with the energy conservation equation (3.30) when leading terms for all scattered modes are included. It is also possible of course to simply use the equation (4.5) under condition (4.10), but this formula would include many extra terms that are smaller than the accuracy of the result. Addition of the higher-order terms of the perturbation series would not expand the validity domain of these formulas given by (4.10), but probably can improve the accuracy of the result inside this domain. We will call this set of formulas CP-I to distinguish it from the CP results for the two grazing modes case which will be labeled as CP-II.

It is also interesting that near the boundary of the validity domain, when $k\eta = O\left(\sqrt{\alpha_{m*}}\right)$ we have $T_{m*}(q_0) = O\left(\frac{1}{\sqrt{\alpha_{m*}}}\right) > 1$, which means that the grazing mode can have a larger amplitude than the incident plane wave. This does not violate the energy conservation principle (3.30) however, since the energy flux across the plane $z = const$ associated with this mode $\left|T_{m*}(q_0)\right|^2 \nu_{m*}$ is bounded when $\alpha_{m*} \to 0$.

Figures 4.5 - 4.7 illustrate our development for the three occurrences of grazing modes $m* = -2$, $m* = 1$, and $m* = -3$ at incidence angles $\alpha_0 \approx 78.5^0$, $\alpha_0 \approx 66.4^0$ and $\alpha_0 \approx 36.9^0$ that were indicated in Figure 4.1. The grazing incidence case will be discussed separately. Numerical data show that all the modes including the grazing mode saturate to the finite limits when $\alpha_{m*} \to 0$. One can see that despite the visual impression of Figure 4.1, the first-order CP fails to predict the correct saturation level, but provides adequate results for the moderately small grazing angles. The CP-I results given by the formulas (4.11) - (4.13) are substantially more accurate in

the transition region between the two saturation levels for the non-grazing modes, but predict the erroneous α_{m*}^{-1} growth for the $\alpha_{m*} \to 0$.

Regarding the specular mode we note that the zero-order CP result $T_0(q_0) \approx 1$ would be quite adequate for the entire range of grazing angles due to the small heights considered. However, the inclusion of the second-order terms, which is usually justified based on energy conservation reasons, blows up the result at the same angles where the CP-I approximation for the non-specular modes becomes invalid.

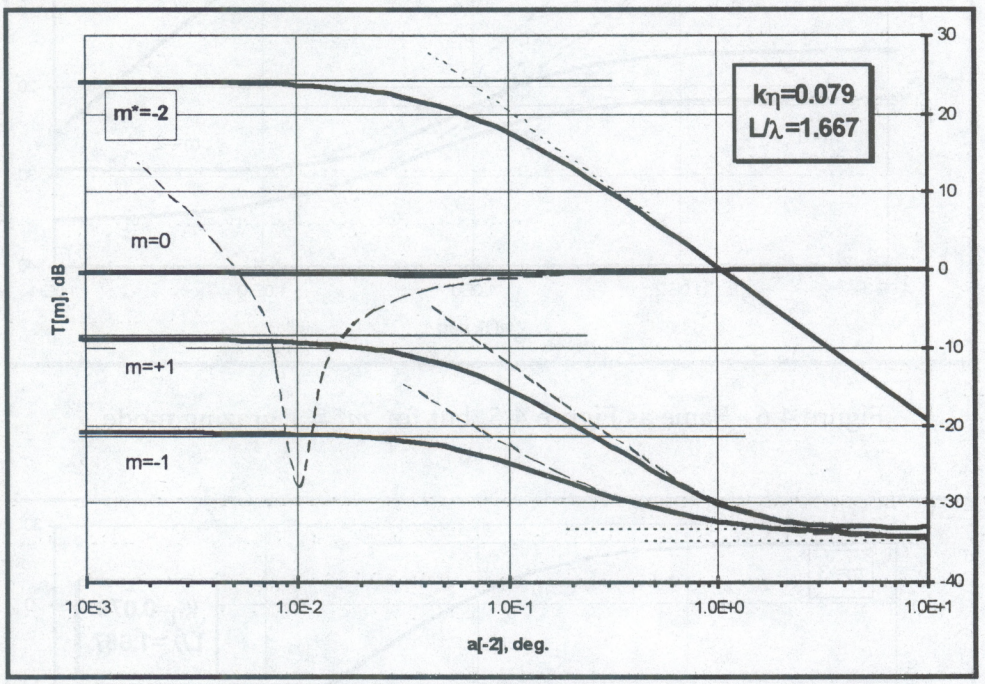

Figure 4.5. Scattering amplitudes for the $m^* = -2$ grazing mode. Heavy solid curves - calculations. Dotted lines - first-order perturbation. Dashed curves - CP-I formulas (4.11) - (4.13).

It is important to note that when $\alpha_{m*} \to 0$, but under condition (4.10), the scattering amplitude for the grazing mode $T_{m*}(q_0)$ indeed becomes larger than the scattering amplitude for all the other modes including the specular. This situation will be used in the following chapter to construct a new GP expansion.

For the grazing incidence case we have $\alpha_0 = \sin^{-1}\left(\frac{\nu_0}{k}\right) << 1$. Due to the reciprocity there is no need to analyze the non-grazing orders: the validity condition for the CP series is the same as for the non-grazing incidence and grazing scattering and is given by (4.10).

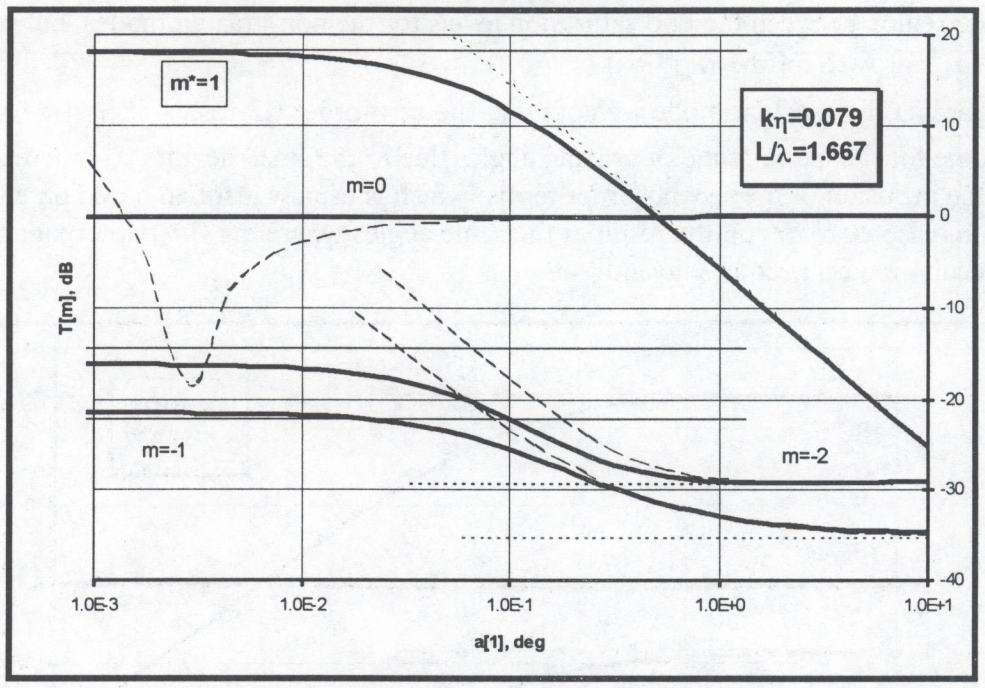

Figure 4.6. Same as Figure 4.5, but for $m^* = 1$ grazing mode.

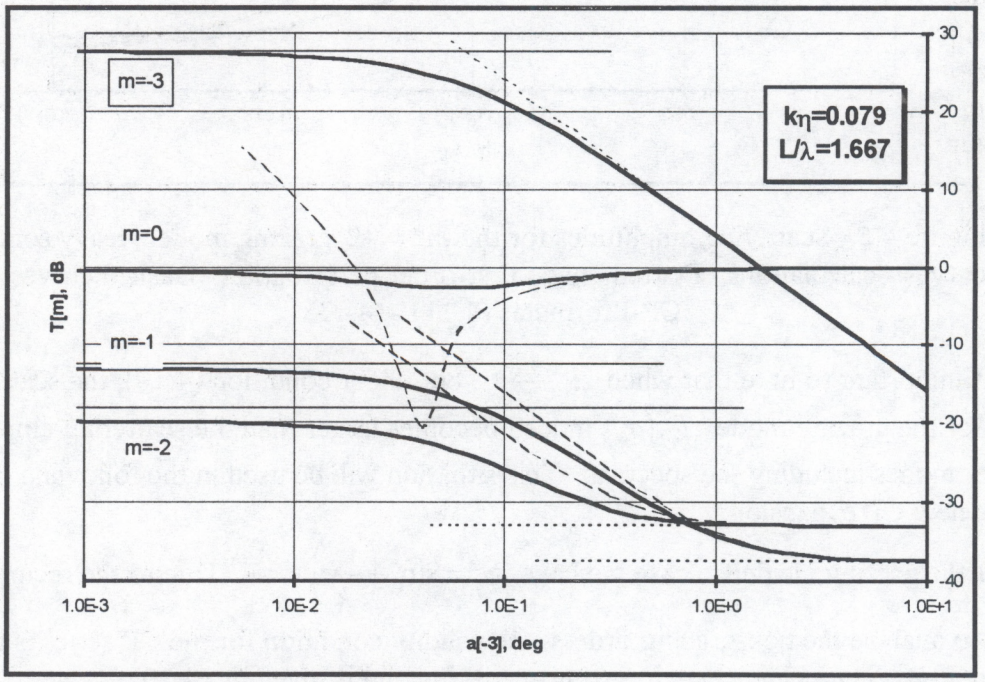

Figure 4.7. Same as Figure 4.5, but for $m^* = -3$ grazing mode.

For the specular reflection coefficient $T_0(q_0)$ the sum in (4.5) has the order $O\left(\frac{k^2\eta^2}{\alpha_0}\right)$, and it is possible to show that the term proportional to the α_0^{-2} is $O\left(\frac{k^4\eta^4}{\alpha_0^2}\right)$. This indicates that the validity condition (4.10) for the CP-I series stands for the specular reflection as well. Estimations for the higher orders support this conclusion. For the generic scattered mode the leading term is $O(k\eta)$, and the sum in (4.5) generates no terms proportional to α_0^{-1}. The lowest order in heights term that is proportional to α_0^{-1} has the order $O\left(\frac{k^3\eta^3}{\alpha_0}\right)$. This proves that the validity condition (4.10) for the CP-I series stands for the grazing incidence as a whole.

Finally the set of CP-I grazing incidence formulas that are valid under condition (4.10) with $m^* = 0$ are as follows:

$$T_0(q_0) = 1 - 2\sum_{n\neq 0} \frac{\left(k^2 - q_0 q_n\right)^2}{v_0 v_n} |\eta_n|^2 + O\left(\frac{k^4\eta^4}{\alpha_{m^*}^2}\right), \tag{4.14}$$

$$T_m(q_0) = -2i\eta_m \frac{\left(k^2 - q_m q_0\right)}{v_m} + O\left(\frac{k^3\eta^3}{\alpha_0}\right), \quad m \neq 0. \tag{4.15}$$

Note that formula (4.15) is reciprocal to (4.12) as expected.

Figure 4.8 presents the comparison of the calculation results to the CP-I formulas (4.14), (4.15). The non-specular modes here are reciprocal to the m^* modes in Figures 4.4 - 4.6, and decrease linearly with α_0 when $\alpha_0 \to 0$. The CP-I formulas provide an adequate approximation at the moderately small incidence angles in the validity domain (4.10) but fail to match this decrease for the extremely small angles.

The most interesting feature of the grazing forward scattering is revealed at the following two charts, Figures 4.9 and 4.10, where we present the quadratic components and the phase of the reflection coefficient $T_0(q_0)$ near grazing for different roughness heights. The complex reflection coefficient rotates on 180° at the complex plane and changes its value from +1 to -1. The magnitude of the reflection coefficient does not change significantly in this process, which is also clear from the charts in Figure 4.8. It is also interesting that the shapes of the curves are practically the same for the wide range of the roughness heights. One can also notice that the critical angle where the phase is 90°is $\propto (k\eta)^2$ which is consistent with our estimation (4.10).

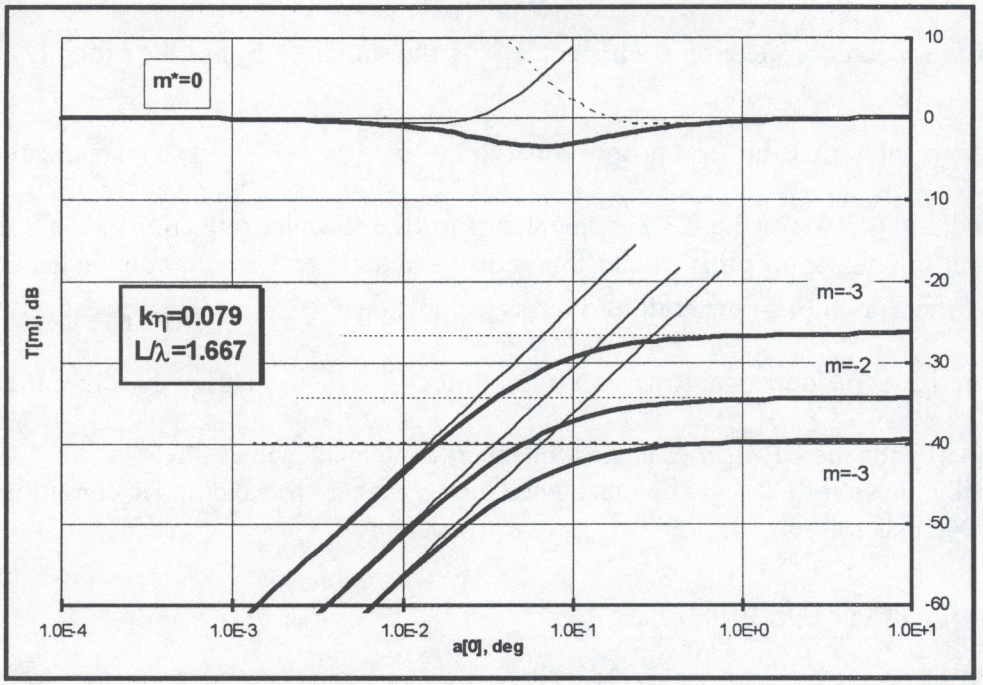

Figure 4.8. Same as Figure 4.5, but for grazing incidence, $m^* = 0$.

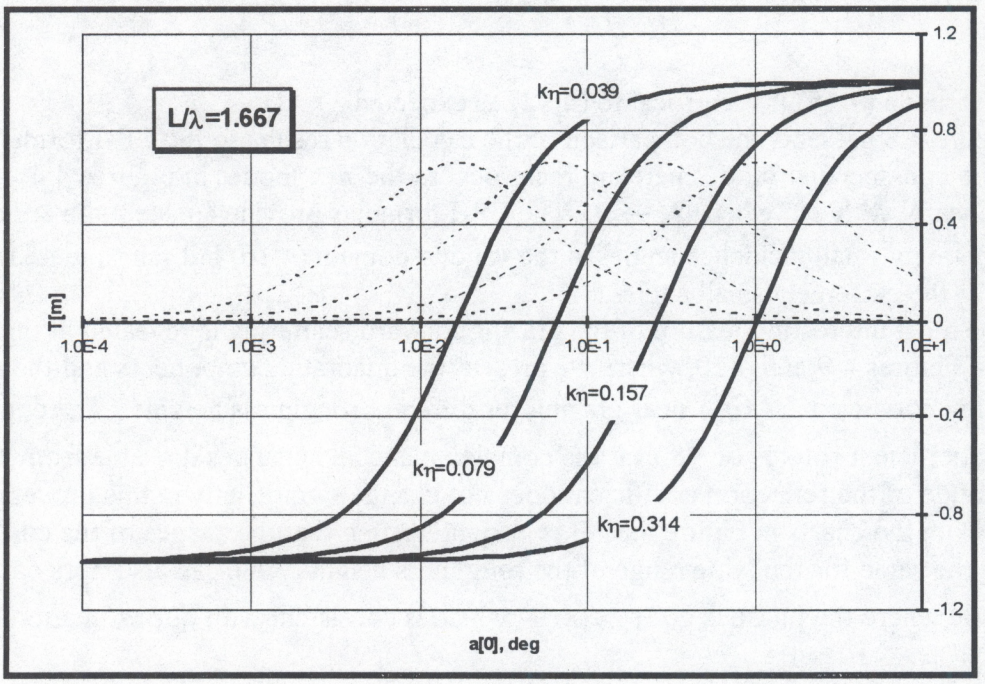

Figure 4.9. Reflection coefficient for grazing incidence, $m^* = 0$. Solid curves – real part. Dashed curves – imaginary part.

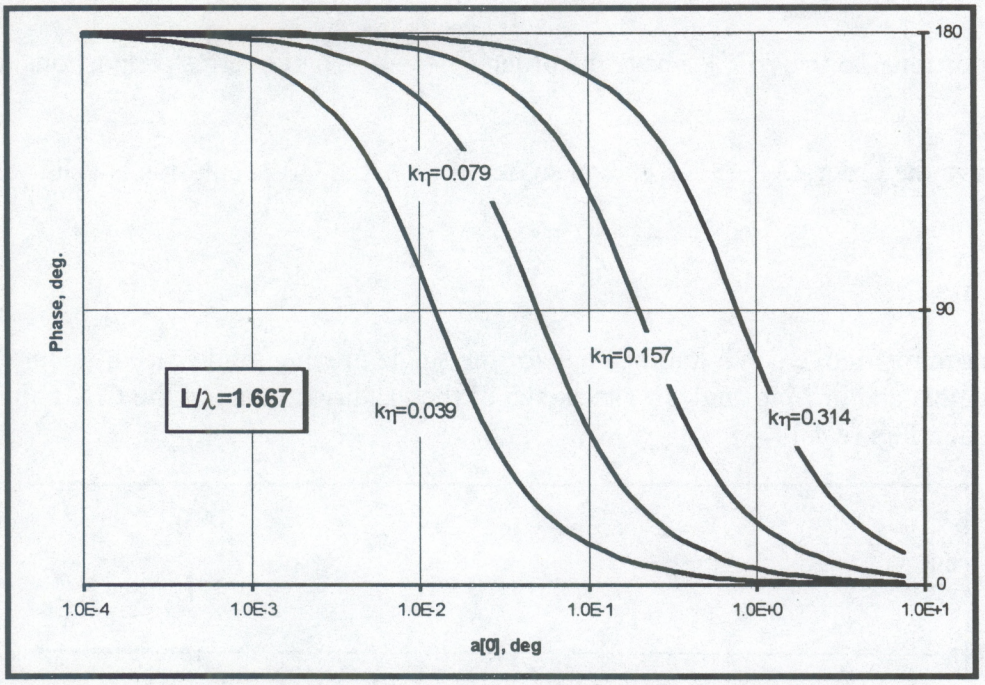

Figure 4.10. Phase of the reflection coefficient for the grazing incidence.

4.3.2 Two Grazing Orders

Consider the non-grazing incidence first. In this case there are two scattering modes that propagate at low grazing angles in the positive and negative directions of the x axis. We denote the numbers of these modes as m^+ and m^-, accordingly. We also assume here that both ν_{m+} and ν_{m-} are of the same order of magnitude, but not necessarily equal to each other. Similar to (4.9) the sum at the right hand part of (4.5) produces two terms inversely proportional to ν_{m+} and ν_{m-} which are larger than all the other terms in the sum. Therefore, the scattering amplitude for the generic mode has the following form:

$$T_m(q_0) = \delta_{m,0} - 2i\frac{\left(k^2 - q_m q_0\right)}{\nu_m}\eta_m$$
$$-2\eta_{m-m^+}\eta_{m^+}\frac{\left(k^2 - q_m q_{m^+}\right)\left(k^2 - q_{m^+} q_0\right)}{\nu_{m^+}\nu_m} - 2\eta_{m-m^-}\eta_{m^-}\frac{\left(k^2 - q_m q_{m^-}\right)\left(k^2 - q_{m^-} q_0\right)}{\nu_{m^-}\nu_m}. \quad (4.16)$$

Similar to the single grazing mode case these additional terms have the order $O\left(\frac{k^2\eta^2}{\alpha_{m^\pm}}\right)$.

However, the higher-order terms behave differently than for the single grazing mode case. The

terms proportional to the $\left(\alpha_{m^{\pm}}\right)^{-2}$ have the order $O\left(\frac{k^3\eta^3}{\alpha_{m^+}\alpha_{m^-}}\right)$, the terms proportional to the $\left(\alpha_{m^{\pm}}\right)^{-3}$ have the order $O\left(\frac{k^4\eta^4}{\alpha^2_{m^{\pm}}\alpha_{m^{\mp}}}\right)$, and so on. Hence, the CP-II solution is valid when

$$\alpha_{m^{\pm}} > k\eta. \tag{4.17}$$

This is a more restrictive condition than one for the single grazing mode case both in terms of allowed heights and grazing angles. The sketch of the validity domain of the CP-II approximation is presented in Figure 4.11.

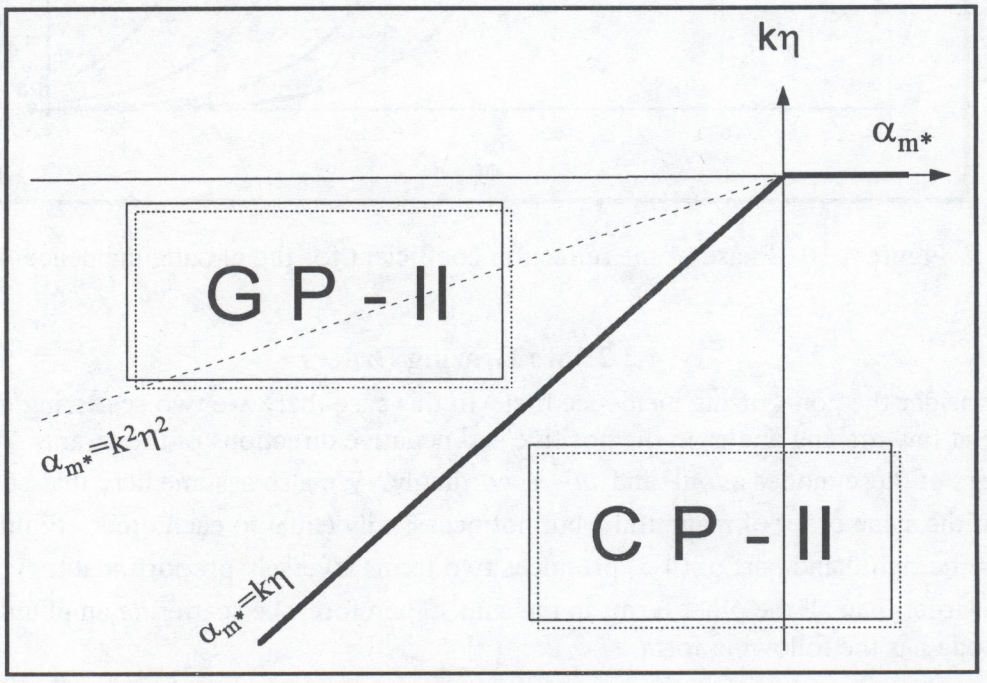

Figure 4.11. Validity domains of the perturbation approximations for two grazing modes.

For the grazing scattered mode, m^+ or m^- from (4.5) we have:

$$T_{m^{\pm}}(q_0) = -2i\frac{\left(k^2 - q_{m^{\pm}}q_0\right)}{v_{m^{\pm}}}\eta_{m^{\pm}} - 2\eta_{m^{\pm}-m^{\mp}}\eta_{m^{\mp}}\frac{\left(k^2 - q_{m^{\pm}}q_{m^{\mp}}\right)\left(k^2 - q_{m^{\mp}}q_0\right)}{v_{m^+}v_{m^-}}. \tag{4.18}$$

This formula and examination of the higher-order terms show that CP-II solution for grazing orders is valid under the same condition (4.17). Note that the second-order in heights terms in (4.16) and (4.18) are smaller than the first-order terms under condition (4.17). They do not extend the validity domain of the first-order formulas, but probably improve the accuracy of the result.

Figure 4.12 presents a comparison of the exact calculations according to (3.18) and (3.21) and the CP-II formulas (4.16) and (4.18). The grazing orders are $m^+ = 2$ and $m^- = -1$. The surface period approached $L = 1.5\lambda$ and the incidence angle was close to $\alpha_0 \approx 109^o$ in order to keep $\alpha_2 = \alpha_{-1} \to 0$. For $k\eta = 0.079$ the critical angle as given by (4.17) is about 4.5^o. This matches the range where the perturbation results are close to computation.

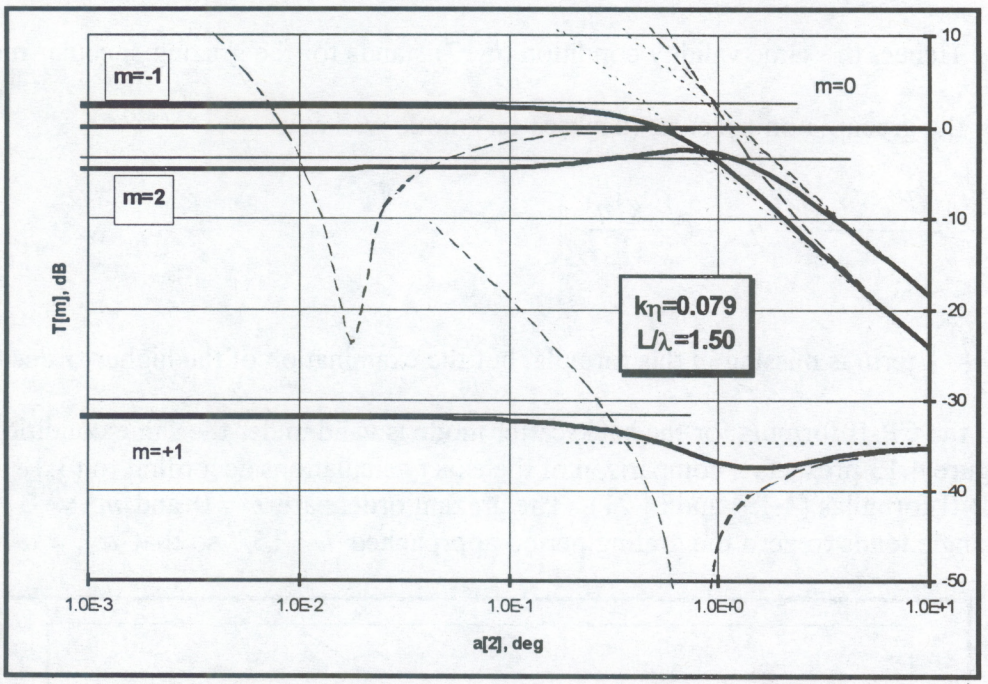

Figure 4.12. Scattering amplitudes for $m^+ = 2$, $m^- = -1$. Heavy solid curves - computations according to (3.18) and (3.21). Dotted lines – first-order perturbation results. Dashed curves – formulas (4.16) and (4.18).

For the grazing incidence we will keep the number $m = 0$ for the grazing specular order and use the notation $m = m^*$ for the second, non-specular grazing order. Once again reciprocity allows us to avoid the examination of the non-grazing scattered modes, but we still do it for the sake of convenience. The sum in the formula (4.5) will contain one large term inversely proportional to α_0. Therefore:

$$T_m(q_0) = -2i\frac{\left(k^2 - q_m q_0\right)}{v_m}\eta_m - 2\eta_{m-m^*}\eta_{m^*}\frac{\left(k^2 - q_m q_{m^*}\right)\left(k^2 - q_{m^*} q_0\right)}{v_m v_{m^*}}, \quad m \neq 0. \tag{4.19}$$

Comparison of the second term at the right-hand part of (4.19) to the first one gives the same validity condition (4.17). This is also supported by the examination of the higher-order terms.

For the grazing specular mode we have from (4.5):

$$T_0(q_0) = 1 - 2|\eta_{m^*}|^2 \frac{\left(k^2 - q_0 q_{m^*}\right)^2}{\nu_{m^*}\nu_0}. \tag{4.20}$$

This formula misses the $O\left(\frac{k\eta}{\alpha_{0,m^*}}\right)$ terms, but we found that the next term has the order $O\left(\frac{k^3\eta^3}{\alpha^3}\right)$. Hence, the same validity condition (4.17) stands for the grazing specular mode.

For the grazing non-specular (backscatter) mode we have:

$$T_{m^*}(q_0) = -2i\frac{\left(k^2 - q_{m^*}q_0\right)}{\nu_{m^*}}\eta_{m^*} + O\left(\frac{k^3\eta^3}{\alpha_{m^*}^2\alpha_0}\right). \tag{4.21}$$

The $O\left(\frac{k^2\eta^2}{\alpha^2}\right)$ term is missing in this formula, but the examination of the higher-order terms shows that the CP-II formula for the backscatter mode is valid under the same condition (4.17).

Figure 4.13 presents a comparison of the exact calculations according to (3.18) and (3.21) and the CP-II formulas (4.19) and (4.21). The grazing orders are $m = 0$ and $m^* = -3$. When the incidence angle tends to zero the grating period approached $L = 1.5\lambda$ so that $\alpha_{-3} = \alpha_0$.

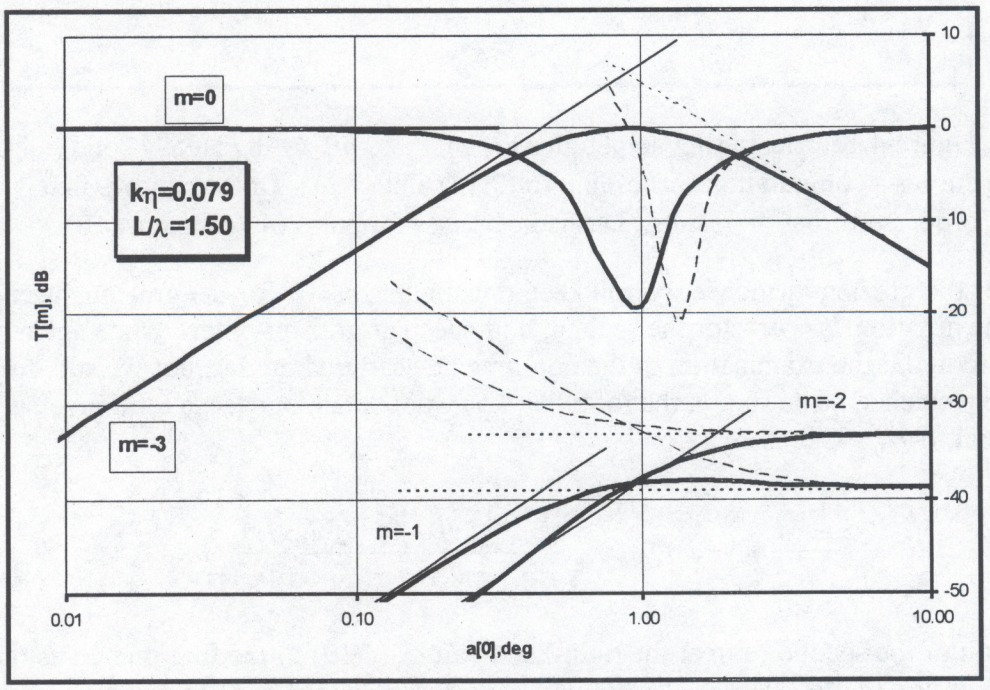

Figure 4.13. Scattering amplitudes for the grazing incidence and $m^* = -3$. Heavy curves – computations according to (3.18) and (3.21). Dotted lines – first-order perturbation results. Dashed lines - CP-II formulas (4.19) - (4.21)..

Similar to the single grazing order case the reflection coefficient for the grazing mode changes it sign from +1 at the moderately small- grazing angles to -1 when $\alpha_0 \to 0$. This is illustrated by Figure 4.14 where we present the trace of the complex $T_0(q_0)$ at the complex plane when the incidence angle changes from $\alpha_0 \approx 10^o$ to $\alpha_0 \approx 0.1^o$. Unlike the single grazing mode case discussed earlier, there is no rotation in the complex plane. It is clear from Figures 4.13 and 4.14 that the reflection coefficient almost vanishes at a grazing angle about twice the estimation (4.17), and then regains its magnitude for the smaller angles but with an opposite sign.

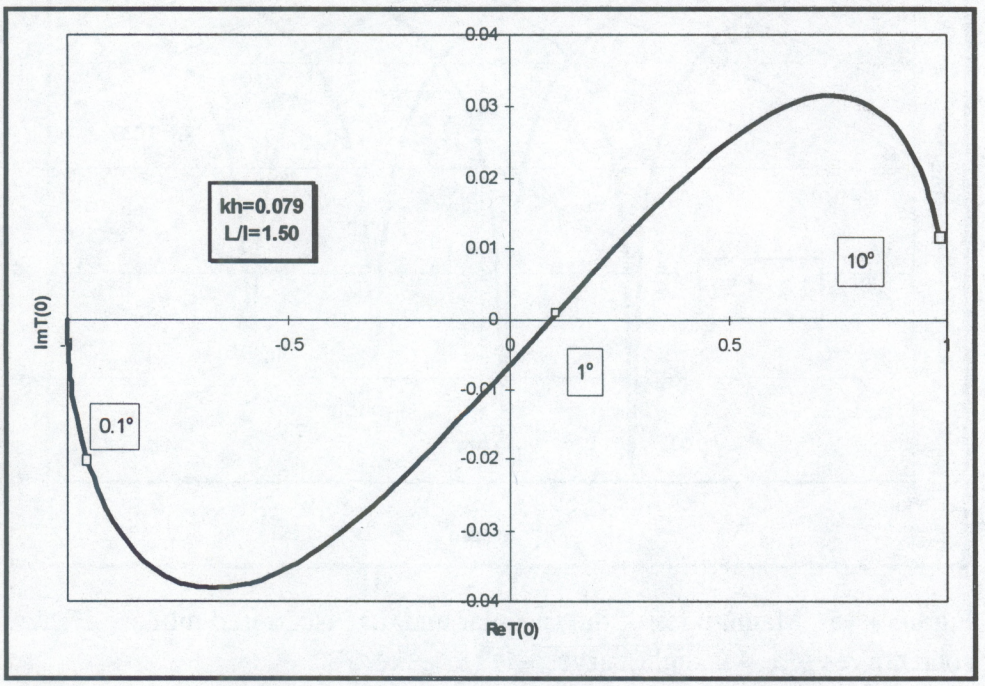

Figure 4.14. Complex reflection coefficient for the grazing incidence in the presence of the backscattered mode.

Figure 4.15 presents the magnitudes of the specular and backscattered modes for the different roughness heights. It is clear that dips of the specular amplitudes correspond to the backscatter maxima, the latest reaching the magnitude of the incident wave. The angular position of the dips is proportional to the $k\eta$ in compliance with our estimation (4.17). The width of the dips decreases for smaller heights, but their depth increases.

Finally for the two-grazing-orders case under condition (4.17) one can use the set of formulas (4.16), (4.18) - (4.21). The general formula (4.5) is also applicable under this condition.

As a conclusion of this chapter we have to stress that the presence of the single grazing mode restricts the validity of the CP formulas by the additional inequality (4.10). CP formulas are not valid in the limit $\alpha \to 0$ even for small in the wavelength scale heights. The presence of the second grazing order imposes an even more restraining requirement (4.17). Our computations presented in Figures 4.5 - 4.12 clearly indicate that there exists a distinctive domain where generic scattered orders saturate at certain levels different from the CP predictions, and the specular grazing mode amplitude changes its sign from the CP value +1 to -1. The objective of the

following two chapters is to develop new approximations that will work for small grazing angle(s) and small heights. More specifically, we are looking for a theory that would work under condition: $1 > (k\eta)^2 > \alpha_{m*}$ for the single grazing mode case, and under condition $1 > k\eta > \alpha_{m^{\pm}}$ when two grazing modes are present.

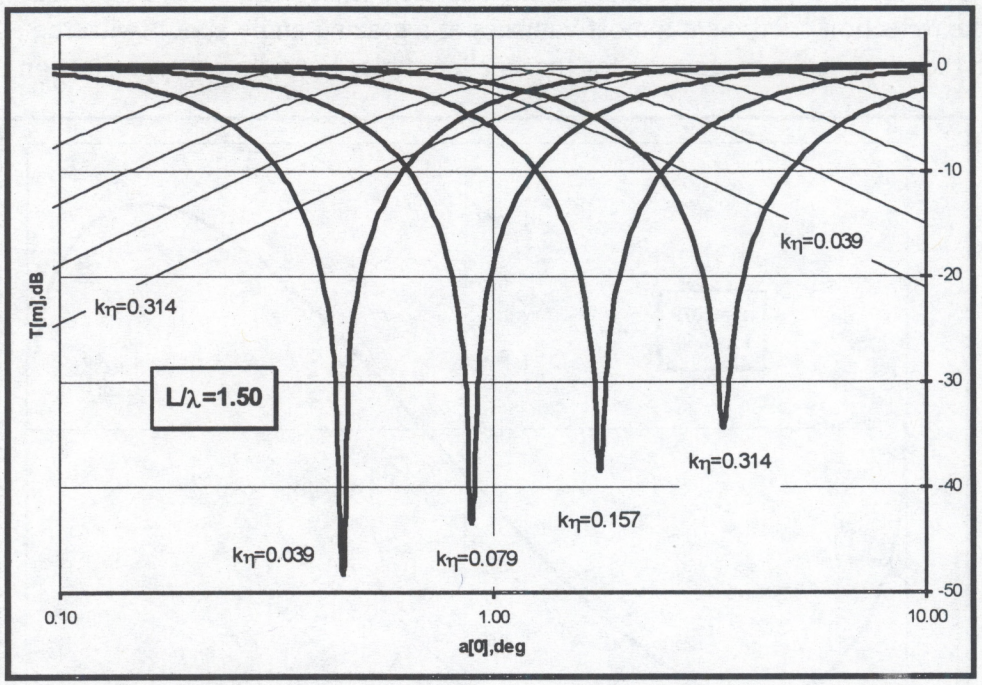

Figure 4.15. Magnitudes of the specular and backscattered modes. Heavy solid curves – $m = 0$, light curves – $m* = -3$.

5. NEW PERTURBATION EXPANSION IN THE PRESENCE OF A SINGLE GRAZING MODE: GP-I

In this chapter we introduce a new perturbation solution of the principal equations (3.18), (3.21) for the case when there is only one m^*-th diffraction order propagating at a small grazing angle. The situation when two grazing orders are present will be addressed in the next chapter. Unlike the CP theory, our development here corresponds to the right-hand part of the formula (1.1). In other words we allow $\alpha_{m^*} \to 0$ first, and after that take advantage of the fact that $k\eta < 1$. We will call this kind of perturbation expansion a GP-I expansion to indicate a presence of a single grazing mode.

We have to consider two separate cases: Non-grazing incidence when $m^* \neq 0$, discussed in Section 5.1, and the grazing incidence case when the specular order is grazing, and $m^* = 0$, is considered in Section 5.2.

5.1 Non-Specular Grazing Order

5.1.1 Failure of the Conventional Perturbation Theory

Numerical results presented in Figures 4.5 - 4.7 clearly indicate that the CP theory is invalid in the presence of a small grazing angle. The rationale for this deficiency is quite clear from equation (3.18). For the case when the m^* order is not specular, equations (3.18) for the Fourier components of the surface field have the following form:

$$\begin{cases} \nu_m e_m(q_0) - i\kappa \sum_{n=-\infty}^{\infty} e_n(q_0)\left[\kappa(m-m^*)(n-m^*) \pm k(m+n-2m^*)\right] p_{m-n}(\nu_m) \\ = 2\nu_0 \delta_{m,0}, \quad m \neq m^* \\ \pm ik\kappa \sum_{n \neq m^*} e_n(q_0)(m^*-n)\eta_{m^*-n} = 0, \quad m = m^*. \end{cases} \tag{5.1}$$

Here, we formally set $\nu_{m^*} = 0$ in (3.18), and use $q_n \approx \pm k + (n-m^*)\kappa$. We also used expansion (3.17) in the m^*-th equation of (5.1, which is actually the discrete analog of (2.34). It is important to note that the e_{m^*} does not enter the m^*-th equation of (5.1). This set of equations does not contain explicitly any small parameters related to the small grazing angle α_{m^*}. Hence, if the matrix of the system (5.1) is not singular, we should be able to obtain the leading order term of the expansion of the surface field in terms of α_{m^*} just by solving (5.1), and the solution would have a zero-order in terms of $\alpha_{m^*} \to 0$.

Consider now CP expansion for the sources in $k\eta$. If we assume that the CP expansion of the surface fields (4.1) is valid, and replace $p_{m-n}(\nu_m) \approx \eta_{m-n}$ everywhere in (5.1), then from the first set of equations in (5.1) we see that $e_n^{(0)} = 2\delta_{n,0}$, and $e_n = O(k\eta)$. This is quite similar to the CP result (4.4), of course. However, obviously this solution cannot satisfy the m^*-th equation of (5.1) since there appear to be no terms to compensate for the relatively large contribution of the $e_0^{(0)}$ to the sum at the left-hand part.

5.1.2 Surface Field

Since the CP approach is not valid for (5.1) we are forced to look for a somewhat different perturbation expansion. The equation corresponding to $m = 0$ is the only equation in the system (5.1) that has the non-zero right-hand part. The rest of the system is homogeneous, meaning that it merely propagates and redistributes the perturbation introduced in the $m = 0$ equation. For the CP-I theory the right-hand part of the $m = 0$ equation is equal to the single term $\nu_0 e_0^{(0)}(q_0)$ at the left hand part since the rest of the terms are at least of order $O(k\eta)$. This type of balance is mandated by the basic form (4.1) of the CP series, and necessarily results in the inconsistency with the m^*-th equation of (5.1) as we have already seen. The solution of this discrepancy is the acceptance that there are some other terms in the $m = 0$ equation that are responsible for the balance of the right-hand part. It is clear that these additional crucial terms should have the order $O\left[(k\eta)^{-1}\right]$. We do not actually know how many of these terms can be involved, but we recognize that if there are several of them, then the analytical solution of (5.1) is questionable. Therefore, we assume that there is only one term of the $O\left[(k\eta)^{-1}\right]$ order. The obvious candidate is the $m = m^*$, of course. Hence, finally we seek a GP-I expansion in the form:

$$e_m(q_0) = \delta_{m,m^*} e_m^{(-1)}(q_0) + e_m^{(0)}(q_0) + e_m^{(1)}(q_0) + \ldots, \tag{5.2}$$

where $e_m^{(p)}(q_0) = O\left[(k\eta)^p\right]$. This form of the new perturbation series will get a more rigorous justification later in this section when we discuss the validity domain of the GP-I expansion.

We substitute (5.2) into (5.1), use the expansion (3.17) for $p_{m-n}(\nu_m)$, and keep the leading terms in $k\eta$ to obtain the following set of homogeneous in $k\eta$ equations:

$$\begin{cases} \nu_m e_m^{(0)}(q_0) \pm ik\kappa(m^* - m)\eta_{m-m^*} e_{m^*}^{(-1)}(q_0) = 2\nu_0 \delta_{m,0}, & m \neq m^* \\ \sum_{n \neq m^*} (m^* - n)\eta_{m^*-n} e_n^{(0)}(q_0) = 0, & m = m^*. \end{cases} \tag{5.3}$$

This is a closed set of equations for $e_{m^*}^{(-1)}(q_0)$ and $e_m^{(0)}(q_0), m \neq m^*$. All terms in each equation of the set are of the same order in $k\eta$. Hence, there are no small parameters in either $k\eta$ nor α_{m^*} left in the problem, and provided that the system (5.3) is not singular, it furnishes the leading-order solution for small α_{m^*} and $k\eta$ in the sense of the right-hand part of (1.1).

In order to solve (5.3) we use the first series of equations in (5.3) to represent $e_m^{(0)}(q_0)$ for $m \neq m^*$ in terms of $e_{m^*}^{(-1)}(q_0)$, and substitute the result into the m^*-th equation. The solution for $e_{m^*}^{(-1)}(q_0)$ is then readily obtained from the m^*-th equation in the form:

$$e_{m^*}^{(-1)}(q_0) = \mp \frac{2i\kappa m^* \eta_{m^*}}{Z}, \tag{5.4}$$

where

$$Z_{EFF} = k\kappa^2 \sum_{p\neq 0} \frac{p^2}{\nu_{p+m^*}} \left|\eta_p\right|^2 = k\kappa^2 \sum_{p\neq 0} \frac{p^2}{\sqrt{2pk\kappa - p^2\kappa^2}} \left|\eta_p\right|^2, \tag{5.5}$$

is the effective impedance of the Neuman surface. The reason for this notation will become clear in Chapter 7. We only note now that $Z_{EFF} = O\left(k^2\eta^2\right)$, does not depend on m^*, direction of the incident wave, and α_{m^*}. Still Z_{EFF} is not a pure geometrical characteristic of the surface because it depends on the radiation frequency. Note also that our single-grazing-mode assumption warrants that the denominator in the sum at the right-hand part of (5.5) is non-zero. In our calculation examples for $k\eta = 0.079$ we have $Z_{EFF} = 0.00045 - 0.011i$. Pending further explanation we also introduce an effective Brewster angle related to the effective impedance in a conventional way:

$$\beta_{EFF} \equiv \sin^{-1}\left(\left|Z_{EFF}\right|\right) \approx \left|Z_{EFF}\right|. \tag{5.6}$$

Our solution (5.4) for $e_{m^*}^{(-1)}(q_0)$ has the $O\left[(k\eta)^{-1}\right]$ order, as was expected. It also is Bragg-like proportional to the η_{m^*}. This can be a problem for a grating with a sparse spectrum, e.g. for sinusoidal grating. If $\eta_{m^*} = 0$, then the scattering to the m^*-th mode is governed by multiple-scattering effects, and our approximation needs to be modified. Note also that (5.4) vanishes when $m^* = 0$, i.e. for the grazing incidence. This case requires a separate analysis, and will be presented in the next section.

The leading terms for the non-grazing orders, $m \neq m^*$, can be obtained by substitution of (5.4) into the first subset of (5.3) and have the following form:

$$e_m^{(0)}(q_0) = 2\delta_{m,0} + 2k \frac{\kappa^2 m^*(m-m^*)\eta_{m^*}\eta_{m-m^*}}{\nu_m Z_{EFF}}, \quad m \neq m^*. \tag{5.7}$$

This result has the expected $O\left[(k\eta)^0\right]$ order, and does not have the Bragg-type form. Instead it looks more like the double-scattering type [compare to the last term in (4.4)] with the first Bragg scattering into the grazing mode, and the second Bragg scattering of the grazing mode into the m-th mode.

5.1.3 Scattering Amplitudes

Similar to the small-grazing-angle expansion of (3.18) that was used to derive (5.1) we present equation (3.21) for the scattering amplitudes in the following form:

$$\begin{aligned} T_m(q_0) &= -\delta_{m,0} + e_m(q_0) \\ &- \frac{i\kappa}{2\nu_m} \sum_{n=-\infty}^{\infty} e_n(q_0)\left[\kappa(m-m^*)(n-m^*) \pm k(m+n-2m^*)\right]\left[p_{m-n}(\nu_m) - p_{m-n}(-\nu_m)\right]. \end{aligned} \tag{5.8}$$

This formula contains no small parameters associated with the small grazing angle.

We substitute (5.4) and (5.7) into (5.8) and retain the leading orders in $k\eta$ to attain:

$$T_m(q_0) \approx \delta_{m,0} + 2k \frac{\kappa^2 m^*(m-m^*)\eta_{m^*}\eta_{m-m^*}}{\nu_m Z_{EFF}}, \quad m \neq m^*. \tag{5.9}$$

$$T_{m^*}(q_0) \approx \mp \frac{2i\kappa m^* \eta_{m^*}}{Z_{EFF}}. \tag{5.10}$$

Formulas (5.9) and (5.10) are the major result for the GP-I expansion. Both formulas are nonlinear in terms of the roughness Fourier amplitudes, and predict the finite limit for the scattering amplitude at grazing. Note that the scattering amplitude for the grazing order increases when the roughness decreases. Obviously this cannot be allowed in the limit of vanishing roughness. Hence, the validity domain of our GP-I expansion should be somehow limited at the small roughness side.

We estimate the validity domain of (5.9) and (5.10) by matching these formulas to the CP-I results (4.11) - (4.13). For $m^* \neq 0$ the CP-I specular reflection coefficient is given by (4.11), and $T_0(q_0) = 1 + O\left(\frac{k^2\eta^2}{\alpha_{m^*}}\right)$. Formula (5.9) for $m = 0$ gives $T_0(q_0) = 1 + O(1)$, and there is a match at $\alpha_{m^*} = O(k^2\eta^2)$. For grazing mode equation (4.12) gives $T_{m^*}(q_0) = O\left(\frac{k\eta}{\alpha_{m^*}}\right)$, and this matches $T_{m^*}(q_0) = O\left(\frac{1}{k\eta}\right)$ at the same boundary $\alpha_{m^*} = O(k^2\eta^2)$. Finally, for the generic mode we have from (4.13) $T_m(q_0) = O(k\eta) + O\left(\frac{k^2\eta^2}{\alpha_{m^*}}\right)$, which again matches the $T_m(q_0) = O(1)$ at $\alpha_{m^*} = O(k^2\eta^2)$.

We recall the small height condition $k\eta < 1$ that was used through the development in this Section, and conclude that our GP-I formulas (5.9) and (5.10) are valid under condition

$$\alpha_{m^*} < k^2\eta^2 < 1. \tag{5.11}$$

This domain is complementary to the validity domain (4.10) of the CP-I theory. Recalling our definition of the effective Brewster angle (5.6) we can also assert that the border between the CP-I and GP-I domains is

$$\alpha_{m^*} \approx \beta_{EFF}. \tag{5.12}$$

Light solid horizontal lines at the left-hand part of the charts in Figures 4.5 - 4.7 represent the GP-I asymptotes calculated according to (5.9) and (5.10). The effective Brewster angle for all charts in Figures 4.5 - 4.7 is $\beta_{EFF} \approx 0.067^0$ which is close to the position where the CP-I and GP-I asymptotes intersect. Note that the accuracy of the GP-I asymptotes varies for the different

diffracted modes.. We discuss this issue in Section 5.3. In the next section we complete our presentation of the GP-I expansion by considering the low grazing incidence case, which has practical importance.

5.2 New Perturbation Expansion for the Low Grazing Incidence

For the low-grazing-angle incidence we have $m^* = 0$ and the specular component is at the low grazing angle. Since we assume that the number of propagating modes is not large, there are no other modes propagating at a low grazing angle.

5.2.1 Surface Field

Similar to (5.1) we set $v_0 = 0$ and $q_n \approx \pm k + \kappa n$ at the left-hand part of the exact equation (3.18) to obtain a new set of equations for the surface field:

$$\begin{cases} v_m e_m(q_0) - i\kappa \sum_{n=-\infty}^{\infty} e_n(q_0)\left[\kappa mn \pm k(m+n)\right] p_{m-n}(v_m) = 0, \quad m \neq 0 \\ \\ \mp ik\kappa \sum_{n\neq 0} e_n(q_0) n\eta_{-n} = 2v_0, \quad m = 0. \end{cases} \tag{5.13}$$

If we assume that all $e_m(q_0) \propto v_0$ then we can eliminate all small parameters associated with the small incidence angle from equations (5.13). Using reasoning quite similar to that used preceding equation (5.2) we seek the GP-I in $k\eta$ solution of (5.13) in the form:

$$e_m(q_0) = \delta_{m,0} e_m^{(-2)}(q_0) + e_m^{(-1)}(q_0) + e_m^{(0)}(q_0) + \ldots. \tag{5.14}$$

We substitute (5.14) into (5.13) and keep only the leading terms in $k\eta$ to attain the system of equation that contains no small parameters when $k\eta \to 0$:

$$\begin{cases} v_m e_m^{(-1)}(q_0) \mp i\kappa k\eta_m m e_0^{(-2)}(q_0) = 0, \quad m \neq 0 \\ \\ \mp i\kappa k \sum_{n\neq 0} n\eta_{-n} e_n^{(-1)}(q_0) = 2v_0, \quad m = 0. \end{cases} \tag{5.15}$$

In order to solve (5.15) we represent $e_m^{(-1)}(q_0)$ for $m \neq m^*$ in terms of $e_0^{(-2)}(q_0)$ from the first series of equations in (5.15), and substitute the result into the m^*-th equation. The solution for $e_0^{(-2)}(q_0)$ is then readily obtained from the $m = 0$ equation of (5.15) in the form

$$e_0^{(-2)}(q_0) = \frac{2v_0}{kZ_{EFF}}. \tag{5.16}$$

The leading terms for the non-grazing orders $e_m^{(-1)}(q_0)$ can be obtained by substitution of (5.16) into the first subset of (5.15), and have the following form:

$$e_m^{(-1)}(q_0) = \pm \frac{2iv_0 m\kappa\eta_m}{v_m Z_{EFF}}, \quad m \neq 0. \tag{5.17}$$

It is worth noting that the leading terms of the surface field have lower orders in roughness heights than for the finite incidence case, and all the Fourier components of the surface field vanish as $O(\alpha_0)$, when the incidence angle approaches zero.

5.2.2 Scattering Amplitudes

When the incidence angle is small equations (3.21) for the scattering amplitude can be presented as follows:

$$T_m(q_0) = -\delta_{m,0} + e_m(q_0) - \frac{i\kappa}{2v_m} \sum_{n=-\infty}^{\infty} e_n(q_0)\left[\kappa mn \pm k(m+n)\right]\left[p_{m-n}(v_m) - p_{m-n}(-v_m)\right]. \tag{5.18}$$

We substitute (5.16) and (5.17) in (5.18) and keep the leading terms in $k\eta$ to obtain the formulas for the scattering amplitudes:

$$T_m(q_0) = \pm \frac{2iv_0 \kappa m \eta_m}{v_m Z_{EFF}}, \quad m \neq 0 \tag{5.19}$$

$$T_0(q_0) \approx -1 + \frac{2v_0}{kZ_{EFF}}. \tag{5.20}$$

GP-I asymptotes calculated using (5.19) and (5.20) are presented as thin solid light lines at the left-hand part of Figure 4.8, and appear to be a good approximation to the direct numerical solution for small incidence angles. It is clear from (5.19) and (5.20) that when $\alpha_0 \to 0$ all diffraction orders besides the specular vanish, and the amplitude for the specular order approaches -1, which is the typical value for the Dirichlet problem rather than for the Neuman problem considered here. This matches our numerical results presented in Figure 4.9. The value of the effective Brewster angle for, $\beta_{EFF} \approx 0.067^\circ$ matches the position of the minimum for the reflection coefficient $T_0(q_0)$, and the intersections of the CP-I and GP-I asymptotes in Figure 4.8. It is also easy to see from Figures 4.9 and 4.10 that the Brewster angle changes as a square of heights, as expected.

In order to determine the validity domain of new formulas we match them to the CP-I formulas (4.15) and (4.14). For the generic scattered order from (4.15) we have $T_m(q_0) = O(k\eta)$, and from (5.19) $T_m(q_0) = O\left(\frac{\alpha_0}{k\eta}\right)$. These values match at $\alpha_{m^*} \propto k^2\eta^2$. For the reflection coefficient formula (4.14) gives $T_0(q_0) = 1 + O\left(\frac{k^2\eta^2}{\alpha_0}\right)$, and from (5.20) we have

$T_0(q_0) = -1 + O\left(\frac{\alpha_0}{k^2\eta^2}\right)$. These values match at $\alpha_{m^*} \propto k^2\eta^2$ also.

Finally, this analysis together with our discussion at the end of the previous subsection show that for the case when a single grazing mode is allowed the CP-I formulas (4.11) -(4.15) and the GP-I expansion (5.9), (5.10) and (5.19), (5.20) form a complete set of asymptotes for the small roughness heights. It is also important to note that the extra, second order in heights, term should be included into the CP-I formula (4.13) in order to have only two asymptotic domains: $\alpha_{m^*} > k^2\eta^2$ and $\alpha_{m^*} < k^2\eta^2 < 1$. If only the first-order in heights terms are used in (4.13) then the intermediate asymptotic domain $k^2\eta^2 < \alpha_{m^*} < k\eta$ has to be considered.

5.3. Second-Order GP-I

Formulas (5.9), (5.10) and (5.19), (5.20) present the leading terms of the GP-I expansion. The following terms have the higher power in $k\eta$ and/or α_{m^*}. Figures 4.6 and 4.7 show that for certain modes the leading GP-I terms are not very accurate even at extremely small grazing angles. The reason for that is that the heights are not small enough. One can obtain better accuracy for the small grazing angles but for moderately small heights if the higher-order terms of the series (5.2) are used to solve (5.1). For the non-grazing incidence the result is then used in (5.8) to obtain the correction terms in the following form:

$$\Delta T_{m^*}(q_0) = \pm\frac{\kappa^2}{Z_{EFF}} \sum_{n,p\neq m^*} \frac{(n-m^*)}{\nu_n}\left[\kappa(n-m^*)(p-m^*) \pm k(2m^*-n-p)\right]\eta_{m^*-n}\eta_{n-p}e_p^{(0)}(q_0), \quad (5.21)$$

$$\Delta T_m(q_0) = \pm ik\kappa\frac{(m-m^*)}{\nu_m}\eta_{m-m^*}\Delta T_{m^*}(q_0) \pm ik\kappa\sum_{p\neq m^*}\frac{(p-m^*)}{\nu_m}\eta_{m-p}e_p^{(0)}(q_0). \quad (5.22)$$

It is clear from the Figure 5.1 that the second-order correction substantially improves the accuracy of the GP-I formulas for moderate heights. Actually we had to terminate our numerical solution of equations (3.18) and (3.21) at $k\eta = 1.57$ due to the increasing error in the energy balance. However, the GP-I solution seems to follow the correct trend.

5.4. Reciprocity of GP-I

One of the important features of the scattering problem is reciprocity. For the discrete scattering amplitudes of the scattering problem for 1-D grating, reciprocity is given by the formula (3.25). Equation (3.25) is an exact relation which is valid for arbitrary heights and incidence and/or scattering angles. It is easy to check that the conventional perturbation expansion (4.5) is reciprocal. Since our GP formulas for the scattering amplitude (5.9), (5.10), (5.19), (5.20) are essentially the rigorous expansions of the exact solution in terms of small angle and small height, we expect that reciprocity is preserved. In this section we check that this is actually true for the first-order GP-I.

If m^* is the order of the single grazing mode for the direct scattering problem then $q_{m^*} \approx \pm k$. Obviously then $p_{m-m^*} \approx \mp k$ in the general reciprocity equation (3.25), and $n^* = m - m^*$ is the order of the grazing mode for the reciprocal problem.

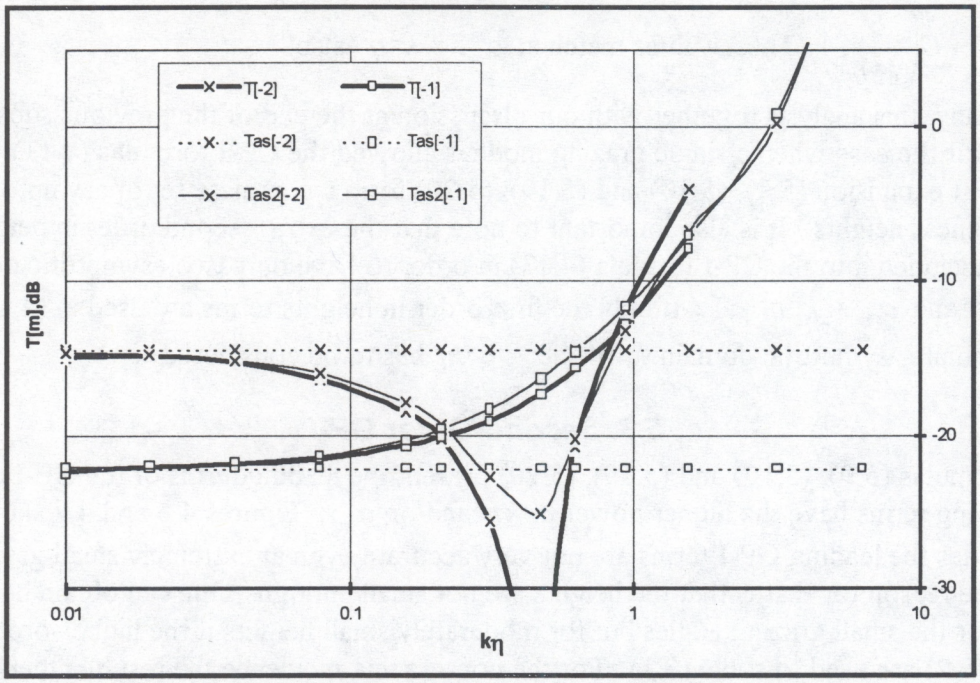

Figure 5.1. Comparison of the first and second-order GP-I results for $m^* = 1$. Heavy solid curves – numerical calculations . Dotted lines - first-order GP-I, (5.19). Light solid curves – second-order GP-I, (5.19) + (5.22).

Non-grazing incidence and scattering. When both ν_0 and ν_m are not small, we can use formula (5.9) for the scattering amplitudes at both sides of (3.25). Hence, in order to check the reciprocity we have to show that:

$$\frac{\delta_{m,0}}{\nu(q_0)} + 2\frac{m^*(m-m^*)\eta_{m^*}\eta_{m-m^*}}{\nu(q_0)\nu(q_m)\sum_{s\neq 0}\dfrac{s^2}{\nu(q_{m^*+s})}|\eta_s|^2} = \frac{\delta_{m,0}}{\nu(p_0)} + 2\frac{n^*(m-n^*)\eta_{n^*}\eta_{m-n^*}}{\nu(p_0)\nu(p_m)\sum_{s\neq 0}\dfrac{s^2}{\nu(p_{n^*+s})}|\eta_s|^2}. \tag{5.23}$$

Equality (5.23) is true since $p_0 = -q_m$, $p_m = -q_0$, $n^* = m - m^*$, $p_{n^*+s} = -q_{m-n^*-s} = -q_{m^*-s}$., and the sum in (5.23) is invariant to the transformation $s \Rightarrow -s$.

Grazing incidence and non-grazing scattering. When ν_0 is small but ν_m is not small, we have $m^* = 0$ and $n^* = m$. Formula (5.19) should be used for the scattering amplitude of the direct problem, and formula (5.10) for the reciprocal problem. Hence, we need to prove that

$$\pm\frac{2im\eta_m}{\nu(q_m)k\kappa\sum_{s=-\infty}^{\infty}\dfrac{s^2}{\nu(q_s)}|\eta_s|^2} = \pm\frac{2in^*\eta_{n^*}}{\nu(p_0)k\kappa\sum_{s=-\infty}^{\infty}\dfrac{s^2}{\nu(p_{n^*+s})}|\eta_s|^2}. \tag{5.24}$$

Since $n^* = m$, $p_0 = -q_m$, $p_{n^*+s} = -q_{m-n^*-s} = -q_{-s}$ and the sum in (5.24) is invariant to the transformation $s \Rightarrow -s$, the equality (5.24) is true.

6. NEW PERTURBATION EXPANSION IN THE PRESENCE OF THE TWO GRAZING MODES: GP-II

In this chapter we examine the case when two grazing diffraction orders are present in the spectrum of the scattered field. As we mentioned in Chapter 4, this can only happen when one grazing mode is propagating in the positive direction of the x axis and the other in the negative direction. This imposes some strict conditions on the wavelength, grating period and incidence angle but we need to address this configuration since it includes the important backscatter case. The new perturbation expansion for this configuration will be dubbed as GP-II.

We have to study two individual cases: non-grazing incidence, section 6.1, and grazing incidence, section 6.2.

6.1 Non-Grazing Incidence

Consider the case when the incident angle is not small, but there are two scattering orders that propagate at low grazing angles. As in Chapter 4, we denote the numbers of these modes as m^+ and m^-, accordingly. It is clear that for this specific case under condition $\nu_{m^+}, \nu_{m^-} << k$ we have:

$$\kappa \approx \frac{2k}{m^+ - m^-}, \quad q_m \approx k\frac{2m - m^+ - m^-}{m^+ - m^-}. \tag{6.1}$$

We do not require here that $\nu_{m^+} = \nu_{m^-}$, but assume that $\nu_{m^-} = O(\nu_{m^+})$ when $\nu_{m^+} \to 0$.

6.1.1 Surface Field

Similar to the previous two sections we let $\nu_{m^+} = \nu_{m^-} = 0$ in equations (3.18) for the scattering amplitudes and use (6.1) to obtain a set of equations that carries no small parameters related to the small scattering angles:

$$\begin{cases} \nu_m e_m(q_0) + ik^2 \sum\limits_{n=-\infty}^{\infty} e_n(q_0)\left[1 - \dfrac{(2m - m^+ - m^-)(2n - m^+ - m^-)}{(m^+ - m^-)^2}\right] p_{m-n}(\nu_m) \\ = 2\nu_0 \delta_{m,0}, \quad m \neq m^+, m^- \\ 2ik^2 \sum\limits_{n \neq m^+} e_n(q_0)\dfrac{m^+ - n}{m^+ - m^-}\eta_{m^+-n} = 0, \quad m = m^+ \\ 2ik^2 \sum\limits_{n \neq m^-} e_n(q_0)\dfrac{n - m^-}{m^+ - m^-}\eta_{m^--n} = 0, \quad m = m^-. \end{cases} \tag{6.2}$$

For $k\eta << 1$ we can show that

$$e_m(q_0)=\left(\delta_{m,0}+\delta_{m,m^+}+\delta_{m,m^-}\right)e_m^{(0)}(q_0)+e_m^{(1)}(q_0)+\ldots. \tag{6.3}$$

We substitute (6.3) into (6.2) and keep the leading terms in $k\eta$ to obtain the following system of equations for the leading orders of $e_m(q_0)$:

$$\begin{cases} \nu_0 e_0^{(0)}(q_0)=2\nu_0 \\ 2ik^2 e_0^{(0)}(q_0)\dfrac{m^+}{m^+-m^-}\eta_{m^+}+2ik^2 e_{m^-}^{(0)}(q_0)\eta_{m^+-m^-}=0, \qquad m=m^+ \\ 2ik^2 e_0^{(0)}(q_0)\dfrac{m^-}{m^+-m^-}\eta_{m^-}-2ik^2 e_{m^+}^{(0)}(q_0)\eta_{m^--m^+}=0, \qquad m=m^- \\ \nu_m e_m^{(1)}(q_0)+2ik^2 e_{m^+}^{(0)}(q_0)\dfrac{m^+-m}{m^+-m^-}\eta_{m-m^+}+2ik^2 e_{m^-}^{(0)}(q_0)\dfrac{m-m^-}{m^+-m^-}\eta_{m-m^-} \\ +ik^2 e_0^{(0)}(q_0)\left[1+\dfrac{\left(m^++m^-\right)\left(2m-m^+-m^-\right)}{\left(m^+-m^-\right)^2}\right]\eta_m=0, \qquad m\neq m^+,m^-. \end{cases} \tag{6.4}$$

The solution of (6.4) can be obtained in a straightforward manner as follows:

$$e_0^{(0)}(q_0)=2. \tag{6.5}$$

$$e_{m^+}^{(0)}(q_0)=\frac{2m^-}{m^+-m^-}\frac{\eta_{m^-}}{\eta_{m^--m^+}}. \tag{6.6}$$

$$e_{m^-}^{(0)}(q_0)=\frac{-2m^+}{m^+-m^-}\frac{\eta_{m^+}}{\eta_{m^+-m^-}}. \tag{6.7}$$

$$\begin{aligned} e_m^{(1)}(q_0)=-\frac{2ik^2}{\nu_m\left(m^+-m^-\right)^2}\Bigg\{&2m^-\left(m^+-m\right)\frac{\eta_{m^-}\eta_{m-m^+}}{\eta_{m^--m^+}} \\ &-2m^+\left(m-m^-\right)\frac{\eta_{m^+}\eta_{m-m^-}}{\eta_{m^+-m^-}}+\left[\left(m^+-m^-\right)^2+\left(m^++m^-\right)\left(2m-m^+-m^-\right)\right]\eta_m\Bigg\}. \end{aligned} \tag{6.8}$$

Equation (6.8) provides the leading orders for $m\neq m^+,m^-,0$, and the first-order correction terms for $m=m^+,m^-,0$.

6.1.2 Scattering Amplitudes

When two grazing diffraction modes are present, the equation (3.21) for the scattering amplitude can be written in a form which does not contain any small parameters associated with the small grazing angles :

$$T_m(q_0) = -\delta_{m,0} + e_m(q_0)$$
$$+\frac{i\kappa^2}{2\nu_m}\sum_{n=-\infty}^{\infty} e_n(q_0)\left[1-\frac{\left(2m-m^+-m^-\right)\left(2n-m^+-m^-\right)}{\left(m^+-m^-\right)^2}\right]\left[p_{m-n}(\nu_m)-p_{m-n}(-\nu_m)\right]. \tag{6.9}$$

Obviously, the last term at the right-hand part of (6.9) is at least of the second order in $k\eta$ when $k\eta \to 0$. Hence, in order to obtain the leading terms of the scattering amplitudes in heights, we only need to keep the first two terms at the right-hand part of (6.9) and use (6.5) - (6.8) for the surface fields. The result is:

$$T_{m^+}(q_0) = \frac{2m^-}{m^+-m^-}\frac{\eta_{m^-}}{\eta_{m^--m^+}}. \tag{6.10}$$

$$T_{m^-}(q_0) = \frac{-2m^+}{m^+-m^-}\frac{\eta_{m^+}}{\eta_{m^+-m^-}}. \tag{6.11}$$

$$T_m(q_0) = \delta_{m,0} - \frac{2ik^2}{\nu_m\left(m^+-m^-\right)^2}\left\{2m^-\left(m^+-m\right)\frac{\eta_{m^-}\eta_{m-m^+}}{\eta_{m^--m^+}}\right.$$
$$\left.-2m^+\left(m-m^-\right)\frac{\eta_{m^+}\eta_{m-m^-}}{\eta_{m^+-m^-}}+\left[\left(m^+-m^-\right)^2+\left(m^++m^-\right)\left(2m-m^+-m^-\right)\right]\eta_m\right\}, \quad m\neq 0, m^+, m^-. \tag{6.12}$$

We observe that similar to the single-grazing mode case (5.9) and (5.10) the grazing scattering amplitudes approach a finite limit when the grazing angle tends to zero. However, the presence of the second grazing mode substantially changes the dependence of the scattering amplitudes on heights. For the generic scattered mode we now have the $\propto k\eta$ dependence compared to the $\propto (k\eta)^0$ for the single-grazing mode case (5.9). The grazing modes themselves are $\propto (k\eta)^0$ instead of $\propto (k\eta)^{-1}$ as given by (5.10).

GP-II asymptotes (6.10) - (6.12) are presented as light solid horizontal lines at the left-hand part in Figure 4.12. They appear to be very accurate for the $k\eta$ value considered. It is instructive to compare the $m=+1$ mode in Figure 4.12 to the $m=-1$ mode in Figure 4.5. In both cases the numerical results show the existence of the two saturation regions for the moderate and very small values of the grazing angles with a transition regions between them. The first-order perturbation and the GP asymptotes provide a good approximation to those saturation

values in both cases. However, the transition regions behave quite differently for these two cases. For the single grazing mode our analysis in Chapter 4 and numerical data in Figure 4.3 indicate that the width of the transition region increases when $k\eta \to 0$. This makes it necessary to consider an intermediate asymptote or complement the first-order CP with the second-order terms which results in the set of formulas (4.11) - (4.13).

In the presence of two grazing modes the transition region changes its position but does not change its width significantly when $k\eta \to 0$. This is quite clear from the comparison of Figure 4.3 to Figure 6.1 which displays the magnitude of $T_{+1}(q_0)$ for different heights. The CP-II formulas (4.16) and (4.18) together with the GP-II formulas (6.10) - (6.12) form a complete set of asymptotes, but the second-order in heights terms in (4.16) and (4.18) are not mandatory. One can expect that they improve the accuracy when $1 > \alpha_{\pm} > k\eta$. However, in the vicinity of the boundary $\alpha_{\pm} \approx k\eta$ it is clear from Figure 4.12 that the higher-order terms do not improve the accuracy in general.

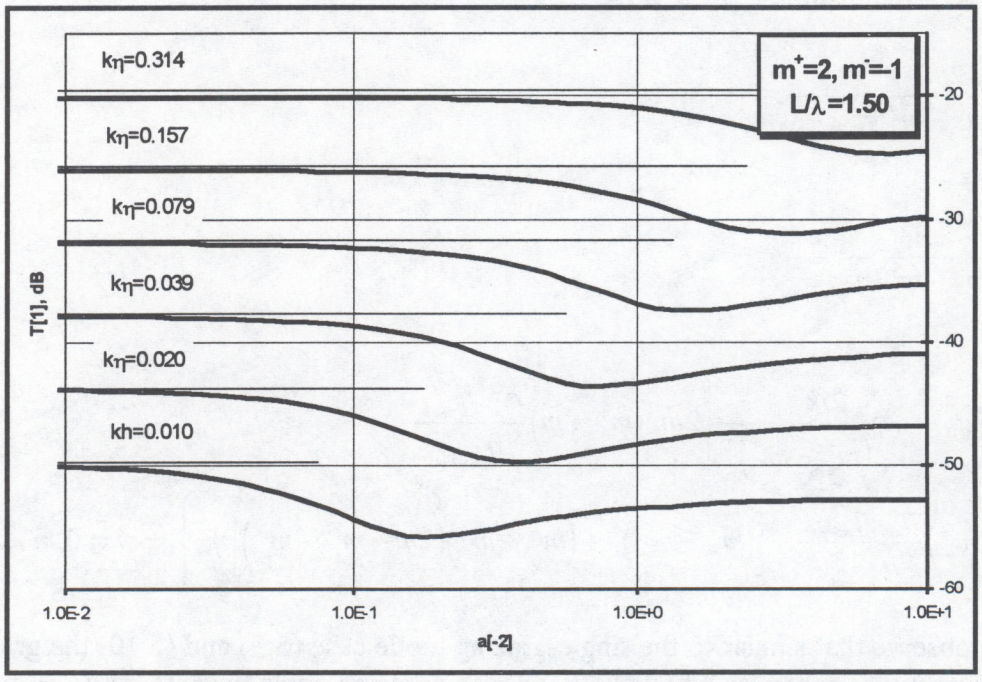

Figure 6.1. Magnitude of $T_{+1}(q_0)$ for various heights.

We complement this discussion of the validity region of the GP-II approximation by comparison to the CP-II results in Section 7.1.

6.2 GP-II Expansion for the Low-Grazing Backscatter

Consider now the case when the incidence grazing angle is small, $\nu_0 << k$, and the m^*-th diffraction orders is also at a low grazing angle: $\nu_{m^*} << k$. When the number of propagating orders $2k/\kappa$ is not large this can happen only when the m^*-th order is close to the backscatter. We do not require here that this is exactly backscatter, or $q_m = -q_0$. We assume, however, that ν_0 and ν_{m^*} are of the same order when $\nu_0 \to 0$.

6.2.1 Surface Field

For $q_0 \approx \pm k$ we have:

$$\kappa \approx \mp \frac{2k}{m^*}, \quad q_n \approx \pm k \frac{m^* - 2n}{m^*}, \tag{6.13}$$

and equation (3.18) for the surface field can be presented in the form not containing any small parameters associated with small grazing angles besides the ν_0 at the right -hand part:

$$\begin{cases} \nu_m e_m(q_0) + \dfrac{2ik^2}{m^*} \displaystyle\sum_{n=-\infty}^{\infty} e_n(q_0)\left(m+n-2\frac{mn}{m^*}\right) p_{m-n}(\nu_m) = 0, & m \neq 0, m^* \\ \dfrac{2ik^2}{m^*} \displaystyle\sum_{n\neq 0} e_n(q_0) n \eta_{-n} = 2\nu_0, & m = 0 \\ \dfrac{2ik^2}{m^*} \displaystyle\sum_{n\neq m^*} e_n(q_0)(m^*-n)\eta_{m^*-n} = 0, & m = m^*. \end{cases} \tag{6.14}$$

We now seek the GP-II solution of (6.14) in the following series form:

$$e_m(q_0) = \delta_{m,m^*} e_{m^*}^{(-1)}(q_0) + e_m^{(0)}(q_0) + e_m^{(1)}(q_0) + \ldots . \tag{6.15}$$

This form of GP-II series is justified by the fact that similar to the two previous cases, the CP series (4.1) fails to accommodate equations (6.14). We also used some trial-and-error method to determine that $e_0(q_0)$ contains no terms inversely proportional to the roughness height. Eventually all this will be justified by matching to the CP-II formulas and comparison with the numerical results.

We substitute (6.15) into (6.14) and keep the leading term in $k\eta$ to obtain the system of equations where each equations is homogeneous in terms of heights:

$$\begin{cases} 2ik^2 \eta_{-m^*} e_{m^*}^{(-1)}(q_0) = 2\nu_0, & m = 0 \\ \nu_m e_m^{(0)}(q_0) + 2ik^2 \dfrac{(m^*-m)}{m^*} \eta_{m-m^*} e_{m^*}^{(-1)}(q_0) = 0, & m \neq 0, m^* \\ \eta_{m^*} e_0(q_0) + \displaystyle\sum_{n\neq 0, m^*} e_n(q_0) \frac{(m^*-n)}{m^*} \eta_{m^*-n} = 0, & m = m^*. \end{cases} \tag{6.16}$$

Solution of (6.16) is straightforward and the result is:

$$e_m^{(0)}(q_0) = 2\frac{(m-m^*)\nu_0}{m^* \nu_m} \frac{\eta_{m-m^*}}{\eta_{-m^*}} \quad m \neq 0, m^*, \tag{6.17}$$

$$e_0^{(0)}(q_0)=\frac{2\nu_0}{(m^*)^2|\eta_{m^*}|^2}\sum_{n\neq 0,m^*}\frac{(m^*-n)^2}{\nu_n}|\eta_{m^*-n}|^2, \tag{6.18}$$

$$e_{m^*}^{(-1)}(q_0)=-\frac{i\nu_0}{k^2\eta_{-m^*}}. \tag{6.19}$$

6.2.2 Scattering Amplitudes

Quite similar to all the previous cases, the leading terms of the scattering amplitude in heights require only the first two terms at the right-hand part of equation (3.21). The results are as follows: For any non-grazing order:

$$T_m(q_0)\approx e_m^{(0)}=2\frac{(m-m^*)\nu_0}{m^*\nu_m}\frac{\eta_{m-m^*}}{\eta_{-m^*}},. \tag{6.20}$$

for the grazing specular order:

$$T_0(q_0)\approx -1+e_0^{(0)}(q_0)=-1+\frac{2\nu_0}{(m^*)^2|\eta_{m^*}|^2}\sum_{n\neq 0,m^*}\frac{(m^*-n)^2}{\nu_n}|\eta_{m^*-n}|^2, \tag{6.21}$$

and for the "backscattered" order:

$$T_{m^*}(q_0)\approx e_{m^*}^{(-1)}(q_0)=\frac{-i\nu_0}{k^2\eta_{-m^*}}. \tag{6.22}$$

Note that the second term in (6.21) is of the order $O(\alpha_0)$, and is smaller than the first one. We keep it, however, in order to comply with the energy conservation principle (3.26).

It is interesting to compare the results for the grazing incidence in the presence of the grazing scattered order (6.20) - (6.22) to our previous results for the grazing incidence when none of the scattered orders is near grazing, equations (5.19) and (5.20). Similar to that earlier case all scattering amplitudes besides the specular vanish in direct proportion to the small incidence angle, and the reflection coefficient approaches -1 when $\alpha_0\to 0$. The height dependence is rather different however: instead of the inverse height dependence for the generic diffraction order we see that the non-grazing orders are not dependent on the roughness height, but depend on the shape of the surface.

Numerical data for the GP-II asymptotes (6.20) - (6.22) are presented as light solid lines at the left-hand part of Figure 4.13. Obviously, formulas (6.20) - (6.22) are very accurate at the small grazing angles. Jointly with the first-order CP-II formulas (dotted lines), they can provide a reasonably good approximation for arbitrary angles for all orders besides specular, where they fail to predict the reflection "dip" discussed in detail at the end of Chapter 4. The incorporation of the second-order CP-II terms allows us to match some fine details of the of $T_0(q_0)$ and $T_{-1}(q_0)$, but increases the error close to the border $\alpha_\pm\approx k\eta$. The accuracy of the GP-II asymptotes for

moderate heights can be improved by including the higher-order in heights terms similar to what was done in the Section 5.3.

6.3. Reciprocity of GP-II

Since our GP-II formulas for the scattering amplitude (6.10) - (6.12), and (6.20) - (6.22) are essentially the rigorous expansions of the exact solution in terms of small angle and small height, one should expect that the reciprocity (3.29) is preserved. In this subsection we check that this is actually true.

We recall that the horizontal components of the mode wave vectors for the direct problem are given by (6.1). Since $p_n = -q_{m-n}$ we have:

$$p_n \approx k\frac{m^+ + m^- + 2(n-m)}{m^+ - m^-}. \tag{6.23}$$

It is clear from (6.23) that the orders of the grazing modes for the reciprocal problem are $n^+ = m - m^-$ and $n^- = m - m^+$.

Non-grazing incidence and scattering in the presence of two grazing modes. When both incidence and scattering directions are not grazing we can use formula (6.12) at both sides of equation (3.25), and therefore need to show that:

$$\begin{aligned}
&-\frac{2ik^2}{\nu(q_0)\nu(q_m)\left(m^+ - m^-\right)^2}\left\{2m^-\left(m^+ - m\right)\frac{\eta_{m^-}\eta_{m-m^+}}{\eta_{m^- - m^+}}\right. \\
&\left.-2m^+\left(m - m^-\right)\frac{\eta_{m^+}\eta_{m-m^-}}{\eta_{m^+ - m^-}} + \left[\left(m^{-} - m^-\right)^2 - \left(m^+ + m^-\right)\left(2m - m^+ - m^-\right)\right]\eta_m\right\} \\
&= -\frac{2ik^2}{\nu(p_0)\nu(p_m)\left(n^+ - n^-\right)^2}\left\{2n^-\left(n^+ - m\right)\frac{\eta_{n^-}\eta_{m-n^+}}{\eta_{n^- - n^+}}\right. \\
&\left.-2n^+\left(m - n^-\right)\frac{\eta_{n^+}\eta_{m-n^-}}{\eta_{n^+ - n^-}} + \left[\left(n^+ - n^-\right)^2 - \left(n^+ + n^-\right)\left(2m - n^+ - n^-\right)\right]\eta_m\right\}.
\end{aligned} \tag{6.24}$$

Substitution of $p_0 = -q_m$, $p_m = -q_0$, $n^+ = m - m^-$, and $n^- = m - m^+$ into the right-hand part of (6.24) proves that this is true.

The special case of specular scattering, $m = 0$, can be checked in a quite similar way but formula (6.10) should be used at the both sides of (3.25) instead of (6.12).

Grazing incidence and non-grazing scattering in the presence of two grazing modes. In this case we have to use formula (6.20) for the direct problem and formula (6.10) or (6.11) for the reciprocal problem. If for definitiveness we choose $q_0 = +k$ and denote m^* the order of the second (backscatter) grazing mode, then $m^+ = 0$, $m^- = m^*$. For the reciprocal problem we have to use formula (6.11) with $n^+ = m - m^*$, and $n^- = m$. Finally, we need to show that:

$$2\frac{(m-m^*)}{m^*\nu(q_m)}\frac{\eta_{m-m^*}}{\eta_{-m^*}} = -2\frac{n^+}{\nu(p_0)(n^+-n^-)}\frac{\eta_{n^+}}{\eta_{n^+-n^-}}. \tag{6.25}$$

Substitution of $p_0 = -q_m$, $n^+ = m - m^*$, and $n^- = m$. into the right-hand part of (6.25) proves that this is true.

Grazing incidence and grazing scattering. There are two cases when both incident and scattering modes are grazing: specular scattering and "backscatter." For the specular mode, $m = 0$ we use formula (6.21) at both sides of the reciprocity formula (3.25):

$$-1+\frac{2}{(m^*)^2|\eta_{m^*}|^2}\sum_{s\neq 0}\frac{(m^*-s)^2}{\nu(q_s)}|\eta_{m^*-s}|^2 = -1+\frac{2}{(n^*)^2|\eta_{n^*}|^2}\sum_{s\neq 0}\frac{(n^*-s)^2}{\nu(p_s)}|\eta_{n^*-s}|^2. \tag{6.26}$$

Since in this case $p_s = -q_{-s}$, and $n^* = -m^*$ (6.26) is true.

For the backscatter case, $m = m^*$, we use formula (6.22) at both sides of the reciprocity formula (3.25):

$$\frac{-i}{k^2\eta_{-m^*}} = \frac{-i}{k^2\eta_{-n^*}}. \tag{6.27}$$

Since in this case $n^* = m^*$, (6.27) is true.

The reciprocity relationship allows us to reduce the number of formulas that are really necessary for calculations. Instead of the complete set of GP-II formulas (6.10) - (6.12), and (6.20) - (6.22), we only need to keep seven formulas (6.12), and (6.20) - (6.22).

7. UNIFORM PERTURBATION APPROXIMATION

In this chapter we propose a more natural form of the GP approximation that uses the real physical parameters of the problem rather than the rigorous but formal presentations obtained in Chapters 5 and 6.

Based on the rigorous CP and GP expansions as starting points we develop uniform approximations that are valid for small heights and arbitrary grazing angles. These uniform approximations tend to the CP and GP results in the appropriate limits, and provide a smooth solution in the transition region between the CP and GP domains.

7.1 "Natural" Form of GP Approximations

Final results of our GP-I and GP-II approximations for scattering amplitudes are presented by the formulas (5.9), (5.10), (5.19), (5.20), (6.10) - (6.12), and (6.20) - (6.22). These formulas are essentially the exact leading terms of the series expansions of scattering amplitudes for $\alpha \to 0$ and $k\eta \to 0$ when $\alpha << k\eta$. Therefore, the dependence on the small grazing angle and heights is presented in the polynomial form in ν_{m^*} and in the rational form in η_n. We now propose the formulas that use the more "natural" parameters such as horizontal components of the wave vectors and characteristic functions of heights. These formulas do not represent the exact leading terms of the appropriate expansions. However the differences are of the same order as the higher order terms of the rigorous series which we neglect anyhow. We believe that this natural form of the solution makes it easier to link the discrete scattering amplitudes of the grating problem to the continuous scattering amplitude of the rough surface problem. There is also a general theoretical result available [5] that the heights enter the final result in the form of the characteristic function only. Therefore, we wanted to check if this can improve the accuracy of our approximations in the present context.

As before we, consider the single grazing order and two grazing order cases separately in subsections 7.1.1 and 7.1.2.

7.1.1 Single Grazing Mode

What we actually intend to do here is replace the exact (in the leading order in ν_{m^*} and $k\eta$) set of equations (5.3) by the set:

$$\begin{cases} \nu_m e_m(q_0) + i\left(k^2 - q_m q_{m^*}\right) p_{m-m^*}(\nu_m) e_{m^*}(q_0) = 2\nu_0 \delta_{m,0}, & m \neq m^* \\ i\sum\limits_{n \neq m^*} \left(k^2 - q_{m^*} q_n\right) p_{m^*-n}(\nu_{m^*}) e_m(q_0) = 0, & m = m^*. \end{cases} \tag{7.1}$$

The solution for the generic non-grazing mode can be obtained from (7.1) and the first two terms of (3.21) in the following form:

$$T_m(q_0) \approx \delta_{m,0} - \frac{2\left(k^2 - q_{m^*} q_m\right)\left(k^2 - q_{m^*} q_0\right) p_{m-m^*}(\nu_m) p_{m^*}(\nu_{m^*})}{\nu_m \sum\limits_{n \neq 0} \dfrac{\left(k^2 - q_{m^*} q_{m^*+n}\right)^2}{\nu_{m^*+n}} p_n(\nu_{m^*+n}) p_{-n}(\nu_{m^*})}. \tag{7.2}$$

This formula replaces (5.9), and can be reduced to (5.9) by setting $q_m = \pm k + \kappa(m - m^*)$ and $P_n(\nu_m) = \eta_n$. In practical calculations it can be costly to store the complex matrix $P_n(\nu_m)$. It is possible, however, to replace $P_n(\nu_m)$ by the vector η_n and use the following formula instead of (7.2) or (5.9):

$$T_m(q_0) \approx \delta_{m,0} - \frac{2\left(k^2 - q_{m^*}q_m\right)\left(k^2 - q_{m^*}q_0\right)\eta_{m-m^*}\eta_{m^*}}{k\nu_m Z_{EFF}(q_{m^*})}. \tag{7.3}$$

Here, we introduce the "natural" form of the effective impedance:

$$Z_{EFF}(q_{m^*}) \approx \sum_{n\neq 0}^{\cdot} \frac{\left(k^2 - q_{m^*}q_{m^*+n}\right)^2}{k\nu_{m^*+n}} |\eta_n|^2. \tag{7.4}$$

This form of the effective impedance depends on the incidence angle, and reduces to (5.5) when $\alpha_{m^*} \to 0$

If we match formula (7.3) to the CP-I results (4.11) and (4.13) we obtain the same validity domain (5.11) of the GP-I. Computations showed that inside the validity domain of the GP-I the difference between the (7.3) and exact asymptote (5.9) is negligible. We expected that formula (7.2) is less restricted on the $k\eta < 1$ side than (7.3). However several numerical examples revealed that this does not happen. Therefore, for further consideration we use only the (7.3) type of formulas which include the actual components of the wave vectors and the Fourier components of the heights. Essentially that means that instead of (7.1) we use the equation set

$$\begin{cases} \nu_m e_m(q_0) + i\left(k^2 - q_m q_{m^*}\right)\eta_{m-m^*} e_{m^*}(q_0) = 2\nu_0 \delta_{m,0}, & m \neq m^* \\ i\sum_{n\neq m^*}\left(k^2 - q_{m^*}q_n\right)\eta_{m^*-n} e_m(q_0) = 0. & m = m^* \end{cases} \tag{7.5}$$

For the grazing scattered mode, instead of (5.10) from (7.5) and (3.21) we have:

$$T_{m^*}(q_0) = \frac{-2i\left(k^2 - q_{m^*}q_0\right)\eta_{m^*}}{kZ_{EFF}(q_{m^*})}. \tag{7.6}$$

Matching of (7.6) to (4.12) shows that our estimation (5.11) of the validity domain of the GP-I expansion is correct for the grazing mode as well.

For the grazing incidence when no other grazing modes are allowed, we can modify equations (5.11) similar to (7.5), and instead of (5.19) we will have:

$$T_m(q_0) = \frac{-2i\nu_0\left(k^2 - q_0 q_m\right)\eta_m}{\nu_m k Z_{EFF}(q_0)} \tag{7.7}$$

for the generic scattered mode. Note that despite the modifications we made, formula (7.6) is reciprocal to (7.5). For the specular grazing mode we have

$$T_0(q_0) = -1 + \frac{2\nu_0}{kZ_{EFF}(q_0)}. \tag{7.8}$$

This formula replaces the exact asymptotic expansion (5.20).

7.1.2 Two Grazing Modes

Quite similar to the single-grazing-order case for the generic non-grazing scattered order and non-grazing incidence, instead of (6.12) we have:

$$T_m(q_0) \approx \delta_{m,0} - \frac{2i}{\nu_m}\left[\left(k^2 - q_0 q_m\right)\eta_m - \frac{\left(k^2 - q_0 q_{m^-}\right)\left(k^2 - q_m q_{m^+}\right)\eta_{m^-}\eta_{m-m^+}}{\left(k^2 - q_{m^-} q_{m^+}\right)\eta_{m^- - m^+}\left(\nu_{m^-}\right)}\right.$$
$$\left. - \frac{\left(k^2 - q_0 q_{m^+}\right)\left(k^2 - q_m q_{m^-}\right)\eta_{m^+}\eta_{m-m^-}}{\left(k^2 - q_{m^-} q_{m^+}\right)\eta_{m^+ - m^-}}\right]. \tag{7.9}$$

Matching this result to the CP-II formula (4.16) shows that at the border $\alpha_{m^\pm} = O(k\eta)$ of the validity domain (4.17) for the CP-II theory both (4.16) and (7.9) have the form $\delta_{m,0} + O(k\eta)$. This supports (4.17) and allows us to estimate the validity region for the GP-II as :

$$\alpha_{m^\pm} < k\eta < 1. \tag{7.10}$$

For the grazing scattered orders and non-grazing incidence we have instead of (6.10) and (6.11):

$$T_{m^+}(q_0) = \frac{-2\left(k^2 - q_0 q_{m^-}\right)\eta_{m^-}}{\left(k^2 - q_{m^-} q_{m^+}\right)\eta_{m^- - m^+}}, \tag{7.11}$$

$$T_{m^-}(q_0) = \frac{-2\left(k^2 - q_0 q_{m^+}\right)\eta_{m^+}}{\left(k^2 - q_{m^+} q_{m^-}\right)\eta_{m^+ - m^-}}. \tag{7.12}$$

The right-hand parts of (7.11) and (7.12) are of the order $O(1)$, but the CP-II result (4.18) is $O\left(\frac{k\eta}{\alpha_{m^\pm}}\right) + O\left(\frac{k^2\eta^2}{\alpha_{m^\pm}^2}\right)$. Obviously they match at the same border $\alpha_{m^\pm} = O(k\eta)$.

The **grazing incidence** and non-grazing scatter case (6.20) can be replaced by

$$T_m(q_0)=\frac{-2\nu_0\left(k^2-q_m q_{m^*}\right)\eta_{m-m^*}}{\nu_m\left(k^2-q_0 q_{m^*}\right)\eta_{-m^*}}. \tag{7.13}$$

This formula is reciprocal to (7.11) and (7.12).

The grazing specular order in the presence of the additional scattering grazing order instead of (6.21) is now given by

$$T_0(q_0)=-1+\frac{2\nu_0}{\left(k^2-q_0 q_{m^*}\right)^2\left|\eta_{m^*}\right|^2}\sum_{n\neq 0,m^*}\frac{\left(k^2-q_n q_{m^*}\right)^2\left|\eta_{n-m^*}\right|^2}{\nu_n}, \tag{7.14}$$

The right-hand part of this formula has the form $-1+O(1)$, and should be compared to the right-hand part of (4.20) which has the form $1+O\left(\frac{k^2\eta^2}{\alpha_m\alpha_0}\right)$. At the border $\alpha_{0,m^*}=O(k\eta)$ both formulas are $O(1)$. This supports our estimations of the validity domains for the CP-II and GP-II series, and explains the transition of the coefficient from +1 to -1 for the slightly rough surface at a small incidence angle.

For the grazing "backscatter" order we have instead of (6.22):

$$T_{m^*}(q_0)=\frac{-2i\nu_0}{\left(k^2-q_0 q_{m^*}\right)\eta_{-m^*}}. \tag{7.15}$$

The right-hand part of this formula is of the order $O\left(\frac{\alpha_0}{k\eta}\right)$, and the comparable CP-II result (4.20) is $O\left(\frac{k\eta}{\alpha_{m^*}}\right)$. They match at the border $\alpha_{0,m^*}=O(k\eta)$.

A numerical check shows that the difference between the natural and exact forms of the GP solutions is negligible in the appropriate validity domains.

7.2. Uniform Perturbation Approximations

In this section we will combine the CP solutions with the GP solutions to create a Uniform Perturbation (UP) solution, which is valid for small heights with or without the grazing order present and reduces to the CP or GP solution when applicable.

7.2.1 Single Grazing Mode: UP-I

We consider the non-grazing incidence first, and assume that only one, m^*-th, grazing mode is present, hence $\nu_{m^*}<<k$. There are two small parameters, α_{m^*} and $k\eta$, now in the basic equation set (3.18), and we intend to develop an approximation that does not use any assumptions regarding the relative value of these two parameters. In order to do this we retain in the exact equation set (3.18) the terms that have been kept in (4.6) or (7.5). The result is the following set of equations:

$$\begin{cases} \nu_0 e_0(q_0) + i\left(k^2 - q_0 q_{m^*}\right)\eta_{-m^*} e_{m^*}(q_0) = 2\nu_0, & m = 0, \\ \nu_{m^*} e_{m^*}(q_0) + i\left(k^2 - q_{m^*} q_0\right)\eta_{m^*} e_0(q_0) + i\sum\limits_{n\neq 0,m^*}\left(k^2 - q_{m^*} q_n\right)\eta_{m^*-n} e_n(q_0) = 0, & m = m^*, \\ \nu_m e_m(q_0) + i\left(k^2 - q_m q_0\right)\eta_m e_0(q_0) + i\left(k^2 - q_m q_{m^*}\right)\eta_{m-m^*} e_{m^*}(q_0) = 0, & m \neq 0, m^*. \end{cases} \tag{7.16}$$

The exact solution of this set is:

$$e_0(q_0) = \frac{2\nu_0}{\Delta}\left[\nu_{m^*} + \sum_{n\neq 0,m^*}\frac{\left(k^2 - q_{m^*} q_n\right)^2}{\nu_n}\left|\eta_{m^*-n}\right|^2\right], \tag{7.17}$$

$$e_{m^*}(q_0) = -\frac{2\nu_0}{\Delta}\left[i\left(k^2 - q_{m^*} q_0\right) + \sum_{n\neq 0,m^*}\frac{\left(k^2 - q_{m^*} q_n\right)\left(k^2 - q_n q_0\right)}{\nu_n}\eta_n \eta_{m^*-n}\right], \tag{7.18}$$

$$e_m(q_0) = -\frac{i}{\nu_m}\left[\left(k^2 - q_m q_0\right)\eta_m e_0(q_0) + \left(k^2 - q_m q_{m^*}\right)\eta_{m-m^*} e_{m^*}(q_0)\right], \tag{7.19}$$

where

$$\begin{aligned} \Delta = {} & \nu_0 \nu_{m^*} + \nu_0 \sum_{n\neq m^*}\frac{\left(k^2 - q_{m^*} q_n\right)^2}{\nu_n}\left|\eta_{m^*-n}\right|^2 \\ & -i\left(k^2 - q_{m^*} q_0\right)\eta_{-m^*}\sum_{n\neq 0,m^*}\frac{\left(k^2 - q_{m^*} q_n\right)\left(k^2 - q_n q_0\right)}{\nu_n}\eta_n \eta_{m^*-n}. \end{aligned} \tag{7.20}$$

We use these results in (3.21) to obtain formulas for scattering amplitudes. These formulas tend to correct limits when $k\eta \to 0$ or $\nu_{m^*} \to 0$ as expected. However, after close examination it becomes clear that these formulas contain some terms that can be omitted without sacrificing this asymptotic correctness. These simplified UP-I formulas have the following form:

$$T_0(q_0) = 1 - \frac{2\left(k^2 - q_{m^*} q_0\right)^2\left|\eta_{m^*}\right|^2}{\nu_0\left[\nu_{m^*} + kZ_{EFF}(q_{m^*})\right]}, \tag{7.21}$$

$$T_{m^*}(q_0) = \frac{-2i\left(k^2 - q_{m^*} q_0\right)\eta_{m^*}}{\nu_{m^*} + kZ_{EFF}(q_{m^*})}, \tag{7.22}$$

$$T_m(q_0)=\frac{-2i\nu_{m^*}\left(k^2-q_m q_0\right)\eta_m-2\left(k^2-q_{m^*}q_0\right)\left(k^2-q_{m^*}q_m\right)\eta_{m-m^*}\eta_{m^*}}{\nu_m\left[\nu_{m^*}+kZ_{EFF}\left(q_{m^*}\right)\right]},\quad m\neq 0,m^*. \tag{7.23}$$

When $k^2\eta^2<\alpha_{m^*}$ these formulas tend to the CP-I limits (4.11) - (4.13). When $k^2\eta^2>\alpha_{m^*}$ formulas (7.21) - (7.23) approach the GP-I formulas (5.9), (5.10) or their natural form (7.3) and (7.6). This further supports our estimation $\alpha_{m^*}=O\left(k^2\eta^2\right)$ of the border between the CP-I and GP-I domains. Note that formula (7.23) is self-reciprocal.

The following two charts present the comparison of the UP-I approximation (7.21) - (7.23) to numerical results, CP-I formulas (4.11) - (4.13) and GP-I formulas (7.3) and (7.6). As expected the UP-I approximation joins the CP-I and GP-I curves smoothly. The uniform approximation appears to be extremely accurate for the four decades range of grazing angles when $k\eta=0.079$, and $\beta_{EFF}\approx 0.067^\circ$. This includes the transition region $\alpha_{m^*}=O\left(k^2\eta^2\right)$ where both CP-I and GP-I are not valid. The accuracy diminishes somewhat for the larger heights as shown in Figure 7.2. This is something one should expect since this approximation is uniform in angles but still requires $k\eta$ to be small.

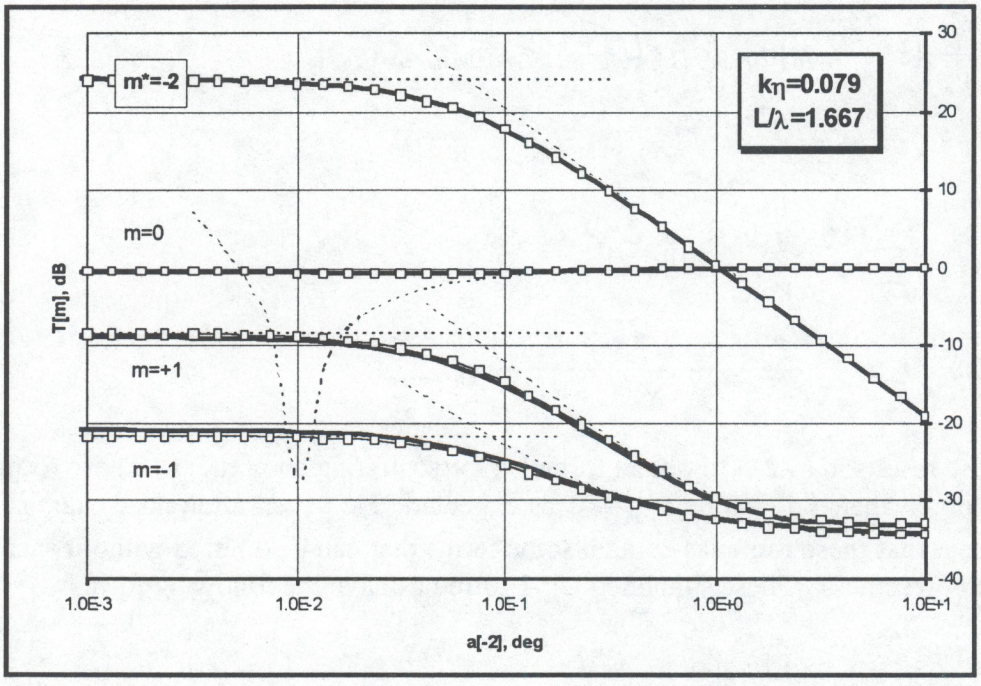

Figure 7.1. Comparison of the UP-I approximation to numerical solution for $m^*=-2$. Heavy solid curves – numerical data. Dashed curves – CP-I and GP-I results. Light solid curves marked with squares – UP-I approximation.

It is interesting that the increase in errors is mostly due to the inaccuracy of the GP-I asymptotes. As we discussed in Chapter 5, this can be fixed by including the second order terms in the GP-I formulas. It is possible of course to build the uniform approximation based on these

more accurate asymptotes. The accuracy for the grazing order remains extremely good even for the $k\eta = 0.314$. The effective Brewster angle for this case is $\beta_{EFF} \approx 1.1^{\circ}$, which is very close to the intersection point of the CP-I and CP-I asymptotes for the grazing and $m^* = 1$ modes.

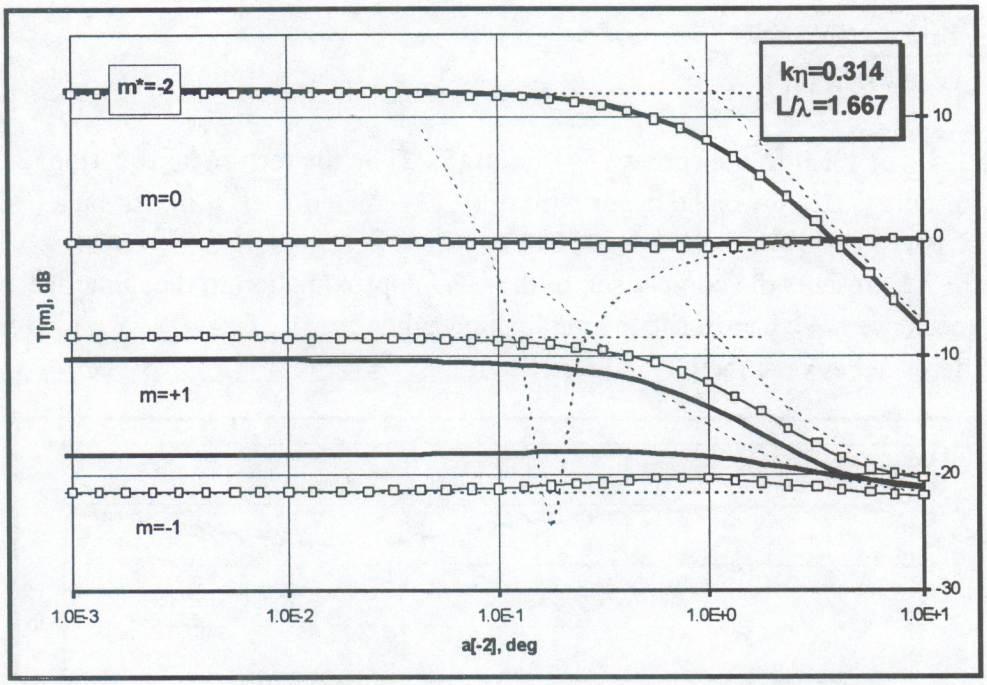

Figure 7.2. Same as Figure 7.1., but for $k\eta = 0.314$.

For the grazing incidence we combine the major terms of the CP equations (4.6) and the GP-I equations (5.15) to form the following equation set for the UP-I surface fields:

$$\begin{cases} v_0 e_0(q_0) + i\sum_{n\neq 0}\left(k^2 - q_0 q_n\right)\eta_{-n} e_n(q_0) = 2v_0, & m = 0 \\ v_m e_m(q_0) + i\left(k^2 - q_m q_0\right)\eta_m e_0(q_0) = 0, & m \neq 0. \end{cases} \tag{7.24}$$

The solution of (7.24) for the surface fields is straightforward, and after substitution in the formula (3.21) for the specular reflection coefficient we have:

$$T_0(q_0) = \frac{v_0 - kZ_{EFF}(q_0)}{v_0 + kZ_{EFF}(q_0)}. \tag{7.25}$$

Comparison of this formula to the reflection coefficient of the plane interface with the impedance boundary condition which is given by the first term at the right-hand part of (4.3) justifies our definitions of the effective impedance (5.5) and (7.4). This formula provides a smooth transition from the CP reflection coefficient +1 to the GP reflection coefficient -1. For $k^2\eta^2 < \alpha_0$ formula

(7.25) reduces to the GP-I result (4.14) with correct orders up to $O\left[(k\eta)^2\right]$. When $k^2\eta^2 > \alpha_0$, formula (7.25) reduces to (5.20) or (7.8) with two correct terms.

For the generic scattered mode we have:

$$T_m(q_0) = \frac{-2i\nu_0\left(k^2 - q_0 q_m\right)\eta_m}{\nu_m\left[\nu_0 + kZ_{EFF}(q_0)\right]}, m \neq 0. \tag{7.26}$$

Formula (7.26) is coupled to the earlier UP-I result (7.22) by the reciprocal equation (3.29). For $k^2\eta^2 < \alpha_0$ formula (7.26) gives the major term of (4.15). When $k^2\eta^2 > \alpha_0$ formula (7.26) reduces to (5.19) or (7.7).

Figure 7.3 presents the comparison of the UP-I approximation to the numerical results for the grazing incidence. We had to use the moderate height, $k\eta = 0.314$, $\beta_{EFF} \approx 1.1^\circ$ to be able to show any difference between the UP and exact solution.

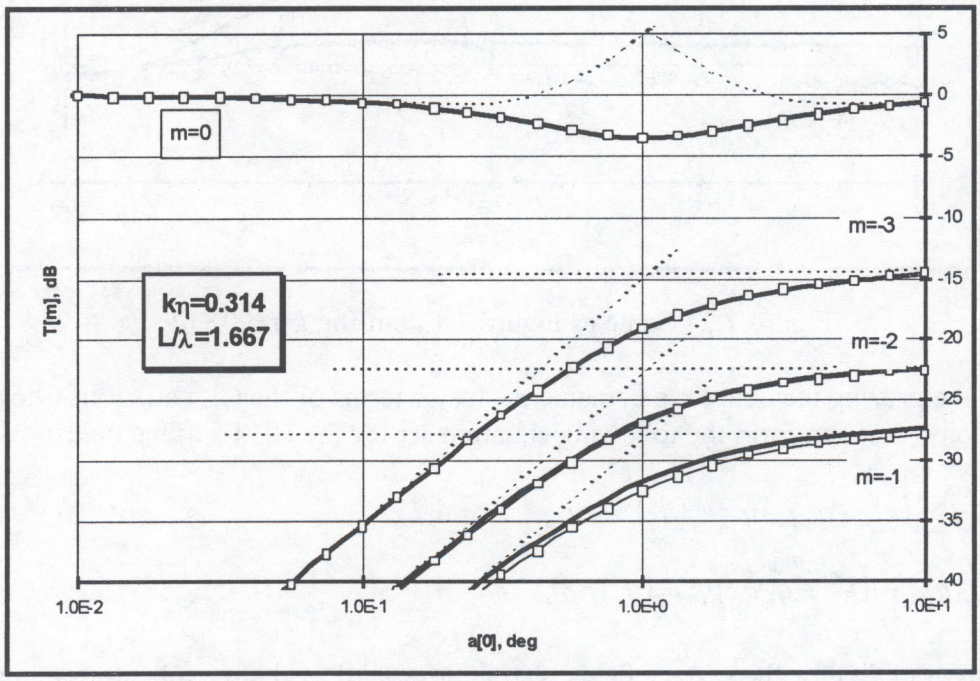

Figure 7.3. Same as Figure 7.2., but for the grazing incidence, $m^* = 0$.

The UP-I appears to be even more accurate for the reflection coefficient, $T_0(q_0)$. In order to show the differences between the exact and UP-I solutions for $T_0(q_0)$ we had to further increase the heights to $k\eta = 0.628$. Figure 7.4 presents the comparison of the exact and the UP-I results for the complex reflection coefficient. UP-I approximation describes the smooth change of the reflection coefficient from +1 to -1 through the rotation at the complex plane without significant changes of the magnitude of the $T_0(q_0)$ when the incidence angle approaches zero. The phase of the reflection coefficient is presented in Figure 7.5, and also shows the remarkable accuracy of the UP-I approximation for moderate heights. Note that the value of the critical angle

is very close to the effective Brewster angle, and increases as a square of height consistently with (5.6).

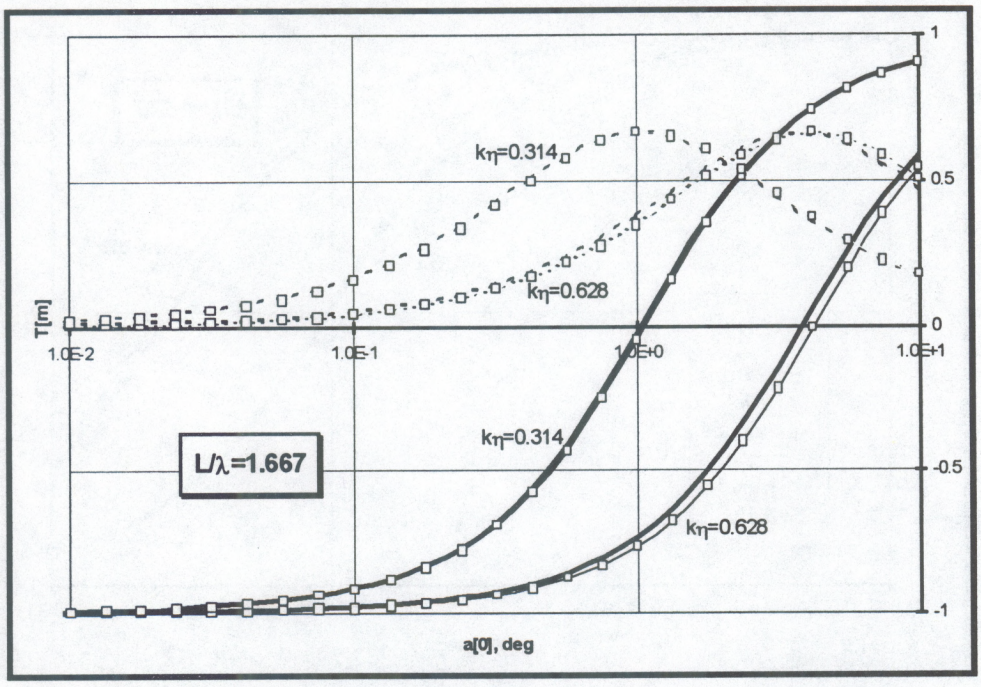

Figure 7.4. Quadratic components of the reflection coefficient $T_0(q_0)$, at small grazing angles. Heavy curves – numerical data. Curves marked with squares – UP-I. Solid curves – real part, dashed curves – imaginary part.

7.2.2 Two Grazing Modes: UP-II

We consider the non-grazing incidence first, and assume that two grazing modes are present with the numbers m^+ and m^-. Similar to the previous subsection we retain in the exact equation set (3.18) the terms that have been kept in the CP equations (4.6) or in the GP-II equations (6.4). The result is the following set of equations for the UP-II approximation:

$$\begin{cases} v_0 e_0(q_0) = 2v_0, \quad m = 0, \\ v_{m^+} e_{m^+}(q_0) + i\left(k^2 - q_{m^+} q_0\right)\eta_{m^+} e_0(q_0) + i\left(k^2 - q_{m^+} q_{m^-}\right)\eta_{m^+-m^-} e_{m^-}(q_0) = 0, \quad m = m^+, \\ v_{m^-} e_{m^-}(q_0) + i\left(k^2 - q_{m^-} q_0\right)\eta_{m^-} e_0(q_0) + i\left(k^2 - q_{m^-} q_{m^+}\right)\eta_{m^--m^+} e_{m^+}(q_0) = 0, \quad m = m^-, \\ v_m e_m(q_0) + i\left(k^2 - q_m q_0\right)\eta_m e_0(q_0) \\ + i\left(k^2 - q_m q_{m^-}\right)\eta_{m-m^-} e_{m^-}(q_0) + i\left(k^2 - q_m q_{m^+}\right)\eta_{m-m^+} e_{m^+}(q_0) = 0, \quad m \neq 0, m^-, m^+. \end{cases} \tag{7.27}$$

The solution of this equation set can be readily obtained by the standard substitution technique. The last equation in (7.27) for $m = 0$ is also used as a correction for the $e_0(q_0) = 2$ solution of the first equation of (7.27). We substitute these surface field components into the equation (3.21) for

the scattering amplitudes, where in fact only the first two terms should be retained, to obtain the scattering amplitudes in the following form:

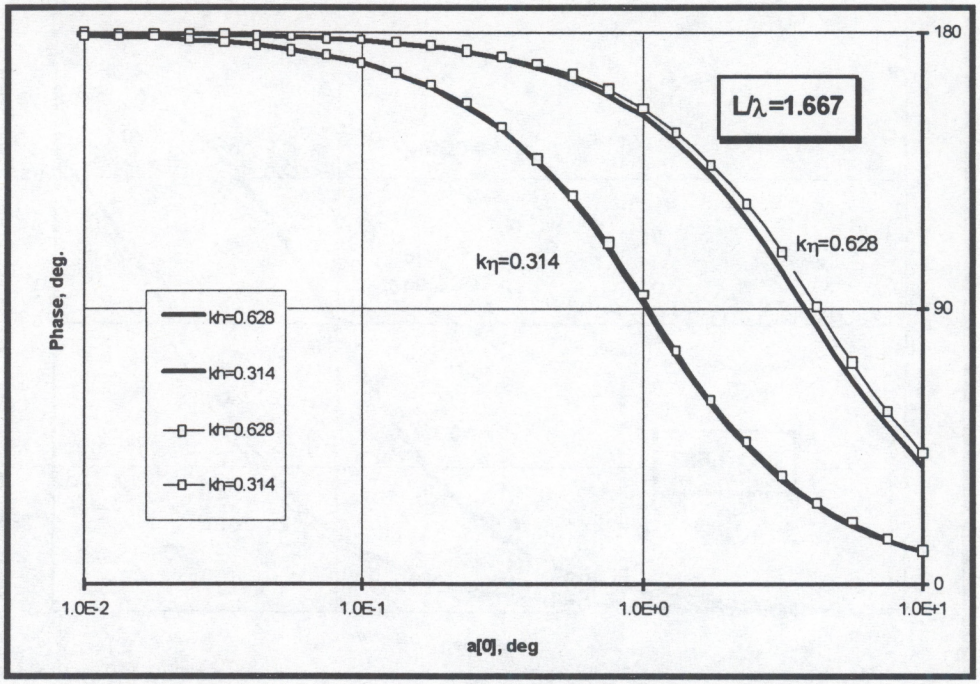

Figure 7.5. Phase of the reflection coefficient $T_0(q_0)$ at small grazing angles. Heavy curves – numerical data. Curves marked with squares – UP-I.

$$T_{m^+}(q_0) = -2i\frac{\left[\nu_{m^-}\left(k^2 - q_{m^+}q_0\right)\eta_{m^+} - i\left(k^2 - q_{m^+}q_{m^-}\right)\left(k^2 - q_{m^-}q_0\right)\eta_{m^+-m^-}\eta_{m^-}\right]}{\nu_{m^+}\nu_{m^-} + \left(k^2 - q_{m^+}q_{m^-}\right)^2\left|\eta_{m^+-m^-}\right|^2}, \tag{7.28}$$

$$T_{m^-}(q_0) = -2i\frac{\left[\nu_{m^+}\left(k^2 - q_{m^-}q_0\right)\eta_{m^-} - i\left(k^2 - q_{m^-}q_{m^+}\right)\left(k^2 - q_{m^+}q_0\right)\eta_{m^--m^+}\eta_{m^+}\right]}{\nu_{m^+}\nu_{m^-} + \left(k^2 - q_{m^+}q_{m^-}\right)^2\left|\eta_{m^+-m^-}\right|^2}, \tag{7.29}$$

$$T_0(q_0) = 1 - \frac{i}{\nu_0}\left[T_{m^-}(q_0)\left(k^2 - q_0q_{m^-}\right)\eta_{-m^-} + T_{m^+}(q_0)\left(k^2 - q_0q_{m^+}\right)\eta_{-m^+}\right], \tag{7.30}$$

$$\begin{aligned} T_m(q_0) = -\frac{1}{\nu_m}\Big[&2\left(k^2 - q_mq_0\right)\eta_m + T_{m^-}(q_0)\left(k^2 - q_mq_{m^-}\right)\eta_{m-m^-} \\ &+ T_{m^+}(q_0)\left(k^2 - q_mq_{m^+}\right)\eta_{m-m^+}\Big], \quad m \neq 0, m^-, m^+. \end{aligned} \tag{7.31}$$

When $k\eta < \alpha_{m^{\pm}}$ these formulas give all the terms retained in the CP-II formulas (4.16) and (4.18). When $k\eta > \alpha_{m^{\pm}}$ they tend to (610) - (6.12) or the "natural" forms of these formulas (7.9), (7.11) and (7.12), as expected. It is also clear from (7.28) - (7.31) that the transition region between these two extreme cases corresponds to $\alpha_{m^{\pm}} \propto k\eta$. This matches our previous estimations (4.17).

Numerical data presented in Figure 7.6 show that UP-II provides a smooth transition between the CP-II and GP-II asymptotes. The UP-II is accurate in the transition region $\alpha_{m^{\pm}} = O(k\eta)$ between the CP-II and GP where neither of the former is valid. As noted for the UP-I case, the inaccuracy of UP-II is mostly related to the offshoot of the GP-II asymptotes for certain modes, and disappears at smaller heights. It can be corrected if higher-order GP-II terms are taken into account.

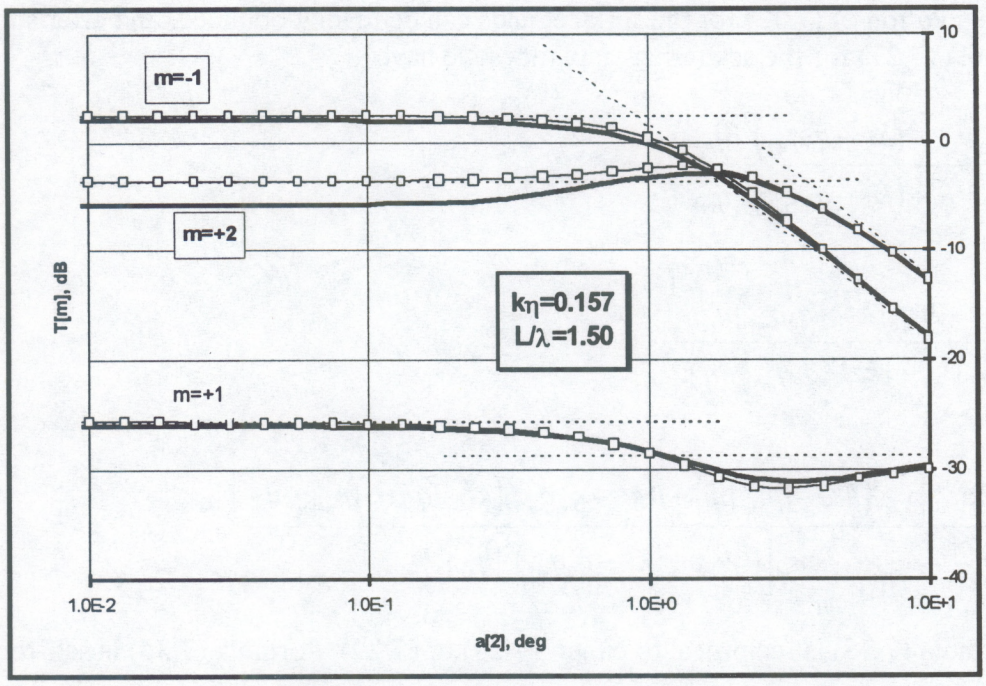

Figure 7.6. Comparison of the UP-II approximation to numerical solution for $m^{+} = +2$, $m^{-} = -1$ and $k\eta = 0.157$. Heavy solid curves – numerical data. Dashed curves – CP-II and GP-II results. Light solid curves marked with squares – UP-II approximation.

For the grazing incidence in the presence of the two grazing modes $m = 0$ (specular) and $m = m^{*}$ (backscatter) equation set that combines the major terms of the conventional perturbation equation (4.6) and the GP-II equation (6.16) has the following form:

$$\begin{cases} \nu_0 e_0(q_0) + i\left(k^2 - q_0 q_{m^*}\right)\eta_{-m^*} e_{m^*}(q_0) = 2\nu_0, \quad m = 0, \\ \nu_{m^*} e_{m^*}(q_0) + i\left(k^2 - q_{m^*} q_0\right)\eta_{m^*} e_0(q_0) = 0, \quad m = m^*, \\ \nu_m e_m(q_0) + i\left(k^2 - q_m q_0\right)\eta_m e_0(q_0) + i\left(k^2 - q_m q_{m^*}\right)\eta_{m-m^*} e_{m^*}(q_0) = 0, \quad m \neq 0, m^*. \end{cases} \tag{7.32}$$

The second term at the left-hand part of the last equation in (6.16) is mostly responsible for the higher-order corrections to the specular reflection coefficient that are similar to (6.21). These corrections are important to keep up with the energy balance. However in this specific case we are more interested in the transition of the specular reflection coefficient from the typical CP value +1 to the GP value -1. Therefore, for the sake of simplicity, we excluded the second term at the left-hand part of the last equation in (6.16) for the present analysis. This term in principle can be included, but it complicates the final formulas significantly.

The solution of (7.32) for the surface fields can be readily obtained, and after substitution in the formula (3.21) for the scattering amplitudes we have:

$$T_0(q_0) = \frac{\nu_0 \nu_{m^*} - \left(k^2 - q_0 q_{m^*}\right)^2 |\eta_{m^*}|^2}{\nu_0 \nu_{m^*} + \left(k^2 - q_0 q_{m^*}\right)^2 |\eta_{m^*}|^2}, \tag{7.33}$$

$$T_{m^*}(q_0) = \frac{-2i\nu_0 \left(k^2 - q_0 q_{m^*}\right)\eta_{m^*}}{\nu_0 \nu_{m^*} + \left(k^2 - q_0 q_{m^*}\right)^2 |\eta_{m^*}|^2}, \tag{7.34}$$

$$T_m(q_0) = \frac{-2i\nu_0 \left[\nu_{m^*}\left(k^2 - q_0 q_m\right)\eta_m - i\left(k^2 - q_m q_{m^*}\right)\left(k^2 - q_{m^*} q_0\right)\eta_{m-m^*}\eta_{m^*}\right]}{\nu_m \left[\nu_0 \nu_{m^*} + \left(k^2 - q_0 q_{m^*}\right)^2 |\eta_{m^*}|^2\right]}. \tag{7.35}$$

Formula (7.35) is reciprocal to either (7.28) or (7.29). Formula (7.34) is self-reciprocal, as expected.

When $k\eta < \alpha_{0.m^*}$ formula (7.33) reduces to the CP-II result (4.20), (7.34) gives the major term of (4.21), and (7.35) gives both terms of (4.19). When $k\eta > \alpha_{0.m^*}$ formula (7.33) gives the major term of (6.21) or (7.14). The correction terms are not reproduced due to the simplifications we mentioned earlier. Formula (7.34) reduces to (6.22) and (7.15), and formula (7.35) approaches (6.20) and (7.13).

UP-II approximation (7.33) - (7.35) is compared to the numerical results, CP-II and GP-II formulas in Figure 7.7. We had to use relatively large heights, $k\eta = 0.314$, in order to show the differences between UP-II and an exact solution for the most interesting forward- and backward-scattered modes. UP-II formulas are fairly accurate in the region of the dip of the reflection coefficient and maximum of the backscattered field where neither CP-II nor GP-II formulas are valid.

It seems enticing to introduce the effective impedance for this grazing incidence/backscatter case as follows:

$$Z_{EFF} = \frac{\left(k^2 - q_0 q_{m^*}\right)^2}{k\nu_{m^*}} |\eta_{m^*}|^2, \tag{7.36}$$

and present the reflection coefficient as similar to (7.25):

$$T_0(q_0) = \frac{\nu_0 - kZ_{EFF}}{\nu_0 + kZ_{EFF}}. \tag{7.37}$$

However, this effective impedance tends to infinity when $\alpha_{m^*} \to 0$ and the Brewster angle does not exist. As we have seen before the critical angle for this case is $\alpha_{m^*} = O(k\eta)$, and it looks like the idea of the effective impedance is not valid here. It is possible however to introduce the more accurate definition of the critical angle as follows:

$$\sin\alpha_C \approx \alpha_C = \frac{\left(k^2 - q_0 q_{m^*}\right)|\eta_{m^*}|}{k} \approx 2k|\eta_{m^*}|. \tag{7.38}$$

At this angle two components of the denominators of (7.33) - (7.35) are equal. For our surface model and $k\eta = 0.314$ we have $\alpha_C = 3.6^o$. This number agrees with the position of the dips in Figure 7.7.

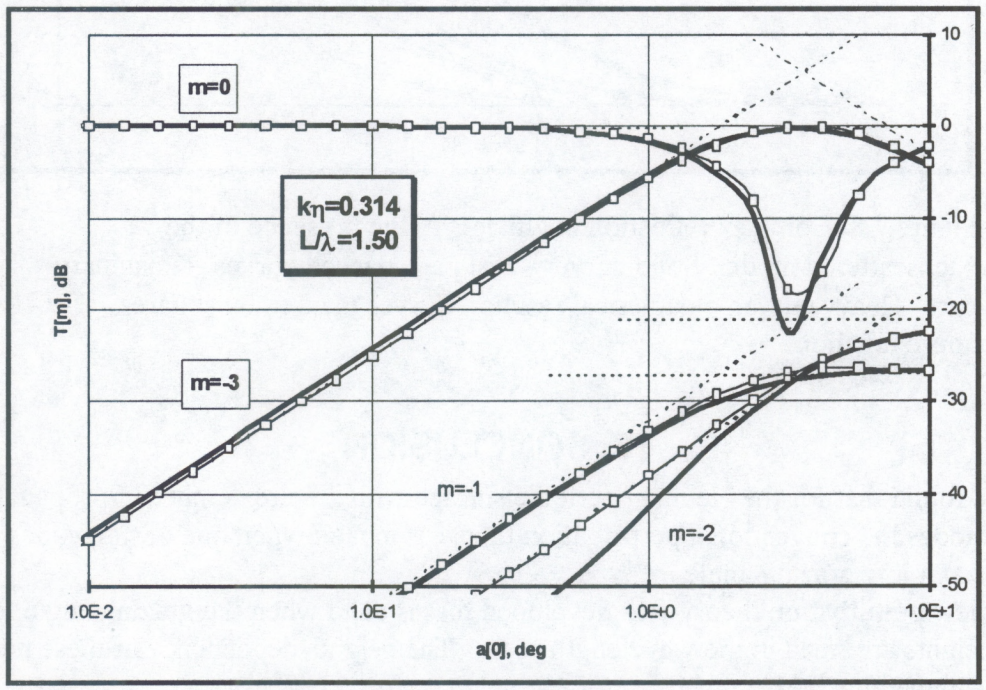

Figure 7.7. Same as Figure 7.6. but for grazing incidence, $m^* = -3$ and $k\eta = 0.314$.

The most interesting feature of the low-grazing forward scattering is the sign inversion of the reflection coefficient. Figure 7.8 presents the quadratic components of the $T_0(q_0)$ calculated

numerically and according to the UP-II formula (7.33). UP-II formulas appear to be fairly accurate even for the moderate heights and predict correct saturation levels for the reflection coefficient. Unlike the singular grazing order case, the transition of the reflection coefficient from +1 to -1 is not a rotation at the complex plane. The reflection coefficient progresses from +1 to -1 mostly along the real axis. This causes the magnitude of the reflection to almost vanish at the incidence angles close to the critical angle. In this situation the energy flux is picked up by the backscattered mode. Note that the reflection coefficient for the UP-II is a real number.

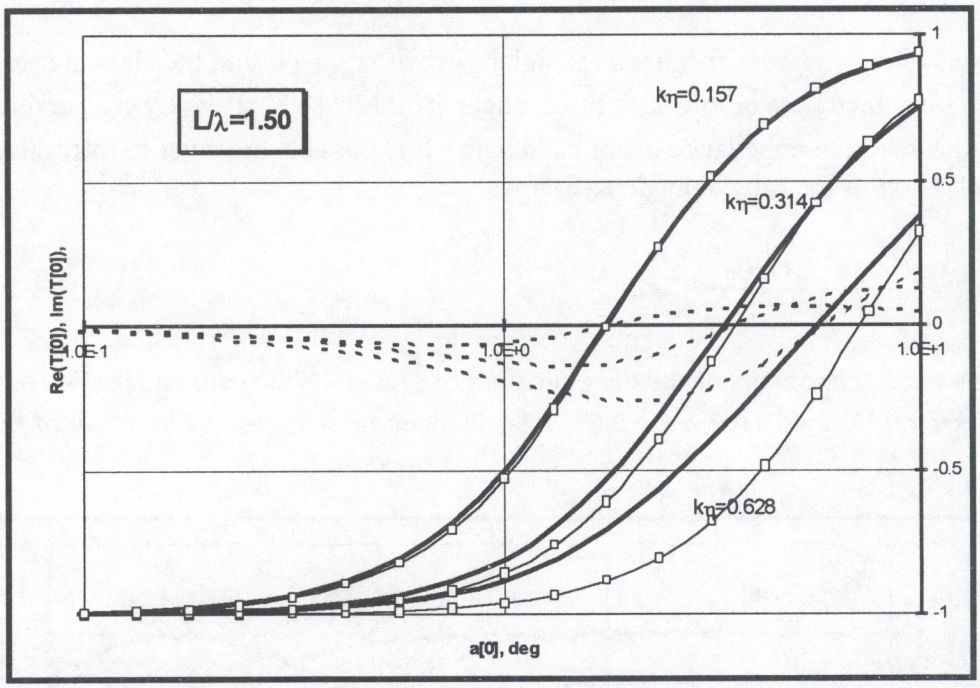

Figure 7.8. Complex reflection coefficient in the presence of the backscattered mode. Solid curves - real part, dashed curves – imaginary part. Heavy curves – numerical results. Curves marked by squares – UP-II approximation.

8. CONCLUSION

We found that for the Neuman periodic surface with a finite number of propagating scattered modes the conventional perturbation theory is invalid when one of the modes propagates at a low grazing angle.

A new perturbation theory was developed that is valid when the grazing angle tends to zero and heights are small in the wavelength scale. The heights dependence of these new formulas is highly nonlinear.

We found that it is necessary to add the second-order term to the conventional first-order perturbation formula to extend the validity domain of the conventional perturbation approximation in the presence of the single grazing mode.

New perturbation theory, together with the conventional perturbation theory, form a complete set of asymptotes for the scattering amplitudes when heights are small in the wavelength

scale. This explains the contradiction between the results of Barrick and Tatarskii/Charnotskii regarding the small grazing angle behavior of the scattering amplitudes: For a single grazing mode Barrick's result is valid under condition (5.11), and Tatarskii/Charnotskii's result is valid under condition (4.10).

We developed a uniform perturbation theory that combines the conventional and new perturbation formulas and is valid for small heights with or without the grazing modes present. We found that the peculiarities of scattering by the Neuman surface in the presence of a single grazing mode can be accurately explained by introduction of the effective surface impedance, which depends on the surface shape and the radiation wavelength but is independent of the direction of the incident wave. The Brewster angle associated with the effective impedance is a critical angle that separates the validity domains of Barrick's and Tatarskii/Charnotskii results. This angle is proportional to the square of the heights when a single grazing mode is present.

Uniform perturbation theory describes a smooth transition of the reflection coefficient for the slightly rough Neuman surface from the value of +1 for the incidence angles larger than the effective Brewster angle to the value of -1 for incidence angles smaller than the effective Brewster angle. In the complex plane this change corresponds to rotation on 180^0 without significant changes in the magnitude of the reflection coefficient.

In the special case of the two grazing modes which includes the low-grazing backscatter we found that the introduction of the effective impedance is not feasible, but there exists a critical angle separating the Barrick's and Tatarskii/Charnotskii's solutions. This angle is proportional to the heights.

The sign inversion of the reflection coefficient in the presence of the two grazing modes is associated with the sharp reduction of its magnitude in the vicinity of the critical angle. At the same time the backscatter coefficient increases to the unit magnitude.

A finite number of propagating modes is crucial for the present development. Transition to the rough surface case is usually achieved through the increase of the surface period. This is associated with the increase of the number of the propagating modes. Formally this adds a new small parameter, the angular separation between adjacent modes or the ratio of the wavelength to the period, to the problem. This third small parameter requires that the asymptotic analysis to be performed in the 3-D parameters space. From a physical standpoint it is hard to believe that when one of the several hundred propagating modes reaches the grazing direction all others are severely affected, as it happens for our example in Figure 4.1.

The example presented in Appendix A for the intrinsically aperiodic case of a surface in the form of the single bump at the plane also shows that our GP asymptotes are not universal in terms of the surface periodicity.

We believe that certain clues regarding scattering behavior at the low-grazing angles can be drawn from the numerical results obtained in the presence of not less than one hundred propagating modes. This requires more substantial numerical efforts, and we consider this to be the next logical step in our study of scattering at low-grazing angles.

REFERENCES

1. Barrick, D. E., 1998. Grazing angle behavior of scatter and propagation above any rough surface. *IEEE Trans. Antennas Propag.* **46**: 73-83.
2. Tatarskii, V. I., and M. I. Charnotskii, 1998. On the universal behavior of scattering from a rough surface for small grazing angles. *IEEE Trans. Antennas Propag.* **46**: 67-72.
3. Tatarskii, V. I., and M. I. Charnotskii, 1998. Universal behavior of scattering amplitudes for scattering from a plane in average rough surface for small grazing angles. *Waves in Random Media.* **8:** 29-40.
4. Bass, F. G., and I. M. Fuks, 1979. Wave scattering from statistically rough surfaces, Pergamon Press. New York. Ch. 2.
5. Tatarskii, V. I., 1997. Formulation of rough-surface scattering theory in terms of phase factors and approximate solutions based on this formulation. *Waves in Random Media.* 7: 557-576.
6. Twersky, V., 1957. On scattering of electromagnetic waves by rough surface. *IRE Trans. Antennas & Propag.* **5:** 81-90.
7. Hutley, M. C., 1982. Diffraction gratings, Academic Press, London, New York. Ch. 6.

APPENDIX A. SCATTERING BY A PLANE WITH A SINGLE BUMP

Let the surface profile of the 1-D scattering problem have a form of a single bump on the otherwise plane surface, i.e. :

$$\eta(x)=\begin{cases} h(x), & |x|\le a \\ 0, & |x|>a \end{cases}, \quad a>h(x)\ge 0. \tag{A.1}$$

We denote $E_{SC}(x,z;q_0)$ the scattered field created by the incident plane wave:

$$E_{IN}(x,z;q_0)=\exp(ixq_0-izv_0) \tag{A.2}$$

under the Neuman boundary condition at the surface.

Consider the auxiliary Neuman scattering problem: scattering of the incident plane wave, $\exp(ixq_0\pm izv_0)$ by the finite symmetrical in z body defined by the equation:

$$|z|\le h(x), \quad |x|\le a. \tag{A.3}$$

We denote the scattering field for this problem as $E_B(x,z;q_0,\pm v_0)$. From the symmetry of the boundary condition we have:

$$E_B(x,z;q_0,-v_0)=E_B(x,z;q_0,+v_0). \tag{A.4}$$

Now it is easy to check that for $z>\eta(x)$ we have:

$$E_{SC}(x,z;q_0)=E_B(x,z;q_0,+v_0)+E_B(x,z;q_0,-v_0). \tag{A.5}$$

The last formula is essentially a result of application of the image theory to this problem.

For the scattered field of the auxiliary problem outside the circle of the radius a enclosing scattering object we have the standard absolutely converging series expansion:

$$E_B(x,z;q_0,+v_0)=\sum_{-\infty}^{\infty}a_n(q_0)h_n^{(1)}(k\rho)\exp(in\alpha), \tag{A.6}$$

where (ρ,α) are the polar coordinates and Fourier coefficients $a_n(q_0)$ depend on the shape and size of the scattering body (A.3).

From (A.4) - (A.6) we have:

$$E_{SC}(x,z;q_0)=2\sum_{-\infty}^{\infty}a_n(q_0)h_n^{(1)}(k\rho)\cos(n\alpha). \tag{A.7}$$

In the far field, $k\rho>>1$ we have:

$$E_{sc}(\rho,\alpha;q_0)=2\sqrt{\frac{2}{i\pi k\rho}}\exp(ik\rho)\sum_{-\infty}^{\infty}i^n a_n(q_0)\cos(n\alpha). \tag{A.8}$$

From the plane wave expansion of the scattered field (3.3) we have

$$E_{sc}(x,z,q_0)=\int\frac{dq}{\nu(q)}T(q_x,q_{0_x})\exp\left[iqx+i\nu(q)z\right]. \tag{A.9}$$

When $x=\rho\cos\varphi$, $z=\rho\sin\varphi$, and $k\rho\to\infty$ from (A.9) we have:

$$E_{sc}(\rho,\alpha,q_0)\approx\sqrt{\frac{2\pi}{ik\rho}}\exp(ik\rho)T(k\cos\alpha,q_0). \tag{A.10}$$

From comparison of (A.8) and (A.9) we have:

$$T(k\cos\alpha,q_0)=\frac{2}{\pi}\sum_{-\infty}^{\infty}i^n a_n(q_0)\cos(n\alpha). \tag{A.11}$$

When $\alpha\to 0$ we have:

$$T(k,q_0)=\frac{2}{\pi}\sum_{-\infty}^{\infty}i^n a_n(q_0). \tag{A.12}$$

It is certainly possible that the sum at the right-hand part of (A.12) is zero for a certain shape of the scatterer (A.3), but there are no reasons to expect that this sum is zero for an arbitrary symmetrical scatterer (A.3). Therefore we conclude that in general the continuous scattering amplitude for the single-bump scattering problem, as defined by (2.4) or (3.3), is $\propto\alpha^0$. This conclusion complies with predictions of Tatarskii/Charnotskii in [2,3], and our discussion of the formula (2.30). However, this contradicts to our GP results (7.6) and (7.11), (7.12) obtained for the periodic surface.

Since the only major difference between the present example and the rest of the paper is in the periodicity of the surface, we are inclined to conclude that there is some singularity associated with the transition from the grating problem to the general rough surface case.

APPENDIX B. DETAILS OF NUMERICAL SOLUTION

In order to obtain a numerical solution of equation (3.18) the number of equations and the number of the Fourier coefficients of the surface field was limited to

$$m_{MIN} \le m.n \le m_{MAX}, \tag{B.1}$$

where the lower boundary of the mode range m_{MIN} was equal to the minimal number of the propagating modes minus 3 - 4 times the number of propagating modes. The upper boundary was determined in a similar way. For example for the $m_0 = 0$ and $m^* = -3$ case of Figure 4.13 the mode range was (-16 ; +13).

All dimensional parameters were normalized by the wave number k, and the final formula for the matrix coefficients was as follows:

$$s_{m,n} = \tilde{v}_m \delta_{m,n} + i(1 - \tilde{q}_m \tilde{q}_n) p_{m-n}(k\tilde{v}_m), \tag{B.2}$$

where ~ denotes the normalized variables. Fourier coefficients $p_n(k\tilde{v}_m)$ were calculated using the 128-point FFT, and the same number of points was used to calculate the Fourier coefficients of heights η_n entering the CP and GP formulas.

The height profile used for all computation has the following form:

$$\eta(x) = \frac{\eta}{5}\left[\cos(\kappa x) + \sin(2\kappa x) - \sin(3\kappa x) + \cos(4\kappa x) - \sin(5\kappa x)\right]. \tag{B.3}$$

The $k\eta$ values used for computation are marked at the charts. The grating period $L = 2\pi\kappa^{-1}$ was fixed at $L = 1.667\lambda$ for all single grazing mode cases. For the two grazing modes case the incidence angle and the grating period were changed simultaneously in order to keep both grazing angles equal while they approach zero. The nominal grating period at the zero-angle grazing was $L = 1.50\lambda$.

The number of the Fourier components for the surface model (B.3) was sufficient to escape the problems discussed in Section 4.2 for all the CP and GP formulas. We avoided using too many high frequency terms to keep the surface slopes moderate. Since in many cases the scattering amplitudes strongly depend on a single Fourier component of the surface, we choose to keep the same amplitude for all the component in order not to avoid the interference between the scattering processes and the surface features. In one case, at the Figure 4.2 this caused all the scattering amplitudes to have practically the same magnitude, and we had to artificially shift the curves to demonstrate their fine features.

The square complex matrix $\{s_{m,n}\}$ was inverted using the regular LU decomposition technique, and the solution for e_n was substituted into the normalized formula (3.21) which was also truncated by (B.1) to calculate the scattering amplitudes.

The energy conservation was controlled during the calculations, and typically the error was less than 10^{-5} for $k\eta \le 0.628$.

*U.S. GOVERNMENT PRINTING OFFICE 1998-0673-018/40109